# Non-leptonic B Meson Decays as a Probe of New Physics

DISSERTATION
zur Erlangung des Grades eines
Doktors der Naturwissenschaften

vorgelegt von
Dipl.-Phys. Martin Jung
geb. am 02.06.1978 in Siegen

eingereicht beim Fachbereich Physik
der Universität Siegen
Siegen 2009

## Gutachter der Dissertation

Prof. Dr. Thomas Mannel
Dr. habil. Alexander Khodjamirian

## Datum der mündlichen Prüfung

17. Juli 2009

Gedruckt auf alterungsbeständigem holz- und säurefreiem Papier, nach ISO 9706.

# Abstract

Despite the tremendous success of the Standard Model, the arguments for the necessity of an extension are compelling. The corresponding energy scale is expected to be $\mathcal{O}(\text{TeV})$; it should lead therefore to visible effects in high-precision flavour observables. While no conclusive effect is seen there up to now, the data reveal certain *puzzles* when compared to Standard Model expectations based on a global fit of the CKM unitarity triangle and general theoretical expectations. The discussion of these tensions in the channels $B \to J/\psi K$, $B \to \phi K$, and $B \to \pi K$, and the deduced constraints for New Physics operators of the class $b \to s\bar{q}q$ form the first project discussed in this thesis. On the other hand, hadronic uncertainties within the Standard Model are still not well understood. Therefore the opposite assumption of large hadronic Standard Model effects in $B \to J/\psi K$ is made in the second project, allowing in addition for a New Physics phase in $B-\bar{B}$ mixing. Finally, the necessity of reliable SM predictions is addressed by developing a framework for the model-independent inclusion of corrections to $U$-spin symmetry predictions.



# Zusammenfassung

Trotz des enormen Erfolgs des Standardmodells ist die Notwendigkeit einer Erweiterung unbestritten. Es wird erwartet, dass die zugehörige Energieskala im TeV-Bereich liegt. Dies sollte zu sichtbaren Effekten in Hochpräzisions-Observablen in der Flavour-Physik führen. Während dort bis heute kein eindeutiger Effekt beobachtet wurde, gibt es doch zumindest gewisse Spannungen, wenn man die Daten mit den Vorhersagen des Standardmodells vergleicht, die aus dem globalen Fit an das Unitaritätsdreieck und allgemeinen theoretischen Erwägungen folgen. Die Diskussion dieser Spannungen in den Kanälen $B \to J/\psi K$, $B \to \phi K$ und $B \to \pi K$, sowie die daraus abgeleiteten Einschränkungen an Operatoren Neuer Physik der Form $b \to s\bar{q}q$ bilden das erste Projekt, das in dieser Arbeit diskutiert wird. Auf der anderen Seite sind die hadronischen Unsicherheiten im Standardmodell nach wie vor nicht gut verstanden. Daher wird im zweiten Projekt die entgegengesetzte Annahme gemacht, dass große Standardmodellbeiträge in Kombination mit Neuer Physik in der $B - \bar{B}$ Mischung für die Abweichungen verantwortlich sind. Schließlich wird diskutiert, wie Einbeziehung von Modell-unabhängigen Korrekturen zu $U$-Spin-Relationen die Zuverlässigkeit einiger Standardmodell-Vorhersagen erhöht werden kann.

# Contents

# Chapter 1

# Introduction

Particle Physics today is at a crossroad: on the one hand, the Standard Model of Elementary Particle Physics (SM) is tremendously successful; there is still no direct measurement in contradiction to it when neutrino masses are included. On the other hand, there is the necessity of physics beyond the SM (New Physics (NP)), preferably at the TeV-scale, associated for example with the hierarchy problem, the question of dark matter and energy, as well as the baryon-antibaryon asymmetry of the universe. In addition, some measurements performed lately, prominently the so-called PAMELA anomaly and the ATIC data, showing both excesses in the cosmic fluxes of electrons and positrons in the $\mathcal{O}(10^2$ GeV) regime, pose questions, which could not be addressed in the SM so far. Finally the SM is unsatisfactory from a theoretical point of view, as it leaves open several questions about e.g. the family structure or the pattern of masses.

On the theory side one has constructed various models in order to address these questions. Ideas include extending the Lorentz symmetry by a symmetry between bosons and fermions (Supersymmetry), adding a fourth family to the spectrum (SM4), embedding the SM gauge symmetry groups in a single one (Grand Unified Theories (GUT)), or treating the four space-time dimensions as arising effectively from a higher dimensional space (Extra Dimensions). Exploring experementally what kind of NP is realized in nature will be a main task in the coming years.

One big step forward in that direction will be the next generation experiments, currently under planning and construction, of which the most prominent one is the Large Hadron Collider (LHC) at CERN. As part of that program, a huge number of new measurements regarding Flavour Physics will be carried out, including

those at LHCb, especially dedicated to this field. Under the important topics in that regime are the Flavour Problem, origin of the masses of and mixing between the fermions, and a possible connection between the quark and lepton sector.

Flavour Physics has a tradition of identifying "NP" in various times: from the postulate of the neutrino over the prediction of the charm quark (including its mass) to the prediction of the third family and the mass of the top quark, low-energy Flavour Physics has been an important complementary tool to the high-energy particle accelerators in the last century.

In this regime lies the focus of this thesis. By now, an enormous amount of data has been gathered regarding $B$ decays, dominated by the dedicated experiments BaBar at SLAC and Belle and KEK, with important addition of several measurements in the $B_s$ system in the D0 and CDF experiments at Tevatron. However, despite the high precision reached there, and in contrast to many situations in the past, there is no striking experimental result at the moment which clearly contradicts theory. It is more the other way around: theory calls for experimental results to contradict the SM, in order to gain more specific information on the structure of a possible extension. This implies, that one has to watch out for emerging discrepancies between the data and the SM, called *puzzles*. Being usually formed by deviations with an approximate significance of around two standard deviations, their interpretation is usually difficult and not conclusive. Another difficulty, which in light of the expected statistics in future experiments will soon become the main issue, is the control of hadronic uncertainties. While in the last decade huge progress has been made in understanding hadronic matrix elements of $B$ decays, the methods developed so far still suffer from relatively large non-factorizable contributions, which prevent in many cases reliable SM predictions to which the data can be compared.

The three projects discussed mainly in this work try to address these issues from different perspectives:

- The first project deals with NP in $b \to s$ transitions. Starting from the observation of different puzzles in this class of decays, the data are fitted under the assumption that one NP operator dominates the effect, and that the SM contributions in these decays are understood reasonably well. In discussing several effects in the same regime within a single, model-independent framework tries to address the issue of the low significance of the single effects.

- In the second project, the opposite assumption is made, namely that non-factorizable SM contributions in $B \to J/\psi K$ are large, but additionally allowing for a NP phase in mixing. This framework implies an approximate symmetry relation to $B \to J/\psi\pi$, which is used to determine the suppressed amplitude parameters, and can be used in the future to discriminate NP from SM effects.

- Finally, the necessity of reliable SM predictions is addressed by developing a framework for the model-independent inclusion of corrections to $U$-spin symmetry predictions. While this generally needs additional input due to a large number of independent parameters, the additional assumptions now mostly can be made for the subleading amplitudes, only, thereby leading to a reduced systematic uncertainty from this method.

All of these analyses will profit enormously from the precision and the new measurements expected from the LHC and a possible Super-$B$ factory.

This work is structured in three main chapters. Chapter 2, "Fundamentals", collects some basic facts about the SM and CP violation, forming the basis of the analysis methods developed in chapter 3. There, the effective field theory framework is introduced, on which both, the QCD Factorization (QCDF) approach and the symmetry based method discussed in the following, rely. In addition, the statistical approach is described, which is used to deal with theoretical and systematic uncertainties. The main part is then given by the "Applications" (chapter 4), where basically the three projects described above are discussed extensively. Finally, conclusions are gathered in chapter 5.

# Chapter 2

# Fundamentals

This chapter collects some basic facts, forming the basis of the analysis methods discussed in chapter 3. As most of this is text book knowledge, the presentation is rather short, mainly fixing notation. Accordingly, it is often referred to the literature for further details.

In the first section, the Standard Model lagrangian is introduced and some of the reasons are given why it is expected to find NP in general, and preferably at the TeV scale. Due to the important role of CP violating quantities in the rest of this work, section 2.2 gives a somewhat more detailed introduction to that topic, and states the necessary expressions for the observables dealed with in the applications. Finally, the last section of this chapter introduces the concept of reparametrization invariance, which arises, because those expressions are non-linear functions of the fundamental parameters, whose extraction becomes therefore non-trivial.

## 2.1 The Standard Model

An exhaustive introduction to the SM [1–3] can clearly not be given here and would be besides the topic of this work; it is referred to the vast amount of literature covering these topics. Examples for text books are given by [4–6], more recent introducing articles are for example [7–10]. This section merely aims at introducing the used notation and motivating why it it necessary to go beyond the SM and search for NP.

The SM describes all known particles and their interactions, apart from grav-

ity. It is formulated as a gauge theory with the product symmetry group

$$\mathcal{G}_{SM} = SU(3)_C \times SU(2)_L \times U(1)_Y \,, \tag{2.1}$$

where $SU(3)_C$ represents the colour symmetry of the strong interactions, $SU(2)_L$ the weak isospin relating left-handed up and down quarks, and the $U(1)_Y$ symmetry under hypercharge transformations. Given the particle content in terms of symmetry multiplets and one coupling constant for each of the three symmetry groups, the gauge symmetry fixes completely the interactions between the fermions and gauge bosons, as well as those between the gauge bosons themselves. The corresponding part of the lagrangian is given by

$$\begin{aligned} \mathcal{L}_{kin} + \mathcal{L}_{gauge} &= \overline{q}_L i\not{D} q_L + \overline{u}_R i\not{D} u_R + \overline{d}_R i\not{D} d_R + \overline{\ell}_L i\not{D} \ell_L + \overline{e}_R i\not{D} e_R + \\ &\quad -\frac{1}{2}\mathrm{Tr}\{\mathbf{G}_{\mu\nu}\mathbf{G}^{\mu\nu}\} - \frac{1}{2}\mathrm{Tr}\{\mathbf{F}_{\mu\nu}\mathbf{F}^{\mu\nu}\} - \frac{1}{4} f_{\mu\nu} f^{\mu\nu} \,, \end{aligned} \tag{2.2}$$

with the following notation:

$$\ell_L = \begin{pmatrix} \nu_L \\ e_L \end{pmatrix} \qquad \text{and} \qquad q_L = \begin{pmatrix} u_L \\ d_L \end{pmatrix} \tag{2.3}$$

denote the left-handed lepton and quark doublet under $SU(2)_L$ respectively, and $e, \nu, d$ and $u$ represent three generations each[1]:

$$\begin{aligned} e_{L.R} &= \begin{pmatrix} e_{L,R} \\ \mu_{L,R} \\ \tau_{L,R} \end{pmatrix} , & \nu_{L,R} &= \begin{pmatrix} \nu_{e,L,R} \\ \nu_{\mu,L,R} \\ \nu_{\tau,L,R} \end{pmatrix} , \\ u_{L,R} &= \begin{pmatrix} u_{L,R} \\ c_{L,R} \\ t_{L,R} \end{pmatrix} , & d_{L,R} &= \begin{pmatrix} d_{L,R} \\ s_{L,R} \\ b_{L,R} \end{pmatrix} . \end{aligned} \tag{2.4}$$

In addition, the quark fields are triplets under $SU(3)_C$, but the corresponding indices are suppressed in the following, unless explicitly stated. $\mathbf{G}_{\mu\nu}$, $\mathbf{F}_{\mu\nu}$ and $f_{\mu\nu}$ denote the field strength tensors for $SU(3)_C, SU(2)_L$ and $U(1)_Y$ respectively. The covariant derivatives differ for each field, depending on the quantum numbers, and contain the corresponding gauge field terms. The hypercharge and weak isospin quantum numbers are listed in table 2.1.

[1]The same symbols are used for the first generation fields, but the differentiation is always obvious from context.

| Field | $I^W$ | $I_3^W$ | $Y$ |
|---|---|---|---|
| $u_L$ | 1/2 | 1/2 | 1/3 |
| $d_L$ | 1/2 | -1/2 | 1/3 |
| $u_R$ | 0 | 0 | 4/3 |
| $d_R$ | 0 | 0 | -2/3 |
| $\nu_L$ | 1/2 | 1/2 | -1 |
| $e_L$ | 1/2 | -1/2 | -1 |
| $e_R$ | 0 | 0 | -2 |

**Table 2.1:** Quantum numbers under hypercharge and weak isospin transformations of the SM matter fields.

However, in this setup masses are not allowed: the gauge bosons have to be massless, because a corresponding mass term is not invariant under the symmetry transformations, leading to a breaking of gauge symmetry. In case of the fermions, $SU(2)_L$ being *chiral* leads to left- and right-handed parts belonging to different multiplets, therefore the symmetry again forbids a mass term.

For these reasons, the gauge symmetry has to be broken, and in order to keep the properties of the gauge symmetry, this breaking has to be spontaneous. In the SM, it proceeds by the *Higgs-mechanism* [11–14], in which a doublet of scalar fields is introduced,

$$\Phi = \begin{pmatrix} \phi_+ \\ \phi_0 \end{pmatrix} , \tag{2.5}$$

which leads to the corresponding potential and kinetic term in the lagrangian,

$$\mathcal{L}_\Phi = (\mathcal{D}^\mu \Phi)^\dagger (\mathcal{D}_\mu \Phi) + \mu^2 \Phi^\dagger \Phi + \frac{\lambda}{4} (\Phi^\dagger \Phi)^2 . \tag{2.6}$$

The mass parameter $\mu^2$ and the self coupling $\lambda$ have to be real to assure the hermitecity of the lagrangian. In addition, this allows *Yukawa couplings* for the fermions,

$$\mathcal{L}_{\text{Yuk}} = -\bar{\ell}_L Y_e \Phi e_R - \bar{q}_L Y_d \Phi d_R - \bar{q}_L Y_u \widetilde{\Phi} u_R + h.c. , \tag{2.7}$$

where

$$\widetilde{\Phi} = i\sigma_2 \Phi^* = \begin{pmatrix} \phi_0^* \\ -\phi_- \end{pmatrix} . \tag{2.8}$$

transforms again as an $SU(2)$ doublet, which allows to give mass to up and down quarks with only one Higgs doublet. The corresponding coupling constants $Y_{u,d,e}$

are discussed in 2.2 in some detail. For $\mu^2 < 0$ this Higgs potential leads to a non-vanishing vacuum expectation value (VEV),

$$|\langle \Phi_0 \rangle| =: \frac{v}{\sqrt{2}} = \sqrt{\frac{-2\mu^2}{\lambda}} > 0\,, \tag{2.9}$$

around which the field is expanded in terms of

$$\Phi = \exp\left(\frac{i\boldsymbol{\xi}\cdot\boldsymbol{\tau}}{2v}\right)\begin{pmatrix} 0 \\ (v+H)/\sqrt{2} \end{pmatrix}. \tag{2.10}$$

This breaks the gauge symmetry spontaneously, $SU(2)_L \times U(1)_Y \to U(1)_{\mathrm{em}}$, leading to one physical Higgs boson $H$ and to masses for the weak gauge bosons as well as the fermions (apart from the neutrinos, which are left massless here, as noted before). The Yukawa couplings allow for flavour-changing interactions and CP violation; these matters will be discussed in section 2.2.

Leaving neutrino phenomenology aside, the SM in this form is capable of accomodating virtually every measurement made so far, although some measurements performed lately, specifically in astrophysical experiments (see e.g. [15, 16]), pose questions which could not be addressed in the SM yet. However, there are several reasons why an extension of this model is necessary in any case:

- **Dark matter:** The evidence for dark matter is by now compelling, see e.g. [17]. Within the SM, while for example neutrinos may contribute, there is no known way to accomodate for the measured value of the dark matter contribution to the energy density of the universe, $\Omega_M \approx 25\%$.

- **Vacuum energy:** Recent observations determine the cosmological constant to be rather small, but non-vanishing [17–19]:

  $$\rho_{\mathrm{vac}} \lesssim 10^{-46}\ \mathrm{GeV}^4 \approx (\text{few meV})^4\,. \tag{2.11}$$

  However, the contribution from the Higgs VEV would naively be given by $\rho_H := \frac{M_H^2 v^2}{8} \gtrsim 10^8\ \mathrm{GeV}^4$, and would be even larger for many extensions of the SM with heavy Higgs bosons. In addition, there are vacuum excitations of all fields, which are not relevant in particle physics, but should play a role in cosmological considerations. Therefore, there seems a huge effect or important principle to be missing, which leads to cancellations between different huge contributions. However, as the only force sensitive to this constant term is gravity, it is extremely difficult to clarify these issues experimentally. For examples of reviews, see [20, 21].

- **Hierarchy problem(s):** While in the SM the fermion and gauge boson masses are protected by the gauge symmetry from becoming huge, because they arise only from symmetry breaking, the mass of the Higgs boson itself is not. In fact, even if it is set to a small value at the Planck or GUT scale, it is driven by renormalization group running to huge values again, due to quadraticly divergent one-loop diagrams. This is called the (large) hierarchy problem. For this problem to be solved, some form of NP has to show up at the TeV scale. In fact, already the circumstance that electroweak precision observable data prefer a light higgs boson [22], but generic NP contributions are favoured to lie above $\sim 5$ TeV, poses a puzzle: the evolution from 5 TeV down to the electroweak scale already induces corrections to the Higgs mass which are larger than its preferred value. This observation is known as the *LEP paradox* [23].

  In addition, the Higgs mechanism leads to masses of the order of $\mathcal{O}(v)$, but only the top quark and the gauge bosons have masses of that order. Leaving neutrinos again aside, the fermion masses cover a range of five orders of magnitude, as can be seen from the ratio $m_e/m_t \lesssim 10^{-5}$, which again is not explained in the SM.

- **Gravity:** Gravity is not described by the SM, and general relativity and the SM are in conflict with each other at the Planck scale. A more complete theory should include all known fundamental forces.

- **Ignorance:** While masses, mixing angles and CP violation are *accomodated for* in the SM, they are not *explained*. A more complete theory could give reasons for the values of these parameters, the number of families, etc. This, however, is only an aesthetical argument.

- **Baryon asymmetry, strong CP violation:** These issues are discussed in the next section.

While these are general problems that need to be addressed by a model beyond the SM, in this work the focus lies on possible influences of NP on flavour observables, without referring to a concrete model. CP violating observables turn out to be especially sensitive; the framework to discuss them is introduced in the next section.

## 2.2 CP Violation

Since its discovery in $K_L \to \pi^+\pi^-$ decays in the famous experiment in 1964 [24], CP violation stayed one of the most interesting and active fields in particle physics. Being found in the $B$ meson system in 2001 [25, 26], the impressive performance of mainly the B factories (BaBar at SLAC, and Belle at KEK), and the experiments D0 and CDF at Fermilab lead to precise measurements of several independent CP violating quantities. From this, a remarkably consistent picture emerges (see figure 2.1), which establishes that the Cabibbo-Kobayashi-Maskawa (CKM) mechanism of CP violation [27, 28], as implemented in the SM (see section 2.2.1), is indeed the main source of low energy CP violation. This prediction by Kobayashi and Maskawa has been rewarded in 2008 with the nobel price.

Actually, the observed consistency comes rather surprising, because of several reasons:

- Within the SM, nonperturbative QCD effects lead to the appearance of a CP violating term in the lagrangian,

$$\mathcal{L}_{\theta_{QCD}} = \frac{\theta_{QCD}}{32\pi^2}\tilde{F}^a_{\mu\nu}F^{\mu\nu\,a}\,, \quad \tilde{F}^a_{\mu\nu} = \epsilon_{\mu\nu\rho\sigma}F^{\rho\sigma\,a}\,, \tag{2.12}$$

  where $F^{\rho\sigma\,a}$ denotes the gluon field strength tensor. Because this term would lead to an electric dipole moment of the neutron, for which

$$d_n < 3 \times 10^{-26}\ \mathrm{e\,cm} \tag{2.13}$$

  has been measured [30], this parameter is constrained to be (see [31] and references therein)

$$\theta_{QCD} < 10^{-9}\,, \tag{2.14}$$

  while from theory $\theta_{QCD} \sim \mathcal{O}(1)$ is expected. This fact is known as the *strong CP problem*. A possible dynamical explanation is given by the *Peccei-Quinn-mechanism* [32, 33], where an additional axial symmetry is spontaneously broken, leading to a Goldstone boson, called *axion*, which gives a dynamical contribution to the angle $\theta_{QCD}$. The minimization of the axion potential then ensures $\theta_{QCD} \sim 0$. However, the axion has not been found so far, despite considerable efforts (see e.g. [34] in [35]). For more details and references to possible alternative explanations, see e.g. [31]. In the following, $\theta_{QCD} = 0$ will be assumed.

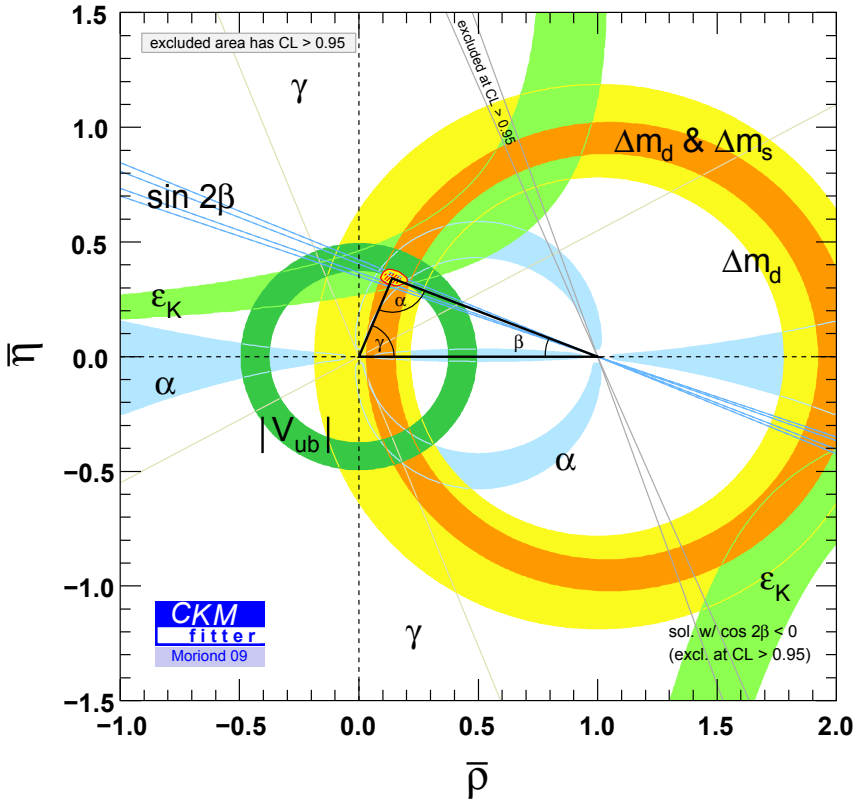


**Figure 2.1:** The global fit to the unitarity triangle, taken from [29]. Shown are various constraints, explained e.g. in [29], in the $\bar{\rho} - \bar{\eta}$-plane, introduced in equation (2.32). The consistency of the CKM mechanism with data is demonstrated by the fact that all constraints have a common overlap, shown in yellow with a red border.

- The baryon-antibaryon asymmetry in the universe requires CP violation [36] and is known to be too large for the CKM mechanism to be the only source of CP violation [37–39]. While this does not necessarily mean that it will be possible to *observe* CP violation from another source, this fact implies that the SM needs an extension at some energy.

- In addition, most NP models have generically a variety of sources for CP violation (including flavour changing neutral currents), so from the aforementioned arguments for NP at a not too high scale (see section 2.1) one

would expect some visible effects at low energies.

As several reviews and textbooks on CP violation are available (e.g. [40–44]), the following description will again only collect the basic facts and expressions which are needed later on in the analysis. After a sketch of the CKM mechanism in the next section, different unitarity triangle fits in the presence of NP are discussed in section 2.2.2. The observables for non-leptonic B decays are introduced in section 2.2.3, and finally a few comments on models beyond the SM are made.

### 2.2.1 CP Violation in the Standard Model

In addition to being gauge and Lorentz invariant, the strong and electromagnetic parts of the SM possess also three discrete symmetries:

- *Charge conjugation* $C$, transforming a particle into its antiparticle,
- *parity transformation* $P$, defined by $x = (x^0, \mathbf{x}) \to x_P = (x^0, -\mathbf{x})$, and
- *time reversal* $T$, implemented by $x = (x^0, \mathbf{x}) \to x_T = (-x^0, \mathbf{x})$.

The weak sector however is only invariant under the combination CPT. The implementation of these symmetries in terms of spinor fields can be deduced by demanding the well known transformation properties of the corresponding currents, and results in unitary representations for $P$ and $C$, while $T$ is implemented as an antiunitary operator. These operators have the following transformation properties[2]:

$$\begin{aligned} P\psi(x)P^{-1} &= \gamma^0\psi(x_P)\,, \\ C\psi(x)C^{-1} &= i\gamma^2\gamma^0\bar{\psi}^T(x)\,, \text{ and} \\ T\psi(x)T^{-1} &= i\gamma^1\gamma^3\psi(x_T)\,. \end{aligned} \tag{2.15}$$

Leaving the strong CP violation aside, the *only* source remaining for CP violation in the Standard Model is the CKM matrix: Given the SM lagrangian including the quark fields,

$$\begin{aligned} \mathcal{L}_q &= \mathcal{L}_q^{kin} + \mathcal{L}_q^{Yuk} \\ &= \bar{q}_L i\not{D} q_L + \bar{d}_R i\not{D} d_R + \bar{u}_R i\not{D} u_R + \\ &\quad \bar{q}_L \phi Y_d d_R + \bar{q}_L \tilde{\phi} Y_u u_R + h.c.\,, \end{aligned} \tag{2.16}$$

[2]The expressions are given for the Dirac matrices in the Dirac representation.

one uses biunitary transformations in order to find the mass eigenstates of the theory:

$$u_{L,R} \to U_u^{L,R} u_{L,R} \qquad \text{and} \qquad d_{L,R} \to U_d^{L,R} d_{L,R}\,, \tag{2.17}$$

satisfying

$$U_d^L Y_d U_d^{R\,\dagger} = \mathrm{diag}(y_d, y_s, y_b) \qquad \text{and} \qquad U_u^L Y_u U_u^{R\,\dagger} = \mathrm{diag}(y_u, y_c, y_t)\,, \tag{2.18}$$

with real entries $y_i \sim m_i$. This leaves the kinetic terms for the right-handed particles invariant and diagonalizes the Yukawa matrices as well as the mass matrices proportional to them. The neutral current interactions do neither mix left- and right-handed fields, nor up- and down-quarks. This implies, that there are no flavour changing neutral currents at tree level (this is usually referred to as GIM-mechanism [45], presented here in a modern language); the only point where an effect is observable is the charged current interaction, where the — again unitary — combination

$$U_u^L U_d^{L\,\dagger} =: V_{CKM} \tag{2.19}$$

appears, which is called the *CKM matrix*:

$$\mathcal{L}_{cc} = \frac{g_2}{\sqrt{2}} J_\mu^+ W^{\mu+} + h.c., \quad \text{with} \quad J_\mu^+ = V_{CKM}^{ij} \bar{u}_{L,i} \gamma_\mu d_{L,j}\,. \tag{2.20}$$

Here $W^{\mu+}$ denotes the gauge boson field. The element $V_{CKM}^{ij}$ gives the coupling constant for the transition $d_j \to u_i$. The transformation property of this part of the lagrangian reads, using equations (2.15),

$$\begin{aligned} \mathcal{L}_{cc} &= W_\mu^+ \bar{u}_L \gamma^\mu V_{CKM} d_L + W_\mu^- \bar{d}_L V_{CKM}^\dagger \gamma^\mu u_L \\ &\overset{\text{CP}}{\to} W_\mu^+ \bar{u}_L \gamma^\mu V_{CKM}^* d_L + W_\mu^- \bar{d}_L V_{CKM}^T \gamma^\mu u_L \end{aligned} \tag{2.21}$$

In order for this matrix to lead to CP violation, in terms of the Yukawa matrices the necessary and sufficient condition is the following [46, 47]:

$$\mathrm{Im}\left(\det\left[Y_d Y_d^\dagger, Y_u Y_u^\dagger\right]\right) \neq 0\,. \tag{2.22}$$

One implication of that is, that the CKM matrix has to carry a (non-trivial, in the sense explained in the following) complex phase, as can be seen from expressions (2.21). For this to be the case, at least three generations are necessary,

because for $N$ generations, one has $2N-1$ unobservable relative phases between the quark fields, and $N(N-1)/2$ (real) mixing angles, leaving

$$N_{phase} = N^2 - (2N-1) - N(N-1)/2 = (N-1)(N-2)/2 \tag{2.23}$$

observable complex phases. This implies, in addition to the existence of at least three generations, that CP violation can only occur in processes in which all three generations take part. For underlying strange or charm decays, this requires at least one loop in the process. Expressing relation (2.22) in terms of low-energy parameters of the theory with aid of ($\Delta m_{ij}^2 = (m_i^2 - m_j^2)$)

$$\mathrm{Im}\det\left[Y_d Y_d^\dagger, Y_u Y_u^\dagger\right] = \Delta m_{tc}^2 \Delta m_{tu}^2 \Delta m_{cu}^2 \Delta m_{bs}^2 \Delta m_{bd}^2 \Delta m_{sd}^2 \, J \,, \tag{2.24}$$

the corresponding conditions are that (a) the *Jarlskog determinant* $J$ defined by

$$\mathrm{Im}\Delta \;:=\; \mathrm{Im}\left[V_{\alpha j} V_{\beta k} V_{\alpha k}^* V_{\beta j}^*\right] =: J \sum_{\gamma,l} \epsilon_{\alpha\beta\gamma}\epsilon_{jkl} \tag{2.25}$$

does not vanish (that is, all four parameters in the CKM matrix have to be non-trivial, for the explicit expression see below), and that (b) within up type and down type quarks separately no degeneracies occur.

Because of equation (2.23), the CKM matrix is parametrized in terms of four real parameters, which are the three mixing angles and one phase in case of the standard parametrization advocated by the PDG ($s/c_{ij}$ denote $\sin/\cos\theta_{ij}$),

$$\begin{aligned} V_{CKM} &= \begin{pmatrix} V_{ud} & V_{us} & V_{ub} \\ V_{cd} & V_{cs} & V_{cb} \\ V_{td} & V_{ts} & V_{tb} \end{pmatrix} \\ &= \begin{pmatrix} c_{12}c_{13} & s_{12}c_{13} & s_{13}e^{-i\delta} \\ -s_{12}c_{23} - c_{12}s_{23}s_{13}e^{i\delta} & c_{12}c_{23} - s_{12}s_{23}s_{13}e^{i\delta} & s_{23}c_{13} \\ s_{12}s_{23} - c_{12}c_{23}s_{13}e^{i\delta} & -c_{12}s_{23} - s_{12}c_{23}s_{13}e^{i\delta} & c_{23}c_{13} \end{pmatrix}, \end{aligned} \tag{2.26}$$

leading to

$$J = c_{12}c_{23}c_{13}^2 s_{12}s_{23}s_{13}\sin\delta \,. \tag{2.27}$$

From this the (generalized) *Wolfenstein parametrization* [48, 49] can be obtained by the following definitions:

$$\begin{aligned} s_{12} &=: \lambda \,, \\ s_{23} &=: A\lambda^2 \,, \\ s_{13}e^{-i\delta} &=: A\lambda^3(\rho - i\eta) \,. \end{aligned} \tag{2.28}$$

Expanding in the small parameter $\lambda = \sin\theta_C \simeq 0.22$ leads to an approximate parametrization in which the hierarchical structure of the matrix becomes obvious, preserving unitarity at every order. The expansion up to order $\lambda^3$ reads

$$V_{CKM} = \begin{pmatrix} 1-\frac{\lambda^2}{2} & \lambda & A\lambda^3(\rho - i\eta) \\ -\lambda & 1-\frac{\lambda^2}{2} & A\lambda^2 \\ A\lambda^3(1-\rho-i\eta) & -A\lambda^2 & 1 \end{pmatrix} + \mathcal{O}(\lambda^4)\,. \tag{2.29}$$

A visualisation of the CKM matrix parameters $\rho, \eta$ can be done using the *unitarity triangle* (UT): The off-diagonal relations from the equation

$$V_{CKM}^\dagger V_{CKM} = V_{CKM} V_{CKM}^\dagger = \mathbf{1} \tag{2.30}$$

represent triangles in the complex plane, two of which are distinguished by having three sides similar in size. The one usually referred to as *the* UT stems from rescaling the relation

$$V_{ub}^* V_{ud} + V_{cb}^* V_{cd} + V_{tb}^* V_{td} = 0\,, \tag{2.31}$$

and is shown in figure 2.2. The area of this triangle is proportional to the Jarlskog determinant. Its apex is given by

$$-\frac{V_{ud}V_{ub}^*}{V_{cb}V_{cd}^*} =: \bar\rho + i\bar\eta = \left(1 - \frac{\lambda^2}{2}\right)(\rho - i\eta) + \mathcal{O}(\lambda^4)\,, \tag{2.32}$$

and the side lengths and angles by

$$\begin{aligned} R_u &:= \left|\frac{V_{ud}V_{ub}^*}{V_{cb}V_{cd}^*}\right|\,, & R_t &:= \left|\frac{V_{td}V_{tb}^*}{V_{cb}V_{cd}^*}\right|\,, \\ \cos\gamma &= \bar\rho/R_u\,, & \sin\gamma &= \bar\eta/R_u\,, \\ \cos\beta &= (1-\bar\rho)/R_t\,, & \sin\beta &= \bar\eta/R_t\,. \end{aligned} \tag{2.33}$$

Later $\beta$ and $\gamma$ instead of $\bar\eta$ and $\bar\rho$ will be used as inputs, because they are almost uncorrelated (in contrast to the latter). The above relations then lead to

$$R_u = \frac{\sin\beta}{\sin(\gamma+\beta)}\,, \tag{2.34}$$

which is valid for $\beta + \gamma < \pi$ and $\beta, \gamma > 0$; these conditions are trivially fulfilled.

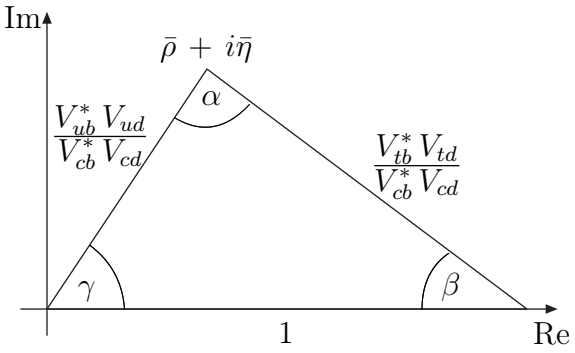


**Figure 2.2:** The unitarity triangle, as explained in the text

Using the unitarity of the CKM matrix, in charmless non-leptonic B decays only the following combinations of CKM elements appear [3]:

$$\lambda_{cs} := V_{cb}V_{cs}^* = A\lambda^2\left(1 - \frac{\lambda^2}{2}\right) + \mathcal{O}(\lambda^6)\,, \tag{2.35}$$

$$\lambda_{cd} := V_{cb}V_{cd}^* = -A\lambda^3 + \mathcal{O}(\lambda^7)\,, \tag{2.36}$$

$$\lambda_{us} := V_{ub}V_{us}^* = A\lambda^4(\bar{\rho} - i\bar{\eta}) + \mathcal{O}(\lambda^6)\,, \tag{2.37}$$

$$\lambda_{ud} := V_{ub}V_{ud}^* = A\lambda^3(\bar{\rho} - i\bar{\eta}) + \mathcal{O}(\lambda^7)\,. \tag{2.38}$$

Of these, $\lambda_{ud}$ and $\lambda_{cd}$, appearing in $b \to d$ transitions, are similar in size,

$$|\lambda_{ud}/\lambda_{cd}| = R_u \sim 0.37\,, \tag{2.39}$$

while $\lambda_{us}, \lambda_{cs}$, appearing in $b \to s$ transitions, exhibit a strong hierarchy:

$$|\lambda_{us}/\lambda_{cs}| \approx \lambda^2/(1-\lambda^2)R_u \sim 2\%\,. \tag{2.40}$$

For transitions with $|\Delta C| = 1$, the combinations

$$V_{cb}V_{ud}^* = A\lambda^2\left(1 - \frac{\lambda^2}{2}\right) + \mathcal{O}(\lambda^6)\,, \tag{2.41}$$

$$V_{ub}V_{cd}^* = -A\lambda^4 R_u e^{-i\gamma} + \mathcal{O}(\lambda^6)\,, \tag{2.42}$$

$$V_{cb}V_{us}^* = A\lambda^3 + \mathcal{O}(\lambda^9)\,, \tag{2.43}$$

$$V_{ub}V_{cs}^* = A\lambda^3 R_u e^{-i\gamma} + \mathcal{O}(\lambda^7) \tag{2.44}$$

are relevant, showing again once a pronounced hierarchy and the other time (almost) none. However, in each decay with defined flavour quantum numbers only one of these factors appears anyway. The hierarchy becomes only relevant when discussing decays to CP eigentstates.

[3] Note that in the literature sometimes also the complex conjugated combinations are denoted as $\lambda_{ij}$.

### 2.2.2 Different Unitarity Triangle Fits

When considering NP, some or all of the constraints shown in figure 2.1 are modified, often rendering the corresponding constraint useless in determining $\bar{\rho}, \bar{\eta}$. However, in order to separate the SM and NP contributions, one has to find a way to determine them without being affected by the NP contributions.

Observables which are considered unaffected by NP, essentially independently of the scenario, are tree level observables, because any NP contribution comparable to the SM tree level one clearly would have been found by now. Therefore these processes are dominated by the SM contribution. From that, the parameter $\lambda$ in the CKM matrix can be determined via superallowed beta decays and semileptonic $K$ decays (mainly). In addition, $|V_{ub}/V_{cb}|$ stays one key ingredient even in the presence of NP. The combination of the different measurements for these observables turns out to be non-trivial. The values used in the analyses in sections 4.1.1 and 4.3 are the averages performed by the CKMfitter group [29], as presented on the conference in Moriond 2009:

$$|V_{ub}| = (3.87 \pm 0.09 \pm 0.46) \times 10^{-3}\,, \quad |V_{cb}| = (40.59 \pm 0.38 \pm 0.58) \times 10^{-3}\,. \tag{2.45}$$

$|V_{ub}|$ is also accessible through the leptonic decay $B \to \tau\nu$. However, in order to turn that measurement into a constraint on $V_{ub}$, one has to know the $B$ meson decay constant $f_B$, which introduces a large theoretical uncertainty of approximately 10%. For that reason this constraint is not used here[4]. However, from the present world average [29]

$$\mathrm{BR}(B^- \to \tau^- \bar{\nu}) = (1.73 \pm 0.35) \times 10^{-4} \tag{2.46}$$

emerges a tension of more than two standard deviations, which depends on the correlation between $\alpha$, $\gamma$, $\sin 2\beta$, $\Delta m_d$, and $\mathrm{BR}(B \to \tau\nu)$. Taking this additional tension into account in the indirect determination of $\beta, \gamma$ would strongly enhance some of the discrepancies discussed later. While the measurement does not enter the determination directly, it is seen as an additional motivation to take the appearing tensions seriously.

There are no other tree-level constraints in this context, apart from the determination of $\gamma$, which is, however, not very restrictive at the moment, as can be seen in figure 2.1.

[4]The CKMfitter collaboration proposes to use the ratio $\mathrm{BR}(B \to \tau\nu)/\Delta m_d$, which shifts the theoretical input from $f_B$ to the bag parameter $B_{B_d}$. However, in that case one has to rely heavily on the corresponding lattice determinations.

Turning to further constraints, one has first to define the model of NP in order to determine the corresponding dependencies. One possible scenario, discussed in section 4.1, is the appearance of NP in decay amplitudes only, leaving the mixing unaffected. In that case the constraint from $B_{d,s}$-mixing still can be used. The corresponding constraint is shown together with the one from $|V_{ub}/V_{cb}|$ in figure 2.3. From that fit, values for $\gamma$ and $\sin 2\beta$ are extracted, given in table 2.3, which are used as inputs in the fits performed in section 4.1 within this NP scenario.

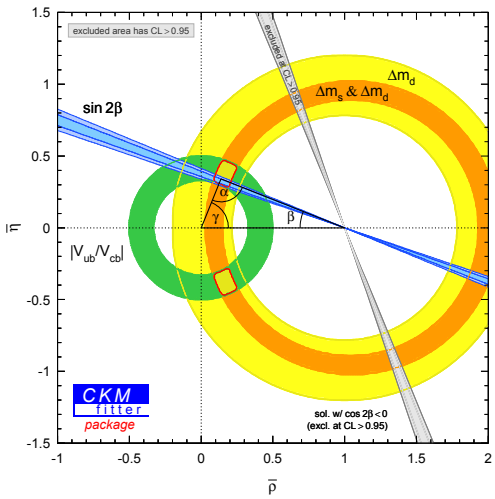


| Quantity | Value |
|---|---|
| $\sin 2\beta$ | $0.746^{+0.014}_{-0.020} \pm 0.081$ |
| $\gamma$ | $(65.7^{+1.8}_{-1.7} \pm 5.5)^\circ$ |

**Figure 2.3:** Global fit to CKM parameters from $\Delta m_d$, $\Delta m_s$ and $|V_{ub}/V_{cb}|_{\text{excl.+incl.}}$. Left: Confidence levels in the $\bar{\eta} - \bar{\rho}$ plane. Right: Fitted values for CKM parameters, where the first error is treated as Gaussian, and the second error, stemming mainly from systematic uncertainties in $|V_{ub}/V_{cb}|$, is treated as flat.

If one allows for NP in the mixing, things get more complicated because the constraint from $\Delta m_{d,s}$ cannot be used any longer easily. In the future, this problem will be solved due to the precise tree level measurements of $\gamma$ in $B \to D\,K$ decays expected from LHCb in particular. For the analysis in section 4.2, this kind of CKM analysis is needed. However, in addition to the constraint from $|V_{ub}/V_{cb}|$, as an estimate for the angle $\gamma$ here simply $\gamma = (65 \pm 10)^\circ$ is used, which is well in accordance with the analyses of the UT in references [29, 50] and the information from $B_{d,s} \to \pi\pi, \pi K, KK$ decays [51]. As mentioned above, this

angle will be determined with only a tiny uncertainty thanks to CP violation measurements in pure tree decays at LHCb. As the analysis in section 4.2 aims at exploiting future precision data, and the extracted value for the angle $\beta$ is essentially independent of the exact choice of $\gamma$, the choice above is considered reasonable. The values used as inputs for that analysis are given in table 2.2.

| Input | Value |
|---|---|
| $R_u$ | $0.423^{+0.015}_{-0.022} \pm 0.029$ |
| $\lambda$ | $0.22521 \pm 0.00083$ |
| $\gamma$ | $(65 \pm 10)^\circ$ |

**Table 2.2:** Input values for the UT analysis depicted in figure 2.4, see also text.

In figure 2.4, the corresponding tension for these inputs can be seen that is also present in more refined fits of the UT for a couple of years [29, 50].

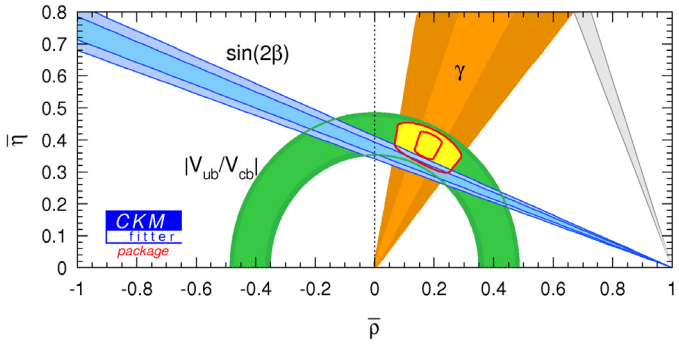


**Figure 2.4:** Constraints in the $\bar{\rho}$–$\bar{\eta}$ plane (1 and $2\,\sigma$ ranges: note that this does not correspond to the 95% CL zones shown usually by CKMfitter).

This fit results in a "true" value for $\beta$, $\beta_{\text{true}} = (24.9^{+1.0}_{-1.5} \pm 1.9)^\circ$, which is, as mentioned above, essentially independent of the error on $\gamma$ for a central value around 65°, and yields $(\sin 2\beta)_{\text{true}} = 0.76^{+0.02+0.04}_{-0.04-0.05}$.

Another possibility would be to transform the measurement of the angle $\alpha$ from $B \to \pi\pi(\rho\pi, \rho\rho)$ decays into one on $\gamma$ by taking the mixing phase explicitly into account instead of identifying it with $2\beta$. However, this would need the

mixing phase $\phi_d$ as an input. This can be extracted from $B \to J/\psi K$, if the common assumption is made that the mixing induced CP asymmetry in that channel equals $\phi_d$. If one wants to avoid that assumption as well, as in the analysis in section 4.2, or to consider models with large contributions to the decay amplitude and mixing, one needs to do a combined fit, which would be quite demanding.

### 2.2.3 CP Violating Observables in B Meson Decays

Obviously, the parameters of interest described in the last section can only be measured indirectly. Therefore in the following the connection between them and the observables measured in experiments is described. This section mostly follows [42, 44].

For a meson $B$, the amplitudes for decaying into a final state $f$ or its CP conjugate state $\bar{f}$ are denoted as

$$\mathcal{A}_f := \langle f|\mathcal{H}|B\rangle\,, \quad \mathcal{A}_{\bar{f}} := \langle \bar{f}|\mathcal{H}|B\rangle\,, \quad \bar{\mathcal{A}}_f := \langle f|\mathcal{H}|\bar{B}\rangle\,, \quad \bar{\mathcal{A}}_{\bar{f}} := \langle \bar{f}|\mathcal{H}|\bar{B}\rangle\,. \tag{2.47}$$

If CP was conserved, the relations $\mathcal{A}_f = \bar{\mathcal{A}}_{\bar{f}}$ and $\mathcal{A}_{\bar{f}} = \bar{\mathcal{A}}_f$ were valid up to non-observable arbitrary phases. For charged decays, the amplitudes $\bar{\mathcal{A}}_f\,, \mathcal{A}_{\bar{f}}$ are obviously zero due to charge conservation. Neutral mesons have the property that they can mix with their anti-particles, so all four amplitudes are non-vanishing. While mixing is abesent on tree level in the SM, because flavour changing neutral currents are forbidden, it proceeds via box diagrams as shown in figure 2.5. At this

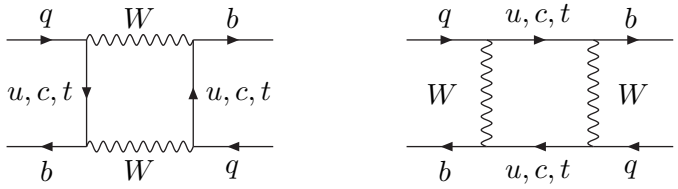


**Figure 2.5:** Box diagrams contributing to $B_q^0$–$\bar{B}_q^0$ mixing ($q \in \{d, s\}$). Figure taken from [42].

point, the GIM mechanism becomes relevant again: the corresponding diagrams can be written without calculation in the following form (taking $B_d$ mixing as an

example):

$$A_{mix} \sim \sum_{q,q'=u,c,t} V_{qb}^* V_{qd} f(q) V_{q'b}^* V_{q'd} f(q')\,. \tag{2.48}$$

Since $V_{CKM}$ is unitary, every contribution common to all intermediate states ($f(q) \to f$) vanishes by $\sum_{q=u,c,t} V_{qb}^* V_{qd} = (V^\dagger V)_{31} = 0$. The only contribution, for which this is not the case, is the one containing the quark masses. This implies for example a strong suppression of $D$- with respect to $K$- and $B$-mixing, due to the smaller mass differences in the down quark sector. In general the order of magnitude of mixing effects can be derived from this and the CKM structure of the corresponding mixing amplitude, while quantitative statements need non-perturbative input.

In order to describe the mixing only, one can employ the *Wigner-Weisskopf-formalism* [52, 53], as long as the characteristic time interval relevant to the process is much larger than the one relevant for strong interactions, which is the case here. In that formalism, the time-evolution can be described by a Schrödinger equation with the effective $2 \times 2$-hamiltonian

$$\mathcal{H} = M - \frac{i}{2}\Gamma \quad (M^\dagger = M, \Gamma^\dagger = \Gamma)\,, \tag{2.49}$$

with the decay width $\Gamma$ leading to the decay of the system and therefore to a non-hermitian hamiltonian. Assuming CPT symmetry, $M_{11} = M_{22} =: M_0$ and $\Gamma_{11} = \Gamma_{22} =: \Gamma_0$ hold. Solving the corresponding eigensystem leads to eigentstates

$$|B_{L,H}\rangle = p|B^0\rangle \pm q|\bar{B}^0\rangle\,, \tag{2.50}$$

for which the mass and width difference are given by

$$\Delta M := M_H - M_L = 2|M_{12}| > 0\,, \quad \Delta\Gamma := \Gamma_H - \Gamma_L = \frac{4\mathrm{Re}(M_{12}\Gamma_{12}^*)}{\Delta M}\,. \tag{2.51}$$

Restricting oneself to CP eigenstates as final states ($\mathrm{CP}|f\rangle = \eta_{\mathrm{CP}}|f\rangle$) leads to the following expressions for the time-dependent CP asymmetry:

$$\begin{aligned} a_{\mathrm{CP}}(t) &:= \frac{\Gamma(\bar{B}(t) \to f) - \Gamma(B(t) \to f)}{\Gamma(\bar{B}(t) \to f) + \Gamma(B(t) \to f)} \\ &= \left[\frac{A_{\mathrm{CP}}^{dir}(B \to f)\,\cos(\Delta M\, t) + S_{\mathrm{CP}}(B \to f)\,\sin(\Delta M\, t)}{\cosh\left(\Delta\Gamma\, t/2\right) - A_{\Delta\Gamma}\left(B \to f\right)\,\sinh\left(\Delta\Gamma\, t/2\right)}\right]\,, \end{aligned} \tag{2.52}$$

where the coefficients usually referred to as *direct* and *indirect* CP violation are given by

$$A_{\mathrm{CP}}^{dir}(B \to f) := -\frac{1 - |\xi|^2}{1 + |\xi|^2}\,, \quad S_{\mathrm{CP}}(B \to f) = \frac{2\mathrm{Im}\,\xi}{1 + |\xi|^2}\,, \tag{2.53}$$

with

$$\xi := \frac{q}{p}\frac{\bar{\mathcal{A}}_f}{\mathcal{A}_f}\,. \tag{2.54}$$

Finally the remaining coefficient is given by

$$A_{\Delta\Gamma}\,(B \to f) = \frac{2\mathrm{Re}\xi}{1+|\xi|^2}\,, \tag{2.55}$$

but is not an independent observable due to

$$A_{\mathrm{CP}}^{dir}(B \to f)^2 + S_{\mathrm{CP}}(B \to f)^2 + A_{\Delta\Gamma}(B \to f)^2 = 1\,. \tag{2.56}$$

Regarding the classification of CP violating effects, one usually distinguishes three effects:

- *CP violation in mixing*: Defined by $|q/p| \neq 1$, this implies different rates for $B \to \bar{B}$ and vice versa. In the SM, $|q/p| \sim 1$ holds to very good approximation; experimentally the upper limit for a deviation is of the order of a few per mille [54]:

  $$|q/p|_d = 1.0024 \pm 0.0023\,, \quad |q/p|_s = 0.9992 \pm 0.0042\,, \tag{2.57}$$

  so $|q/p| = 1$ will be assumed in the following.

- *CP violation in decay*: Independent of mixing, this is the only form of CP violation that can occur for charged particles. It is defined by $|\bar{\mathcal{A}}_{\bar{f}}/\mathcal{A}_f| \neq 1$, and is therefore equivalent to a non-vanishing coefficient $A_{\mathrm{CP}}^{dir}$ in equation (2.53). For $|q/p| = 1$, it is equal to the direct CP asymmetry. As $\bar{\mathcal{A}}_f$ and $\mathcal{A}_f$ differ only in the signs for the weak phases, the corresponding amplitude has to have two parts with a strong *and* weak phase difference for this coefficient to be non-vanishing.

- *CP violation in the interference of mixing and decay*: For this effect, it is sufficient to haveIm $\xi \neq 0$. It occurs with a non-trivial mixing phase, even if the strong phases in the decay amplitude vanish, and is usually expressed in terms of the coefficient $S_{\mathrm{CP}}$ in equation (2.53). The corresponding strong phase difference is generated by the time-evolution of the system. One important application is the case, in which one amplitude dominates the process, e.g. $B \to J/\psi K_S$, which will be discussed in detail later. In this case, the simple relation

  $$S_{\mathrm{CP}} = -\eta_{CP}\sin\phi \tag{2.58}$$

holds, where $\phi$ denotes the mixing phase and equals $\phi_d = 2\beta$ in $B_d$ decays in the SM.

### 2.2.4 Beyond the SM

As mentioned in the introduction to this section, one major puzzle in flavour physics today may be stated as the question, why the description of CP violation by the CKM mechanism works so well. Given the high precision in several flavour observables, for any generic extension of the SM at the TeV scale one would have expected a signal by now. This issue has to be adressed by any NP model in order for it to be viable. In most cases this is achieved by imposing additional symmetries, which forbid the "dangerous" operators leading to large observable effects, especially those inducing flavour changing neutral currents. One principle emerging from the apparent absence of new sources of flavour violation is called *minimal flavour violation* [55, 56]. It describes a class of models, in which the Yukawa matrices are in fact the only source of flavour violation, and govern the higher-dimensional interactions arising from NP as well, leading to a predictive framework. The possible operators are obtained by a spurion analysis, demanding formally the invariance of the hamiltonian under the flavour symmetry group[5]

$$G_F = SU(3)_{Q_L} \times SU(3)_{U_R} \times SU(3)_{D_R} \,. \tag{2.59}$$

Basically, this suppresses all NP contributions to processes which are suppressed in the SM, especially flavour changing neutral currents. In addition, all weak phases can be expressed by the one in the SM.

Matrix elements of NP operators are usually parametrized by their absolute value, and an unknown strong and weak phase. However, in general for each process several such contributions will occur, whose combination does not transform as a single contribution with respect to CP. However, as shown in [57], they can always be combined into *two* contributions with definite weak phases. As in many cases the experimental information does not suffice to include two unknown contributions, further assumptions are necessary. One option, used below, consists of assuming the dominance of contributions with one weak phase, corresponding either to the dominance of one NP operator or of several operators with the same weak phase. Another option, advocated in [58], consists of neglecting all strong phases in matrix elements of NP operators. This results in a combined

[5] Additional $U(1)$ symmetries are omitted here.

contribution with one effective weak phase and a strong phase difference to the SM contributions. The resulting parametrization is the same, but the interpretation of the results is different. One connected problem regarding possible new weak phases in general is the impossibility of identifying the new phase whithout fixing the hadronic matrix elements in the SM. This issue is discussed in the next section.

## 2.3 Reparametrization Invariance

As can be seen in section 2.2.3, the measurable observables are non-linear functions of the fundamental parameters one is interested in. Therefore the extraction of these parameters exhibits complications, even when the observables are known with good precision. One of the most obvious examples is the extraction of the angle $\beta$ from the time-dependent CP asymmetry in $B \to J/\psi K$. Even in an idealized scenario, where $S_{\mathrm{CP}} = -\sin 2\beta$ holds and vanishing experimental uncertainty is assumed, there is a fourfold ambiguity resulting from the fact that the whole set $\phi = \{\beta, \pi+\beta, \pi/2-\beta, 3\pi/2-\beta\}$ leads to the same value of $\sin 2\phi$. The measurement of $\cos 2\beta$, for example using $B \to J/\psi K^*$ [59], excludes two of the solutions, but only theoretical input on strong phases can resolve the last one [60]. While this is an example of a discrete invariance, there are also continuous transformations which leave all observables invariant. This observation is called *reparametrization invariance* (see e.g. [57, 61, 62]). Explicitly, as soon as a given isospin amplitude has contributions with two different phases, it can be written as

$$\mathcal{A} = \mathcal{A}_0(1 + re^{i\Delta\phi_s}e^{i\Delta\theta_W}), \tag{2.60}$$

where $A_0$ can be chosen to be real, and $re^{i\phi_s}e^{i\Delta\theta_W}$ parametrizes the second part of the amplitude, with the corresponding relative strong and weak phase. This expression is, however, invariant under the following reparametrization[6]:

$$\begin{aligned} \mathcal{A}_0' &= \mathcal{A}_0\left(1 + \xi\, r_0\, e^{i\Delta\phi_s}\right), \\ e^{i\Delta\theta_W'} &= \frac{e^{i\Delta\theta_W} - \xi}{\sqrt{1 - 2\,\xi\,\cos\Delta\theta_W + \xi^2}}, \\ r' e^{i\Delta\phi_s'} &= re^{i\Delta\phi_s}\frac{\sqrt{1 - 2\,\xi\,\cos\Delta\theta_W + \xi^2}}{1 + \xi r e^{i\Delta\phi_s}}, \end{aligned} \tag{2.61}$$

[6] There is no standard convention how to express this transformation. The expressions given here are the ones from [63].

with $\xi$ being an arbitrary real number.

The most important consequence of these equations is that the weak phase difference $\Delta\theta_W$ is in fact not an observable in these kinds of processes, as long as none of the other parameters is fixed in another way, for example calculated in QCDF. The points $\Delta\theta_W = 0, \pi$ cannot be reached with the transformation above, however. This reflects the obvious fact, that an amplitude with a single weak phase cannot be equivalent to one with two different phases.

When considering the SM or a specific NP scenario, the phase difference is obviously fixed from theory (e.g. in the SM to be $\gamma$), so other processes can be used in order to determine it, which, when used as an input, breaks the invariance. Therefore the hadronic matrix elements can be determined in this case. In addition, if one can find a process where the same quantities enter with a different weight, the invariance is broken as well. This is for example the case when considering amplitudes with different CKM structures, related by $U$-spin or $SU(3)$.

# Chapter 3

# Methods

This chapter introduces the tools which are used later in the different analyses. All of the analayses are carried out in an effective theory framework, therefore an introduction to effective field theories is given first. That section ends with introducing the SM weak effective hamiltonian and giving an idea of how to include NP effects. This framework leaves us with the necessity to find a method for determining the matrix elements of the effective operators. Two complementary methods are introduced, starting with QCDF, which uses the fact that $B$ meson decay amplitudes factorize in the heavy-quark limit to reduce these amplitudes to a set of basic non-perturbative objects, namely form factors, light-cone distribution amplitudes and decay constants. Large non-factorizable contributions render precise predictions in this framework difficult. Section 3.3 introduces therefore an alternative framework, which relates matrix elements using symmetry arguments. Here, the focus lies on $U$-spin related decays, whose precision in turn is severely limited by the relatively large strange quark mass. A framework is introduced, in which these effects are taken into account, performing an expansion in the stange quark mass over the chiral symmetry breaking scale. Finally, in section 3.4 the statistical approach RFit is introduced, which is used later for the quantitative analysis of present data.

## 3.1 Effective Field Theory for Weak Decays

Effective field theories (EFT) are a basic tool in theoretical physics. They are applicable whenever there are largely different scales $\Lambda_{1,2}$ with $\Lambda_2/\Lambda_1 \ll 1$ in a problem. In particle physics, these scales are typically expressed in terms of

energy[1]. Examples for applications are given in table 3.1.

| **EFT** | $\mathbf{\Lambda_1}$ | $\mathbf{\Lambda_2}$ |
|---|---|---|
| Chiral perturbation theory | $4\pi f_\pi \sim m_\rho$ | $E$ |
| Non-relativistic QCD (NRQCD) | $m_Q$ | $v^2 m_Q, v m_Q$ |
| Effective weak interactions | $M_W$ | $m_{b,c}$ |

**Table 3.1:** Examples for effective field theories and the relevant scales.

With a few exceptions, one of which is to be mentioned later, the *decoupling theorem* [64] ensures that the effects of the large scale vanish as $\Lambda_1 \to \infty$, i.e. that the corresponding series in $\Lambda_2/\Lambda_1$ converges. This reflects essentially the fact known from every-day experience, that in order to solve a problem at a certain level of detail, information of other detail levels are often not necessary. For example, in order for a chemist to make successful predictions for atomic reactions, he neither needs to know the quark structure of the nucleons nor the movement of the earth around the sun.

The advantages of the formalism developed in the present section are mainly the following:

- The computation in the effective theory is usually simpler than in the full theory, and sometimes even only feasible in the effective theory framework.

- Through the separation of the scales, the problem is divided in different parts, which can be worked at separately. In addition, usually different low energy problems are to be solved in a specific framework. Then the high-energy part can be calculated once and for all, leaving only the low-energy part to be calculated for each problem.

- If the high-energy theory or the transition to low energies is unknown, one might still identify possible low-energy operators using the known low-energy particle content, symmetries, and other known properties of that theory, treating the corresponding coefficients as unknowns to be determined by experiment (as done e.g. in chiral perturbation theory).

[1] Conventionally $\hbar = c = 1$, which implies $[E] = [p] = [m] = [x^{-1}] = [t^{-1}]$.

- In some cases, in the effective theory new symmetries appear, which were not there or not apparent in the full theory, and which allow additional predictions and calculations. A well-known expample are the two additional symmetries appearing in heavy-quark effective theory (HQET), namely the heavy flavour symmetry and the heavy-quark spin symmetry, both of which are absent in full QCD and help making model-independent predictions for heavy-quark systems.

- Still, at least for a known high-energy theory, using the effective theory framework seems not to be necessary at first sight. Actually, it *is* necessary when choosing a mass independent regularization scheme, and doing otherwise results in complications more severe than performing the calculation as described below. The reason, as explained in more detail in section 3.1.2, lies in the appearance of large logarithms of the form $\log\left(\frac{\Lambda_1}{\Lambda_2}\right)^2$, which spoil the power-counting in the perturbative series: $\alpha_s \log\left(\frac{\Lambda_1}{\Lambda_2}\right)^2 \sim 1$. These effects can be treated by means of the *renormalization group*, which allows to sum up at a given order $n$ all terms of the form $\alpha_s^n \left[\sum_{m=0}^{\infty}\left(\alpha_s \log\left(\frac{\Lambda_1}{\Lambda_2}\right)^2\right)^m\right]$.

Hand in hand with the development of effective field theories went a paradigm shift: while for some time only renormalizable theories were considered "good" theories in the sense of predictive ones, the picture now is that of a chain of effective theories, e.g.

$$\begin{aligned}\text{Fermi's theory} \;&—\; \text{Standard Model} — \text{SUSY (?)} — \text{String Theory (??)}\\ &—\; \text{M theory (???)} — (????)\ ,\end{aligned}$$

and it is a question of the desired precision of the calculation if higher dimensional operators are relevant. Each effective theory in that chain is predictive, because in the effective theory framework at each step in the expansion only a finite number of operators appear, and a finite number of insertions of them is necessary. As mentioned above, it is one of the strengths of this method, that in order to discuss one chain link it is not necessary to know the whole chain.

This section proceeds as follows: the first part consists of a description of the operator product expansion, the mathematical framework used in effective field theories. This is followed by introducing the concept of renormalization group improved perturbation theory in section 3.1.2. Finally, in section 3.1.3,

the framework is presented which forms the basis of all applications discussed later, namely the weak effective hamiltonian.

Again the following treatment is rather schematical; for a comprehensive overview see [65], where also all citations to the original literature can be found which are mostly omitted here. An introductory lecture on these topics is [66], and a text book treatment of these issues can be found in [67].

### 3.1.1 Operator Product Expansion in Weak Decays

Within the operator product expansion one performs an expansion of non-local operators containing the heavy degrees of freedom in terms of the small ratio $\Lambda_2/\Lambda_1$. This results in local operators of higher dimension, in which the heavy degrees of freedom have been removed. The expansion becomes possible, because the non-local lagrangian is *analytic* in the whole range of $\Lambda_2/\Lambda_1 < 1$. This is the mathematical expression for the intuitive fact that for a process which probes a theory at a certain energy — that is, with a certain resolution — effects of distances much smaller than the probed one are not visible and effects with much larger wavelenghts are constant.

To see how this works in some more detail, consider now the part of the generating functional containing the $W$ boson,

$$Z_W \sim \int [dW^+][dW^-] \exp\left[i \int d^4x \, \mathcal{L}_W\right] . \tag{3.1}$$

Here $\mathcal{L}_W$ is the corresponding part of the SM lagrangian,

$$\mathcal{L}_W = -\frac{1}{2}\left(\partial_\mu W^+_\nu - \partial_\nu W^+_\mu\right)\left(\partial^\mu W^{-\,\nu} - \partial^\nu W^{-\,\mu}\right) + M_W^2 W^+_\mu W^{-\,\mu} + \mathcal{L}_{cc}\,, \tag{3.2}$$

with $\mathcal{L}_{cc}$, already appearing in equation (2.20), including the interaction with the quark fields. As the aim is to deal with $B$ meson decays, no $W$ bosons are appearing in the initial or final state, so a corresponding source is not necessary[2]. After "quadratic enhancement" in the exponent, this functional integral takes a gaussian form and can be explicitly performed, resulting in

$$Z_W \sim \exp\left[-i \int d^4x d^4y \left\{\frac{g_2^2}{2} J^-_\mu(x) \Delta^{\mu\nu}(x,y) J^+_\nu(y)\right\}\right] , \tag{3.3}$$

[2]This is to be contrasted with the situation in HQET, where the heavy quark, which is to be integrated out there, is part of at least the initial state and remains in the theory as a static source of flavour.

where $\Delta^{\mu\nu}(x,y)$ denotes the $W$ propagator. The action for the quarks including one $W$ boson exchange becomes therefore

$$\mathcal{S}_q = \int d^4x \left\{ \mathcal{L}_{kin} - \frac{g_2^2}{2} \int d^4y \left[ J_\mu^-(x) \Delta^{\mu\nu}(x,y) J_\nu^+(y) \right] \right\} , \tag{3.4}$$

with a non-local interaction term. The key observation is now, that, up to this point, the expression is *exact* (with only one insertion considered and no external $W$ fields) — therefore the expansion of this expression in $k^2/M_W^2$ to all orders is equivalent to the full theory. Truncating the series yields a systematic approximation to it, with the first term reading

$$\Delta^{\mu\nu}(x,y) = \frac{g^{\mu\nu}}{M_W^2} \delta^{(4)}(x-y) + \mathcal{O}\left( \frac{k^2}{M_W^4} \right) . \tag{3.5}$$

This removes the $W$ boson as dynamical degree of freedom, giving the well known *local* interaction term ($V = V_{CKM}$ in the following)

$$\mathcal{L}_{int} = -\frac{4G_F}{\sqrt{2}} V_{ij}^* V_{i'j'} (\bar{d}_L^j u_L^i)(\bar{u}_L^{i'} d_L^{j'}) =: -\frac{4G_F}{\sqrt{2}} V_{ij}^* V_{i'j'} \mathcal{O}_2^{iji'j'} , \tag{3.6}$$

which is the gerneralized version of Fermi's four fermion interaction in a modern language. This is the desired result concerning the expansion in the inverse $W$ boson mass, because the corresponding expansion parameter is exceedingly small. However, strong interaction corrections from above the scale $\mu$ need to be taken into account for a reasonable precision. As the relevant scale is at least of the order of the $b$ quark mass, this can be done in a perturbative framework, thanks to asymptotic freedom.

In order to include these effects, first thing to note is that loop effects induce new operator structures, due to (a) colour exchange by gluons, (b) the fact that the gluon does not distinguish the $(V-A)$ from $(V+A)$ structure, and (c) the difference of the $Z, \gamma$ couplings to the gluon ones. The good news is, that all these effects are calculable. The calculation, which again is only sketched in the following, results in the following structure: the effective hamiltonian is represented as

$$\mathcal{H}_{\text{eff}} = \sum_i C_i(\mu) \mathcal{O}_i , \tag{3.7}$$

whith the effective operators $\mathcal{O}_i$ forming the extended operator basis, and the *Wilson coefficients* $C_i(\mu)$ as effective coupling constants. The information on the high-energy behaviour of the theory is encoded in the Wilson coefficients, which

are therefore in general non-trivial functions of the corresponding parameters, i.e. $M_{W,Z}, m_t$ in case of the SM. In addition, they depend on $\alpha_s$ and $\mu$. For the hadronic amplitudes of interest follows

$$A \sim \sum_i C_i(\mu)\langle \mathcal{O}_i \rangle(\mu)\,, \tag{3.8}$$

where the matrix elements of the effective operators depend only on the properties of the theory below $\mu$ — the problem has been *factorized* in a high- and low-energy part. Importantly, as indicated in the formula, these matrix elements depend on the scale $\mu$; because this scale is arbitrary, the physical amplitudes cannot depend on it, so the dependence of the matrix elements has to cancel that of the Wilson coefficients. As the series is truncated in $\alpha_s$, a residual scale dependence of the neglected order remains, which is often taken as an estimate of the uncertainty introduced by the truncation. These issues are discussed further in section 3.1.2.

When the high-energy theory is known, as is the case in the present calculation, one is able to determine the operator basis and calculate the corresponding Wilson coefficients explicitly. This is done by requiring that at each scale where a heavy degree of freedom is removed, the amplitudes in the full and effective theory are equal. This procedure is called *matching* the full theory on the effective theory (or one effective theory on another for the chain picture). Importantly, as this procedure involves only the high-energy part of the theory, it is universal, that is, especially independent of the hadronic initial and final states. For that reason, this calculation can be performed by considering artificial amputated Green functions, which involve only the corresponding quark transition instead of a transition between hadrons.

As the simplest example, consider the one loop diagrams of the current-current diagram depicted in figure 3.1: while the corresponding tree diagram is matched on the operator $\mathcal{O}_2$ as described above, diagrams (b) and (c) introduce a new colour structure. Therefore the operator basis is enhanced to

$$\mathcal{H}_{\text{eff}}^{cc}(\bar{d}_L^j \to \bar{u}_L^i u_L^{i'} \bar{d}_L^{j'}) \sim C_1(\mu)\mathcal{O}_1^{iji'j'} + C_2(\mu)\mathcal{O}_2^{iji'j'}\,, \tag{3.9}$$

with the operator $\mathcal{O}_1^{iji'j'} = (\bar{d}_{L,a}^j u_{L,b}^i)(\bar{u}_{L,b}^{i'} d_{L,a}^{j'})$, where $a, b$ are colour indices, assumed to be equal within brackets before. For the matching, one has to compute the corresponding one loop diagrams in the effective theory, as shown in figure 3.2.

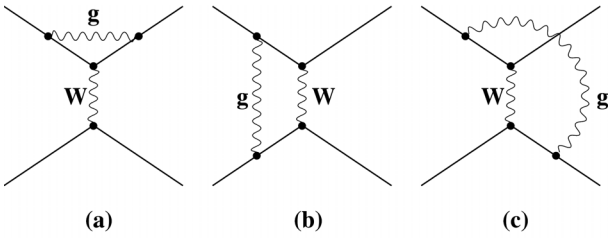


**Figure 3.1:** Examples for one loop diagrams in the SM, i.e. the full theory, making the extension of the operator basis necessary. Figure taken from [65].

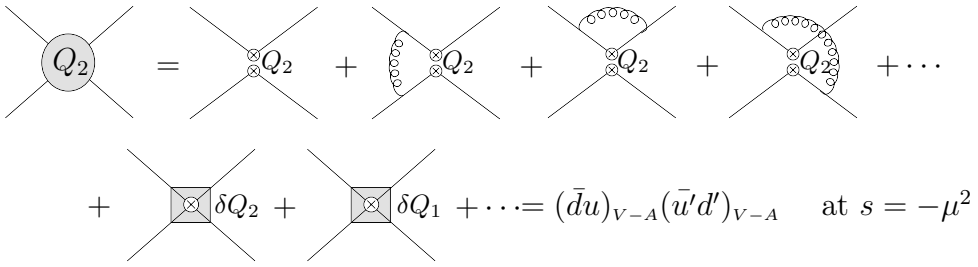


**Figure 3.2:** Contributions to the renormalization of the operator $\mathcal{O}_2$ in the effective theory. The divergencies of the full theory cancel in the first line. For the new divergencies *both* the counterterms for $\mathcal{O}_{1,2}$ are needed, as a consequence of operator mixing. Figure taken from [68].

However, after using renormalized fields and couplings, these diagrams still contain divergencies. This leads to the necessity to renormalize the couplings $C_i$, which allows to remove the infinite parts; this is also known as *operator renormalization*. As a new aspect, the renormalization of e.g. the operator $\mathcal{O}_2$ involves also counterterms proportional to $\mathcal{O}_1$ (and vice versa) — the operators *mix* with each other, that is, their scale dependence becomes correlated. Explicitly, the calculation yields [65]

$$\begin{aligned} C_1(\mu) &= -3\frac{\alpha_s(\mu)}{4\pi}\ln\frac{M_W^2}{\mu^2} + \mathcal{O}(\alpha_s^2)\,, \\ C_2(\mu) &= 1 + 3\frac{\alpha_s(\mu)}{4\pi}\ln\frac{M_W^2}{\mu^2} + \mathcal{O}(\alpha_s^2)\,. \end{aligned} \tag{3.10}$$

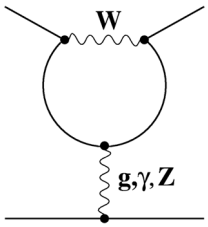


**Figure 3.3:** Example for a penguin diagram, possible for $i = i'$, as explained in the text. Figure taken from [65].

While equation (3.9) gives the full hamiltonian for $i \neq i'$, the operator basis is larger for $i = i'$, especially when including electroweak corrections. The additional operators, $\mathcal{O}_{3\ldots6}$ and $\mathcal{O}_{7\ldots10}$, are called *penguin* and *electroweak penguin* operators respectively; they originate from diagrams as depicted in figure 3.3.

When including the full basis, the calculation becomes a lot more involved, but the calculation does not change in principle. The results of the corresponding calculations, performed at next to leading order (NLO) with corresponding additional complications, are collected in [65] and its results are given in the last subsection. Before turning to that, the concept of renormalization group (RG) improved perturbation theory is introduced in this context.

### 3.1.2 RG improved Perturbation Theory

In equation (3.10) one problem becomes obvious which was mentioned before: the expansion parameter is multiplied by large logarithmic terms, spoiling the perturbative expansion. Therefore the expansion has to be reorganized, counting $\frac{\alpha_s(\mu)}{\pi} \sim 0.1$, while $\frac{\alpha_s(\mu)}{\pi} \ln \frac{M_W^2}{\mu^2} \sim 1$, leading to an expansion of the form

$$\begin{aligned}
\text{LL } (\mathcal{O}(\alpha_s^0)): &\quad \sum_n k_n^{(0)} \left(\frac{\alpha_s(\mu)}{\pi} \ln \frac{M_W^2}{\mu^2}\right)^n \\
\text{NLL } (\mathcal{O}(\alpha_s^1)): &\quad \frac{\alpha_s}{\pi} \sum_n k_n^{(1)} \left(\frac{\alpha_s(\mu)}{\pi} \ln \frac{M_W^2}{\mu^2}\right)^n \\
\text{NNLL } (\mathcal{O}(\alpha_s^2)): &\quad \left(\frac{\alpha_s}{\pi}\right)^2 \sum_n k_n^{(2)} \left(\frac{\alpha_s(\mu)}{\pi} \ln \frac{M_W^2}{\mu^2}\right)^n \\
\ldots &\quad \ldots
\end{aligned} \tag{3.11}$$

extending the sums to all orders. The orders are denoted as "leading logarithmic approximation" (LL), "next-to-leading logarithmic approximation" (NLL) and so on. The resummation of these terms is achieved by using the renormalization group. This is shown below, following the presentation given in [66].

Starting point is the observation, that because the scale $\mu$ is unphysical, the physical amplitudes cannot depend on it. Given a set of linearly independent operators $\{\mathcal{O}_i\}$ which closes under renormalization (that is, it forms a basis for the problem given), this implies

$$\frac{d}{d\ln\mu}\sum_i C_i(\mu)\langle\mathcal{O}_i\rangle(\mu) = 0\,, \tag{3.12}$$

where the logarithmic derivative has been chosen for convenience. $\{\mathcal{O}_i\}$ forming a basis,

$$\frac{d}{d\ln\mu}\langle\mathcal{O}_i\rangle(\mu) = -\sum_j \gamma_{ij}(\mu)\langle\mathcal{O}_j\rangle(\mu) \tag{3.13}$$

holds, where the *anomalous dimension* $\gamma$ has been introduced. Without operator mixing, $\gamma_{ij} = \gamma_i\delta_{ij}$, while in general $\gamma$ represents a non-diagonal matrix. For the case discussed before with only $\mathcal{O}_{1,2}$ present it is at one-loop order given by

$$\gamma(\alpha_s) = \frac{\alpha_s}{4\pi}\begin{pmatrix} -6/N & 6 \\ 6 & -6/N \end{pmatrix}. \tag{3.14}$$

Inserting equation (3.13) in (3.12) yields

$$\sum_i \left\{\frac{d}{d\ln\mu}C_i(\mu) - \sum_j C_j(\mu)\gamma_{ji}(\mu)\right\}\langle\mathcal{O}_i\rangle(\mu) = 0\,, \tag{3.15}$$

which, because of the assumed independence of the $\mathcal{O}_i$ , translates into

$$\frac{d}{d\ln\mu}C_i(\mu) - \sum_j C_j(\mu)\gamma_{ji}(\mu) = 0\,. \tag{3.16}$$

Observing finally that $\gamma(\mu) = \gamma(\alpha_s(\mu))$, i.e. that the anomalous dimension depends on the scale only through the coupling constant, and collecting the Wilson coefficients in the vector $\mathbf{C}$ yields

$$\frac{d}{d\alpha_s(\mu)}\mathbf{C}(\mu) - \frac{\gamma^T(\alpha_s(\mu))}{\beta(\alpha_s(\mu))}\mathbf{C}(\mu) = \mathbf{0}\,, \tag{3.17}$$

where $\beta(\alpha_s(\mu))$ denotes the usual QCD beta function, defined by

$$\frac{d}{d\ln\mu}\alpha_s(\mu) = \beta(\alpha_s(\mu))\,. \tag{3.18}$$

The equation can be integrated, with a possible complication arising due to $[\gamma(\mu), \gamma(\mu')] \neq 0$.

To see that this sums the large logarithms, consider the simplest case, where only one operator is present: Expanding all terms in the equation to leading order in $\alpha_s$,

$$\gamma(\alpha_s) \approx \gamma_0 \frac{\alpha_s}{4\pi}\,, \quad \beta(\alpha_s) \approx -2\alpha_s\beta_0 \frac{\alpha_s}{4\pi}\,, \quad C(M_W) \approx 1\,, \tag{3.19}$$

yields

$$C_{LL}(\mu) = \left(\frac{\alpha_s(\mu)}{\alpha_s(M_W)}\right)^{-\frac{\gamma_0}{2\beta_0}}\,. \tag{3.20}$$

Using then

$$\frac{\alpha_s(\mu)}{\alpha_s(M_W)} \approx 1 + \beta_0 \frac{\alpha_s(M_W)}{4\pi} \ln\frac{M_W^2}{\mu^2} \tag{3.21}$$

results in

$$C_{LL}(\mu) = 1 - \frac{\gamma_0}{2}\frac{\alpha_s(M_W)}{4\pi}\ln\frac{M_W^2}{\mu^2} + \mathcal{O}\left(\frac{\alpha_s^2}{\pi^2}\ln^2\frac{M_W^2}{\mu^2}\right)\,, \tag{3.22}$$

showing the structure (3.11). However, in this case obviously also the resummed result for $\alpha_s$ should be used, which is (again at one-loop order)

$$\frac{\alpha_s(\mu)}{\alpha_s(M_W)} = \frac{1}{1 - \beta_0 \frac{\alpha_s(M_W)}{4\pi}\ln\frac{M_W^2}{\mu^2}}\,. \tag{3.23}$$

Including operator mixing, the solution is obtained by diagonalizing $\gamma$ at the matching scale, evolving the eigenvectors $\tilde{\mathbf{C}}(\mu)$, whose renormalization is just multiplicatively, and changing back to the basis $\mathbf{C}(\mu)$. Again, all details can be found in [65].

### 3.1.3 The SM Weak Effective Hamiltonian

The last subsections introduced the necessary ingredients for the calculation of the effective hamiltonian relevant for $B$ decays. In the following, it is referred to

$b \to D$ transitions, with $D = d, s$ and $\Delta C = 0$. The operator basis is chosen as[3]

$$\begin{aligned}
\mathcal{O}_1^q &= (\bar{q}_i b_j)_{V-A} (\bar{D}_i q_j)_{V-A}\,, & \mathcal{O}_2^q &= (\bar{q}_i b_i)_{V-A} (\bar{D}_j q_j)_{V-A}\,,\\
\mathcal{O}_3 &= (\bar{D}_i b_i)_{V-A} \sum_q (\bar{q}_i q_i)_{V-A}\,, & \mathcal{O}_4 &= (\bar{D}_i b_j)_{V-A} \sum_q (\bar{q}_j q_i)_{V-A}\,,\\
\mathcal{O}_5 &= (\bar{D}_i b_i)_{V-A} \sum_q (\bar{q}_i q_i)_{V+A}\,, & \mathcal{O}_6 &= (\bar{D}_i b_j)_{V-A} \sum_q (\bar{q}_j q_i)_{V+A}\,,\\
\mathcal{O}_7 &= \frac{3}{2}(\bar{D}_i b_i)_{V-A} \sum_q e_q (\bar{q}_i q_i)_{V+A}\,, & \mathcal{O}_8 &= \frac{3}{2}(\bar{D}_i b_j)_{V-A} \sum_q e_q (\bar{q}_j q_i)_{V+A}\,,\\
\mathcal{O}_9 &= \frac{3}{2}(\bar{D}_i b_i)_{V-A} \sum_q e_q (\bar{q}_i q_i)_{V-A}\,, & \mathcal{O}_{10} &= \frac{3}{2}(\bar{D}_i b_j)_{V-A} \sum_q e_q (\bar{q}_j q_i)_{V-A}\,,
\end{aligned} \tag{3.24}$$

where $i, j$ are colour indices, and $V \pm A$ refer to the projectors $(1 \pm \gamma_5)/2$. Using the input values listed in table 3.2, and the powercounting for the evolution as described in [69], the result for the coefficients at one exemplary scale is given in table 3.3. For this work, however, mainly the corresponding orders of magnitude are relevant, which are taken to be

$$C_{1,2} \sim 1\,, \quad C_{3\ldots6} \sim \lambda\,, \text{ and } C_{7\ldots10} \sim \lambda^2\,. \tag{3.25}$$

| Quantity | Value |
|---|---|
| $M_W$ | $(80.403 \pm 0.029)$ GeV |
| $M_Z$ | $(91.1876 \pm 0.0021)$ GeV |
| $\bar{m}_t(m_t)$ | $(164.6 \pm 2.7)$ GeV |
| $\sin^2(\theta_W)$ | 0.23122 |
| $\alpha$ | 1/129 |
| $\alpha_s(M_Z)$ | 0.1176 |
| $\mu_b$ | 4.2 GeV |

**Table 3.2:** Input quantities from [35] for the reevaluation of the Wilson coefficients.

[3]Note that [66,69,70] use another notation, with $\mathcal{O}_{1,2}$ exchanged. In addition, the operators differ by a factor of 4 to those in [65,69,70], because there the subscripts $V \mp A$ refer to $1 \mp \gamma_5$.

| $C_1$ | $C_2$ | $C_3$ | $C_4$ | $C_5$ | $C_6$ |
|---|---|---|---|---|---|
| -0.189 | 1.081 | 0.014 | -0.035 | 0.010 | -0.042 |
| $C_7/\alpha$ | $C_8/\alpha$ | $C_9/\alpha$ | $C_{10}/\alpha$ | | |
| $-0.015$ | 0.058 | $-1.225$ | 0.203 | | |

**Table 3.3:** Wilson coefficients at $\mu = 4.2$ GeV, evaluated at NLO, using the inputs from table 3.2.

Putting now all ingredients together, the effective hamiltonian for charmless B decays ($b \to D, D \in \{d, s\}$) is given as

$$\mathcal{H}_{\text{eff}}^{b\to D} = \frac{4G_F}{\sqrt{2}} \left[ \sum_{i=1,2} \sum_{q=u,c} \lambda_{qD} C_i \mathcal{O}_i^q - \sum_{i=3}^{10} \lambda_{tD} C_i \mathcal{O}_i \right] . \tag{3.26}$$

Note that usually the unitarity relation

$$\sum_q \lambda_{qD} = 0 \tag{3.27}$$

is used, in order to eliminate one of the CKM factors. In the applications below, $\lambda_{tD}$ is replaced.

One interesting point to note concerns the matching conditions for the penguin operators. Exemplarily,

$$C_4(M_W) = C_6(M_W) = \frac{1}{2}\tilde{E}_0(x)\frac{\alpha_s(M_W)}{4\pi}\,, \quad C_7(M_W) = \frac{3}{2}f(x)\frac{\alpha_s(M_W)}{4\pi}\,, \tag{3.28}$$

where

$$x = \frac{m_t^2}{M_W^2}\,, \quad \tilde{E}_0(x) = -\frac{7}{12} + \mathcal{O}(1/x)\,, \text{ and } f(x) = \frac{x}{2} + \frac{3}{3}\ln x + \mathcal{O}(1/x)\,. \tag{3.29}$$

Contrary to the expectation from the decoupling theorem, they do not vanish in the limit $m_t \to \infty$, and in case of the electroweak penguins they even grow with growing top mass. The reason is that removing the top quark from the theory violates gauge symmetry, which in turn spoils renormalizability — which is a condition for the theorem to hold. This in turn implies, that electroweak penguins are phenomenologically relevant in some decays (e.g. $B \to \pi K$), despite their tiny couplings.

Given the picture developed above of the SM as the renormalizable part of an effective theory, the question arises how to go beyond the SM in a model-independent way. As noted above already, in principle it is obvious how to do this: analogously to $\chi PT$, one has to identify the possible operators compatible with the SM symmetries, multiply them with unknown coupling constants and determine these using experimental information. The operators have been identified some time ago [71], however, it turns out that the number of coupling constants is huge, even when considering only those operators relevant for quark flavour changing processes. This renders a completely general analysis impossible. One possible assumption leading to a predictive framework has already been sketched in section 2.2.4, namely minimal flavour violation. Another possibility is to use family symmetries (for basic papers, see e.g. [72–74]), which explain the hierarchies observed in the fermion masses and mixings as a result of symmetry breaking. These issues are not discussed further in the following, instead the assumption described in section 2.2.4 is used.

The formalism presented in this section forms the basis of the applications given in chapter 4. This chapter proceeds by introducing some more concepts relevant in this context and used later, beginning with the method of QCDF.

## 3.2 QCD Factorization

An open problem remains the calculation of the matrix elements of the effective operators. One step in that direction has been the observation that the matrix elements *factorize* in the heavy-quark limit. The physical picture beyond this statement is the following: Consider for example the decay $B^- \to D^0 K^-$ in the $B$ meson rest frame. The $c$ quark produced in the decay is relatively heavy and therefore slow, and will combine easily with the slow spectator quark to form the $D$ meson. The light quark pair, on the other hand, is energetic and in a colour singlet mode, so it will leave the interaction region fast and probably without a strong interaction. Therefore, the process factorizes into a $B \to D$ subprocess and the emission of the kaon. This is Bjorken's argument of *colour-transperancy* [75]. This picture led in a first step to an approach known as *naive factorization*, where hadronic matrix elements of products of currents are expressed schematically as

$$\langle M_1 M_2 | (b\bar{q}_1)(q_2\bar{q}_3) | B \rangle \to \langle M_1 | (b\bar{q}_1) | B \rangle \langle M_2 | (q_2\bar{q}_3) | 0 \rangle \sim F^{B\to M_1} f_{M_2} \,, \qquad (3.30)$$

possibly plus ($M_1 \leftrightarrow M_2$) and Fierz transformed operator combinations.

However, it is easily seen that this cannot be correct: in this form, the matrix element is expressed in terms of observable quantities and therefore does not contain any scale nor renormalization scheme dependence. This, however, is necessary to cancel those from the Wilson coefficients, as mentioned before. Therefore the above equation cannot hold beyond tree level. In addition, it is not obvious why the argument should hold for charmless decays, where all emitted quarks are enegeretic, or for colour octet intermediate states. A solution for these problems has been provided with the QCDF approach [69,70,76], where the physical picture described above enters a systematic expansion in $\alpha_s$ and $\Lambda_{QCD}/m_b$, to be described in the following.

The central statement in QCDF can be expressed through two formulas, illustrated in figure 3.4. Representing the final state meson which contains the $B$ meson spectator quark as $M_1$, they read

$$\langle M_1 M_2|\mathcal{O}_i|\bar{B}\rangle = \sum_j F_j^{B\to M_1}(m_2^2) \int_0^1 du\, T_{ij}^I(u)\, \Phi_{M_2}(u)\,, \tag{3.31}$$

for the case where $M_1$ is a heavy meson and

$$\begin{aligned}\langle M_1 M_2|\mathcal{O}_i|\bar{B}\rangle \;=\; & \sum_j F_j^{B\to M_1}(m_2^2) \int_0^1 du\, T_{ij}^I(u)\, \Phi_{M_2}(u) \;+\; (M_1 \leftrightarrow M_2) + \\ & \int_0^1 d\xi du dv\, T_i^{II}(\xi,u,v)\, \Phi_B(\xi)\, \Phi_{M_1}(v)\, \Phi_{M_2}(u)\end{aligned} \tag{3.32}$$

if $M_{1,2}$ are both light. Here $T_{ij}^{I,II}(u(,\xi,v))$ denote hard-scattering functions which are perturbatively calculable, the $\Phi_M(u)$ are light-cone distribution amplitudes (LCDA), and $u, v, \xi$ are longitudinal momentum fractions. These equations hold to leading order in $\Lambda_{QCD}/m_b$, but to all orders in $\alpha_s$. In [69, 70, 76] the hard-scattering kernels are calculated at NLO; recently NNLO accuracy has been achieved [77–83].

In the case of a heavy-light final state, equation (3.31) mainly reflects the physical picture described above, taking into account possible hard gluon exchanges and describing with the LCDA the probability of hadronization of the given quark pair for a certain momentum configuration. In this case, the second process depicted in figure 3.4 is power-suppressed. If the final state consists of two light mesons, it becomes relevant: it describes processes where the spectator quark participates, as in hard spectator scattering and annihilation processes (which

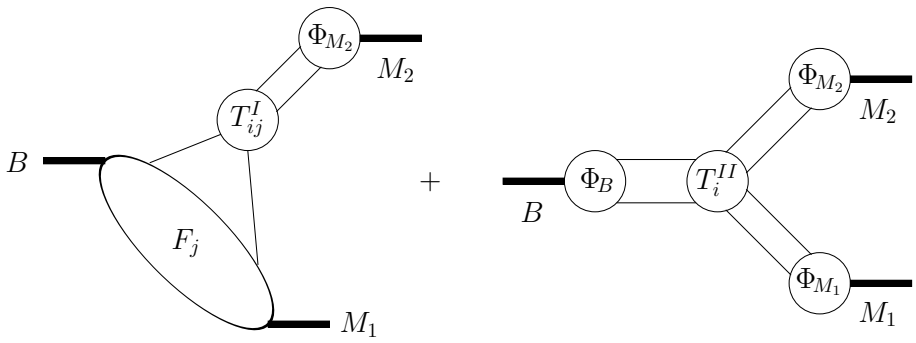


**Figure 3.4:** Illustration of the factorization formulas (3.31,3.32), as described in the text. Figure taken from [69].

are formally power-suppressed, see below); this leads to the explicit appearance of the $B$ meson LCDA. For factorization to hold, these processes must be sufficiently suppressed when soft gluons are involved. This is indeed the case [69], as the leading soft contributions cancel due to colour-transperancy and the subleading contributions are power-suppressed due to the behaviour of the LCDAs for these momentum configurations. Several more comments are in order:

- In the heavy-quark limit, factorization achieves a reduction of the full hadronic amplitude to a few, still non-perturbative objects, which have to be calculated by means of non-perturbative methods, such as light-cone sum rules or lattice QCD, or taken from experiment. However, the progress afforded by this method is nevertheless enormous: The remaining objects, namely LCDAs, form factors and decay constants, have a much simpler structure, depending on at most two mesons. For these, the calculation with non-perturbative methods is gernerally possible, in contrast to the full matrix elements. In addition, they are universal, so even if they could not be calculated, they can be determined by independent measurements.

- The LCDAs describe the distribution of quarks within hadrons, depending on the longitudinal momentum fraction and the renormalization scale. For the relatively simple case of the lowest Fock state for a meson (i.e. $(\bar{q}q')$) they can be defined using the following bi-local matrix element (for

definiteness, the pion is chosen):

$$\langle \pi(p)|\bar{u}(x)\gamma_\mu\gamma_5[x,-x]d(-x)|0\rangle|_{x^2=0} =: -ip_\mu f_\pi \int_0^1 du\, e^{ipx(u-\bar{u})}\Phi_\pi(u,\mu)\,, \tag{3.33}$$

where $[-x,x]$ represents a path-ordered gauge factor to render the expression gauge invariant, and $\bar{u}=1-u$. This definition corresponds to

$$\Phi_\pi(u,\mu) = \int \frac{d^2k_\perp}{16\pi^3}\Psi^{(\mu)}_{q\bar{q},\pi}(u,\mathbf{k}_\perp)\,, \tag{3.34}$$

that is, the LCDA equals the corresponding wave function integrated over the transverse momentum components. The leading twist amplitude in the asymptotic limit, corresponding to the renormalization scale set to infinity, then is given by

$$\Phi_M^{\text{asym}}(u) = 6u\bar{u}\,, \tag{3.35}$$

leading to the normalization $\int_0^1 du\Phi_M^{\text{asym}}(u) = 1$. For finite values of the renormalization scale, LCDAs are expanded in terms of Gegenbauer moments,

$$\Phi_M(u,\mu) = 6u\bar{u}\left[1+\sum_{i=1}^{\infty}\alpha_i^M(\mu)C_i^{(3/2)}(u-\bar{u})\right], \tag{3.36}$$

with $C_i^{(3/2)}(u)$ denoting the Gegenbauer polynomials and $\alpha_i^M(\mu)$ the Gegenbauer moments. This expansion is usually truncated after the second term in the sum. Higher Fock states are power-suppressed in the heavy-quark limit, and so are higher twist contributions. However, chirally enhanced two-particle twist-3 contributions are taken into account, see below.

- At leading order ($\alpha_s^0$), $T_{ij}^{II}(\xi,u,v)$ vanishes, and $T_{ij}^I(u) = T_{ij}^I$ becomes independent of $u$. The integrals are then evaluated trivially to give the corresponding decay constants, so in this limit naive factorization is recovered.

- Factorization does not hold if the emitted meson is heavy, as for example in $B^- \to \pi^0 D^-$. For quarkonia, it does hold formally, because quarkonia are relatively small. "Formally", because this holds only in the formal heavy-quark limit $m_b, m_c \to \infty$: the size of charmonium is actually proportional to $1/(\alpha_s m_c)$, which clearly does not allow for the approximation $r_{c\bar{c}} \ll 1/\Lambda_{QCD}$. Therefore, in practice QCDF is not expected to work well in this case. In addition, power-suppressed corrections are expected to be

larger ($\mathcal{O}(\Lambda_{QCD}/(\alpha_s m_b))$). Finally, in the important case of $B \to J/\psi K$, the leading order amplitude is colour suppressed, therefore the relative importance of the power-suppressed terms is increased additionally. For these reasons, the results for $B \to J/\psi K$ in QCDF will not be used in this work.

- Even if factorization is applicable, problems appear with some *chirally enhanced* terms: these are terms, which are formally of order $\Lambda_{QCD}/m_b$, but are numerically large. This results from the large value of the quark condensate, as appearing in

$$2\mu_\pi := \frac{2m_\pi^2}{m_d + m_d} = -4\frac{\langle q\bar{q}\rangle}{f_\pi^2} \sim 3 \text{ GeV} \gg \Lambda_{QCD}\,. \tag{3.37}$$

  As they are formally power-suppressed, factorization no longer holds, which is signalled by appearing divergencies related to the fact that the asymptotic twist-3 LCDAs do not vanish at the endpoints. At the moment, there is no known method for calculating these divergencies model-independently. The model-dependent treatment advertised in [69, 70, 76] leads in many cases to relatively large uncertainties.

In the following, the resulting structure for the hadronic amplitudes is discussed in some more detail, however, the discussion remains qualitative. For details of the calculation and references, see again [69, 70, 76].

Relevant NLO contributions are shown in figure 3.5. They are usually categorized as vertex corrections, penguin diagrams and hard spectator interactions. While the first two categories contribute to $T_{ij}^I(u)$, the last one is the only contribution to $T_{ij}^{II}(u)$ which is not formally power-suppressed. They all include chirally enhanced contributions. Additionally, enhanced annihilation diagrams arise which are not shown. Qualitatively, the following picture emerges:

- **Vertex corrections:** These corrections are one source for imaginary parts at $\mathcal{O}(\alpha_s)$. There exist chirally enhanced contributions which are finite. The factorizable diagrams contributing to the form factor are not shown.

- **Penguin diagrams:** Again the diagrams contain no divergencies, even the formally power-suppressed parts are finite. The imaginary parts arising from these contributions correspond basically to the *Bander-Silverman-Soni-mechanism* [84], and lead again to strong phases of $\mathcal{O}(\alpha_s)$.

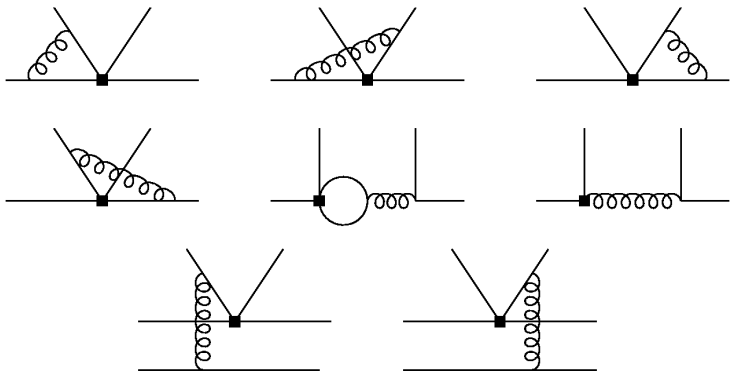

**Figure 3.5:** Calculable NLO ("non-factorizable") diagrams in QCDF: Vertex corrections (first line and first diagram in the second row), penguin diagrams (rest of the second row) and hard spectator interactions (third row). Figure taken from [70].

- **Hard spectator interactions:** Also here only the relevant diagrams are shown, i.e. those which are not included in the form factor. As mentioned above, while the leading twist contributions result in a finite part for $T_{ij}^{II}(u)$, the diagrams containing the twist-3 LCDA lead to divergencies of the form

$$X_H^M := \int_0^1 \frac{dy}{1-y} \Phi_p^M(y)\,, \tag{3.38}$$

  where the asymptotic form for $\Phi_p^M(y)$ has to be used, that is, $\Phi_p^M(y) \equiv 1$. In [69, 70, 76], these terms are estimated to be $\mathcal{O}(\ln m_b/\Lambda_{QCD})$ and are treated using the parametrization

$$X_H = \left(1 + \rho_H e^{i\phi_H}\right) \ln \frac{m_B}{\sqrt{\Lambda_{QCD} m_b}}\,, \text{ with } \rho_H \in [0,1]\,,\ \phi_H \in [0, 2\pi]\,, \tag{3.39}$$

  which is clearly model-dependent. In particular, the parameter $X_H$ is taken to be universal, which introduces correlations between different isospin amplitudes.

- **Annihilation contributions:** These contributions are proportional to the $B$ meson wave function at the origin (the quarks have to "meet" to annihilate), and therefore are power-suppressed. The chirally enhanced contributions again exhibit divergent behaviour. In [69, 70, 76], the corresponding divergencies are treated completely analogously to those in the hard spectator interactions, leading to another phenomenological parameter $X_A$.

The fact that imaginary parts only arise at $\mathcal{O}(\alpha_s)$ or $\mathcal{O}(\Lambda_{QCD}/m_b)$ implies that the strong phases generated this way are small, unless the leading contribution is suppressed. However, there are several mechanisms which lead to such suppression, e.g. CKM suppression, colour suppression, or penguin suppression, so the statement "strong phases are small in QCDF" has to be taken with care. The picture arising in QCDF for imaginary parts differs from the one obtained by considering hadronic intermediate states: while each intermediate state may lead to a sizable imaginary part, QCDF predicts that there are cancellations, which cannot be traced due to the large number of possible states. A similar cancellation occurs in the two hard spectator scattering diagrams in figure 3.5: both are infrared divergent and have therefore important soft contributions, however, their sum is infrared finite and gives a perturbatively calculable contribution to the hard scattering kernel.

Concluding this section, it should be emphasized again that QCDF contributed a lot to the present understanding of non-leptonic decays. However, power corrections render precise predictions problematic. Soft collinear effective theory (SCET) [85–88] is a rigorous effective theory framework similar to HQET, designed to deal with situations in which light degrees of freedom have large energies. In SCET, different fields are introduced for one meson, in order to take the different scaling behaviour of the different degrees of freedom into account. It was hoped to solve the problem of divergencies in power-suppressed terms within this framework, but as of today this goal has not been achieved, at least not for exclusive decays.

## 3.3 Symmetry based Methods

Another option for determining matrix elements is to use symmetries which relate them. If the symmetry-related decays have a larger number of independent observables than the resulting parametrization of the reduced matrix elements has parameters, one can perform a fit to determine the matrix elements. While this results in a model-independent, data driven method to determine hadronic matrix elements, there are several problems which need to be addressed:

- The method is not applicable to all decays, because the number of parameters needed to describe a set of decays varies.

- The analytical dependence on fundamental parameters within the reduced amplitudes is lost in the process.

- In many cases the corrections to the symmetry limit are not accessible. This often re-introduces model-dependence. The possible model-independent inclusion of such subleading matrix elements is part of this thesis and discussed in sections 3.3.4 and 4.3.

However, given the difficulties in calculating hadronic matrix elements model-independently, determining them this way may simply be the only option at the moment.

This section proceeds as follows: first the Wigner-Eckart-theorem [89, 90] is briefly discussed, as it is the basic mathematical tool which this method relies on. Then isospin is introduced in section 3.3.2, which was the first flavour symmetry to be discovered, long before the underlying quark model was established. In the following subsection 3.3.3, this symmetry is extended to include the strange quark, which leads to the $SU(3)$ flavour symmetry. The $SU(3)$ includes in addition to isospin also $U$-spin as a subgroup, on which the main focus lies in this part of the work. It is discussed in the last subsection.

### 3.3.1 The Wigner-Eckart Theorem

The Wigner-Eckart theorem correlates matrix elements of irreducible tensor operators with respect to angular momentum eigenstates. Let $T^{(j)}_m$ be such an operator and $\alpha_{i,f}$ additional quantum numbers not related to the considered angular momentum, then

$$\langle f; j_f, m_f, \alpha_f | T^{(j)}_m | i; j_i, m_i, \alpha_i \rangle = \langle j_i, j, m_i, m | j_i, j, j_f, m_j \rangle \frac{\langle \alpha_f, j_f || T^{(j)} || \alpha_i, j_i \rangle}{\sqrt{2j_f + 1}} , \tag{3.40}$$

where

$$\langle j_i, j, m_i, m | j_i, j, j_f, m_j \rangle = C^{j_f, m_f}_{j m j_i m_i} \tag{3.41}$$

represents the corresponding Clebsch-Gordan coefficient and $\langle \alpha_f, j_f || T^{(j)} || \alpha_i, j_i \rangle$ is a *reduced matrix element* independent of $m, m_i$ and $m_f$. To see this, one uses the tranformation properties of a tensor operator,

$$\left[ J_z, T^{(j)}_m \right] = m T^{(j)}_m \quad \text{and} \quad \left[ J_\pm, T^{(j)}_m \right] = \sqrt{j(j+1) - m(m \pm 1)}\, T^{(j)}_{m \pm 1} , \tag{3.42}$$

which imply for example

$$\begin{aligned}\sqrt{j_f(j_f+1)-m_f(m_f+1)}\langle j_f, m_f+1|T^{(j)}_m|j_i m_i\rangle = \\ \sqrt{j_i(j_i+1)-m_i(m_i-1)}\langle j_f, m_f|T^{(j)}_m|j_i, m_i-1\rangle + \\ \sqrt{j(j+1)-m(m-1)}\langle j_f, m_f|T^{(j)}_{m-1}|j_i, m_i\rangle\,.\end{aligned} \tag{3.43}$$

With this relation, one can use the highest-weight construction to arrive at equation (3.40). An example for the application of this theorem is given in the next subsection.

### 3.3.2 Isospin

Historically Werner Heisenberg introduced the concept of neutron and proton being different "spin" orientations (in the sense of mathematical representation) of the same particle in order to explain the observation that the strong interaction does not differentiate between the two. After the development of the quark model the concept shifted to relate up and down quark; from this the original relation can be deduced. Isospin symmetry expresses the fact, that the QCD lagrangian exhibits an $SU(2)$ symmetry when up and down quark masses are set equal. Correspondingly, up and down quark form a fundamental doublet under this symmetry,

$$\begin{bmatrix} |u\rangle \\ |d\rangle \end{bmatrix} = \begin{bmatrix} |\frac{1}{2}\ +\frac{1}{2}\rangle \\ |\frac{1}{2}\ -\frac{1}{2}\rangle \end{bmatrix}_I, \quad \begin{bmatrix} |\bar{d}\rangle \\ |\bar{u}\rangle \end{bmatrix} = \begin{bmatrix} |\frac{1}{2}\ +\frac{1}{2}\rangle \\ -|\frac{1}{2}\ -\frac{1}{2}\rangle \end{bmatrix}_I, \tag{3.44}$$

where the sign for $\bar{u}$ arises because the antiparticles are written as doublets instead of anti-doublets.

Corrections to this limit arise at the percent level, $\mathcal{O}((m_d - m_u)/2\Lambda_{QCD})$ and $\mathcal{O}(\alpha)$, the mass difference being one source and the different electric charge the other.

One trivial example to be referred to later on consists of the two decays $B^0 \to J/\psi K^0$ and $B^+ \to J/\psi K^+$, when considering the leading transition operator (colour indices suppressed) $\mathcal{O} = (\bar{b}c)(\bar{c}s)$, being obviously an isospin singlet. $(K^+, K^0)$ and $(B^+, B^0)$ form doublets under isospin, and no other quantum numbers are involved, so the Wigner-Eckart theorem (3.40) implies

$$\langle B^0|\mathcal{O}|J/\psi K^0\rangle = \langle B^+|\mathcal{O}|J/\psi K^+\rangle\,. \tag{3.45}$$

As the Wigner-Eckart theorem relates irreducible tensor operators, it is necessary to express the effective hamiltonian (3.26) in these terms. As the operators for $b \to s$ and $b \to d$ transitions form different representations, they may be discussed separately. For $b \to s$ transitions, as mentioned above, the $\mathcal{O}^c_{1,2}$ operators form singlets and so do the penguin operators, because only the combination $\bar{u}u+\bar{d}d$ appears. Electroweak penguin operators and the remaining tree operators $\mathcal{O}^u_{1,2}$ can be decomposed into operators with definite isospin by using

$$\bar{u}u = \frac{1}{2}\left[(\bar{u}u+\bar{d}d)+(\bar{u}u-\bar{d}d)\right] \quad \text{and} \quad \bar{d}d = \frac{1}{2}\left[(\bar{u}u+\bar{d}d)-(\bar{u}u-\bar{d}d)\right], \tag{3.46}$$

so both classes of operators are given as the sum of $\Delta I = 0$ and $\Delta I = 1$ terms. While the matrix elements of the different operators with identical representations are in principle independent, there is no way to seperate them, unless they are multiplied by different CKM factors. Concerning $b \to d$ transitions, the additional down quark implies $\mathcal{O}^c_{1,2} \sim (1/2,+1/2)$, $\mathcal{O}_{3-6} \sim (1/2,+1/2)$ and $\mathcal{O}_{7-10}, \mathcal{O}^u_{1,2} \sim (1/2,+1/2)\oplus(3/2,+1/2)$. From these considerations, the following decompositions arise:

$$\begin{aligned}
\mathcal{H}^{b\to s} &\sim \lambda_{cs}\left[(\mathbf{1})_{T,P,EWP}+(\mathbf{3})_{EWP}\right]+\lambda_{us}\left[(\mathbf{1})_{T,P,EWP}+(\mathbf{3})_{T,EWP}\right], \\
\mathcal{H}^{b\to d} &\sim \lambda_{cd}\left[(\mathbf{2})_{T,P,EWP}+(\mathbf{4})_{EWP}\right]+\lambda_{ud}\left[(\mathbf{2})_{T,P,EWP}+(\mathbf{4})_{T,EWP}\right].
\end{aligned} \tag{3.47}$$

These will be used implicitly when isospin decompositions are given in chapter 4.

In $b \to d$ transitions, the only operator combination proportional to $\lambda_{cd}$ contibuting to the $\Delta I = 3/2$ amplitude is the sum of electroweak penguin operators containing up and down quarks. This fact can be used for the following approximation: neglecting the contributions from the operators $\mathcal{O}_{7,8}$ which have tiny Wilson coefficients ($C_{7,8} \lesssim 5\% \times C_{9,10} \sim \alpha C_{1,2}$), one can use Fierz identities in combination with isospin to derive the relation [91, 92]

$$\mathcal{H}^{EW}_{\Delta I=3/2} = -\frac{3}{2}\frac{\lambda_{td}}{\lambda_{ud}}\frac{C_9+C_{10}}{C_1+C_2}\mathcal{H}^{tree}_{\Delta I=3/2}. \tag{3.48}$$

As this relation relies only on the properties of the weak effective hamiltonian and isospin, it is expected to hold again on the percent level and can be used to relate two of the reduced matrix elements.

### 3.3.3 SU(3)

The extension of isospin symmetry to include the third light quark is in principle straight forward. In that case, the doublet above is extended to the fundamental triplet

$$\begin{bmatrix} |u\rangle \\ |d\rangle \\ |s\rangle \end{bmatrix} = \begin{bmatrix} |1\ +1\rangle \\ |1\ \ 0\rangle \\ |1\ -1\rangle \end{bmatrix} . \tag{3.49}$$

However, some complications arise: first of all, the strange quark mass is not as small as that of up and down quark, $m_s \sim \Lambda_{QCD}$. For that reason, corrections of the order 30% are expected, so the use for precise predictions is questionable, unless a reliable way to treat these corrections is found. In addition, the group theoretical structure of these decays is more complicated, because for example in decays into two (different) octets all representations in

$$\mathbf{8} \otimes \mathbf{8} = \mathbf{1} \oplus \mathbf{8}_S \oplus \mathbf{8}_A \oplus \mathbf{10} \oplus \bar{\mathbf{10}} \oplus \mathbf{27} \tag{3.50}$$

contribute, and the effective hamiltonian is complicated as well. For two-body non-leptonic $B$ decays, the relations have been worked out in [93, 94]. However, when aiming at including corrections to the symmetry limit, the expressions become very cumbersome. More importantly, one would like to take into account that isospin is unbroken to a very good approximation. Therefore it seems more convenient and appropriate to discuss the different subgroups of the full flavour $SU(3)$ separately, taking isospin to be unbroken. The other two possibilities to identify $SU(2)$ subgroups of flavour $SU(3)$ run under the names $U$-spin and $V$-spin. Among these, the generators of $U$-spin, under which the $d$ and the $s$ quark form a fundamental doublet, commute with the charge operator, which makes this subgroup particularly interesting with respect to electroweak interactions. Therefore, this subgroup is discussed in the following.

### 3.3.4 U-spin and its breaking

Under $U$-spin the down and strange quark form a doublet. A priori, it is as badly broken as the full flavour $SU(3)$, since the masses of the two quarks are substantially different, $m_s - m_d \sim m_s$. This results in a breaking, since the

relevant mass term in the lagrangian reads

$$\begin{aligned}\mathcal{L}_{s\text{mass}} &= m_d\bar{d}d + m_s\bar{s}s = \frac{1}{2}(m_s+m_d)(\bar{d}d+\bar{s}s) + \frac{1}{2}\Delta m(\bar{s}s-\bar{d}d) \\ &= \frac{1}{2}(m_s+m_d)\bar{q}q + \frac{1}{2}\Delta m\bar{q}\tau_3 q\,, \end{aligned} \tag{3.51}$$

where

$$q = \begin{pmatrix} d \\ s \end{pmatrix} \tag{3.52}$$

is the $U$-Spin quark doublet. Thus the breaking term can be described as a triplet spurion

$$\mathcal{H}_{\text{break}} = \frac{1}{2}\Delta m\tau_3 = \epsilon B_0^{(1)}\,, \tag{3.53}$$

where $\epsilon \sim \Delta m$ and $B_0^{(1)}$ is an irreducible tensor-operator with $j=1$ and $j_3=0$ of $U$-spin.

When considering a matrix element of some operator $\mathcal{O}(x)$ which can be decomposed into irreducible tensor-operators of $U$-spin, $U$-spin breaking to leading order can be considered by evaluating

$$\langle\tilde{f}|\mathcal{O}(0)|\tilde{i}\rangle = \langle f|\mathcal{O}(0)|i\rangle + (-i)\int d^4x\,\langle f|T[\mathcal{O}(0)H_{\text{break}}(x)]|i\rangle + \dots\,, \tag{3.54}$$

where the states $\tilde{f}$ and $\tilde{i}$ include the breaking term, while the states $f$ and $i$ are the $U$-spin-symmetric states. A general analysis of $U$-spin breaking can be perfomed by a group theoretical analysis of the breaking term, by decomposing the $T$ product of the operator $\mathcal{O}$ with $H_{\text{break}}$ into irreducible tensor operators $T^{(j)}_{j_3}$ of $U$-spin.

The simplest, non-trivial case emerges if the operator $\mathcal{O}$ is an $U$-spin doublet, which is denoted by $\mathcal{O}^{(1/2)}_{j_3}$. In this case, the last term in (3.54) decomposes into

$$\begin{aligned}(-i)\int d^4x\,T\left[\mathcal{O}^{(1/2)}_{\pm1/2}(0)H_{\text{break}}(x)\right] &= (-i\epsilon)\int d^4x\,T\left[\mathcal{O}^{1/2}_{\pm1/2}(0)B_0^{(1)}(x)\right] \\ &= \sqrt{\frac{2}{3}}\left[K^{(3/2)}_{\pm1/2} \mp \sqrt{\frac{1}{3}}K^{(1/2)}_{\pm1/2}\right]. \end{aligned} \tag{3.55}$$

Aside from the trivial example of the currents $j=\bar{u}\Gamma q$, $q=d,s$, also the effective weak hamiltonian for $B$ decays is a pure $U$-spin doublet, even if electroweak penguins are included. The latter is true due to the fact that the $s$ and the $d$ quark carry the same electroweak quantum numbers. Thus from the group

theoretical point of view the weak effective hamiltonian may be decomposed into its irreducible tensor components according to

$$\begin{aligned} H_{\text{eff}}^{\Delta C=\pm 1} &= \frac{4G_F}{\sqrt{2}}\left[V_{cb}V_{ud}^* P_{1/2}^{(1/2)} + V_{cb}V_{us}^* P_{-1/2}^{(1/2)}\right], \\ H_{\text{eff}}^{\Delta C=0} &= \frac{4G_F}{\sqrt{2}}\left[V_{cb}V_{cd}^* Q_{1/2}^{(1/2)} + V_{ub}V_{ud}^* R_{1/2}^{(1/2)} + V_{cb}V_{cs}^* Q_{-1/2}^{(1/2)} + V_{ub}V_{us}^* R_{-1/2}^{(1/2)}\right], \end{aligned} \tag{3.56}$$

where the operators $P_{j_3}^{(1/2)}$, $Q_{j_3}^{(1/2)}$ and $R_{j_3}^{(1/2)}$ are renormalization group invariant combinations of four-quark operators. Their transformation properties under isospin, relevant when combining both symmetries, are given in table 3.4.

In the following this group theoretical decomposition is used to discuss $U$-spin and its breaking in various $B$ decays. To this end, one has to identify the $U$ spin multiplets of hadronic states. Starting from the definiton of the fundamental quark doublets (using the same sign convention as in [95]),

$$\begin{bmatrix} |d\rangle \\ |s\rangle \end{bmatrix} = \begin{bmatrix} |\frac{1}{2}\ +\frac{1}{2}\rangle \\ |\frac{1}{2}\ -\frac{1}{2}\rangle \end{bmatrix}, \quad \begin{bmatrix} |\bar{s}\rangle \\ |\bar{d}\rangle \end{bmatrix} = \begin{bmatrix} |\frac{1}{2}\ +\frac{1}{2}\rangle \\ -|\frac{1}{2}\ -\frac{1}{2}\rangle \end{bmatrix}, \tag{3.57}$$

the decaying $B$ mesons transform as

$$\left|B^+\right\rangle = \left|u\bar{b}\right\rangle = |0,0\rangle\,, \quad \begin{bmatrix} |B^0\rangle = \left|(d\bar{b})\right\rangle \\ |B_s\rangle = \left|(s\bar{b})\right\rangle \end{bmatrix} = \begin{bmatrix} \left|\frac{1}{2},+\frac{1}{2}\right\rangle \\ \left|\frac{1}{2},-\frac{1}{2}\right\rangle \end{bmatrix}. \tag{3.58}$$

The mesons in the final state are in terms of $U$-spin

$$\begin{aligned} \begin{bmatrix} |K^+\rangle = |(u\bar{s})\rangle \\ |\pi^+\rangle = \left|(u\bar{d})\right\rangle \end{bmatrix} &= \begin{bmatrix} \left|\frac{1}{2},+\frac{1}{2}\right\rangle \\ -\left|\frac{1}{2},-\frac{1}{2}\right\rangle \end{bmatrix}, \\ \begin{bmatrix} |\pi^-\rangle = -|(\bar{u}d)\rangle \\ |K^-\rangle = -|(\bar{u}s)\rangle \end{bmatrix} &= \begin{bmatrix} -\left|\frac{1}{2},+\frac{1}{2}\right\rangle \\ -\left|\frac{1}{2},-\frac{1}{2}\right\rangle \end{bmatrix}, \\ \begin{bmatrix} |K^0\rangle = |(\bar{s}d)\rangle \\ \sqrt{3}/2\,|\eta_8\rangle - 1/2\,|\pi^0\rangle = \left|\bar{s}s - \bar{d}d\right\rangle \\ \left|\bar{K}^0\right\rangle = \left|(\bar{d}s)\right\rangle \end{bmatrix} &= \begin{bmatrix} |1,+1\rangle \\ |1,\ \ 0\rangle \\ -|1,-1\rangle \end{bmatrix}, \\ \begin{bmatrix} |K^{*0}\rangle = |(\bar{s}d)\rangle \\ 1/\sqrt{2}\,|\phi\rangle - 1/2\,|\rho^0\rangle - 1/2\,|\omega\rangle = \left|\bar{s}s - \bar{d}d\right\rangle \\ \left|\bar{K}^{*0}\right\rangle = \left|(\bar{d}s)\right\rangle \end{bmatrix} &= \begin{bmatrix} |1,+1\rangle \\ |1,\ \ 0\rangle \\ -|1,-1\rangle \end{bmatrix}. \end{aligned} \tag{3.59}$$

From this the decomposition of the neutral states is derived as

$$\begin{aligned}
|\pi^0\rangle &= -\frac{1}{2}|1,0\rangle + \frac{\sqrt{3}}{2}|0,0\rangle_8 \ , \\
|\eta\rangle &= \sqrt{\frac{2}{3}}|1,0\rangle + \frac{\sqrt{2}}{3}|0,0\rangle_8 - \frac{1}{3}|0,0\rangle_1 \ , \\
|\eta'\rangle &= \frac{1}{2\sqrt{3}}|1,0\rangle + \frac{1}{6}|0,0\rangle_8 + \frac{2\sqrt{2}}{3}|0,0\rangle_1 \ , \\
|\rho^0\rangle &= -\frac{1}{2}|1,0\rangle + \frac{\sqrt{3}}{2}|0,0\rangle_8 \ , \\
|\omega\rangle &= -\frac{1}{2}|1,0\rangle - \frac{\sqrt{3}}{6}|0,0\rangle_8 + \sqrt{\frac{2}{3}}|0,0\rangle_1 \ , \\
|\phi\rangle &= \frac{1}{\sqrt{2}}|1,0\rangle + \frac{1}{\sqrt{6}}|0,0\rangle_8 + \frac{1}{\sqrt{3}}|0,0\rangle_1 \ ,
\end{aligned} \tag{3.60}$$

where the subscript $1, 8$ on the two $U$-spin singlet states refers to the $SU(3)$ transformation properties of the corresponding state. Frome these definitions, the relations discussed in section 4.3 can be derived, simply using Clebsch-Gordan tables.

| Operator | $(\Delta I, \Delta I_z)$ |
|---|---|
| $\Delta C = 1$ : | |
| $P^{(1/2)}_{+1/2}$ | $(1,-1)$ |
| $P^{(1/2)}_{-1/2}$ | $(1/2,-1/2)$ |
| $\Delta C = 0, b \to d$ | |
| $Q^{(1/2)}_{+1/2}$ | $(1/2,-1/2) \oplus (3/2,-1/2)$ |
| $R^{(1/2)}_{+1/2}$ | $(1/2,-1/2) \oplus (3/2,-1/2)$ |
| $\Delta C = 0, b \to s$ | |
| $Q^{(1/2)}_{-1/2}$ | $(0,0) \oplus (1,0)$ |
| $R^{(1/2)}_{-1/2}$ | $(0,0) \oplus (1,0)$ |

**Table 3.4:** Classification of irreducible $U$-spin operators in terms of isospin.

In the $U$-spin limit, there is one additional relation between observables which can be derived [96,97]: The key observation is that due to CKM unitarity all CP violation in the standard model is proportional to the Jarlskog invariant, see

equation (2.25). In particular, all CP violating rate differences,

$$\Delta\Gamma = \Gamma(B \to f) - \Gamma(\overline{B} \to \overline{f}) \tag{3.61}$$

are proportional to Im$\Delta$. Exchanging the roles of the $d$ and the $s$ quark will flip the sign of Im$\Delta$ in $\Delta\Gamma$ as can be seen in (2.25). This relation may be combined with the group theory of $U$-spin using the transformation properties of tensor operators given in equation (3.42) or using the Wigner-Eckart theorem directly. Then for two processes $\#1, \#2$, related by exchanging all down and strange quarks, the relation

$$\frac{A_{\mathrm{CP}}(\#1)}{A_{\mathrm{CP}}(\#2)} = -\frac{\bar{\Gamma}(\#2)}{\bar{\Gamma}(\#1)} \tag{3.62}$$

holds, where $\bar{\Gamma}$ denotes the CP-averaged rate. This implies that in the $U$-spin limit there is one independent observable less for every pair related in the way described above.

## 3.4 Statistical Approach

Hadronic uncertainties play an important role in determining fundamental SM parameters as well as in discovering NP. The translation of measurements into fundamental parameters is usually only possible with theoretical input on the hadronic physics (e.g. the bag parameter $B_K$, or the $B$ meson decay constant $f_B$), taken from non-perturbative methods as lattice QCD or light-cone sumrule calculations. The treatment of the uncertainties of these kinds of calculations as well as experimental systematic uncertainties is not straight forward. In fact, it is not even well-defined. For that reason, there exist different approaches for handling them, prominently represented by the UTfit collaboration [50], advertising an approach with bayesian treatment of these uncertainties, and the CKMfitter group [29], which has developed the frequentist approach RFit [98]. For a recent discussion about the two approaches, see [99–102]. In this work, the RFit scheme is used, as described in the following. The presentation follows [98], where a more complete discussion and references to the original literature can be found.

### 3.4.1 The RFit Approach

The goal of the analysis is to quantify the agreement between a theory and a set of given measurements. Furthermore, if the theory turns out to be viable in

that step, the fundamental parameters entering that theory are to be determined. Dealing with a strongly interacting theory like QCD, this requires input on quantities, which were in principle determined by the theory, but are in practice hard or even impossible to calculate. In the following a framework for this analysis is described, as it is implemented in the software package CKMfitter.

Given are $N_{exp}$ measurements $\{x^i_{exp}\}$ with corresponding theoretical expressions $\{x^i_{theo}(y_{mod})\}$, depending on $N_{mod}$ model parameters $\{y^j_{mod}\}$. These parameters are divided in two subgroups:

- There are $N_{theo}$ parameters which are fundamental parameters of the theory, e.g. $\beta, m_q$, denoted as $\{y^i_{theo}\}$, which to determine is the primary goal;
- The remaining $N_{QCD} = N_{mod} - N_{theo}$ parameters are not fundamental, but appear because solving QCD is extremely difficult if not impossible.

There are two different steps in the analysis:

- Quantifying the agreement between the measurements and the theory under consideration as a whole, i.e. asking the question if the theory is capable of explaining the measurements.
- Estimating the parameters $y_{theo}$ of the considered theory, assuming the theory is correct; This is called model dependent metrology. In this step only the *relative* $\chi^2$ is relevant.

In any case the basic quantity to be considered is the likelihood function or the $\chi^2$-function respectively:

$$\mathcal{L}(y_{mod}) = \mathcal{L}_{exp}\left(x_{exp} - x_{theo}(y_{mod})\right)\mathcal{L}_{theo}(y_{QCD})\,, \tag{3.63}$$

$$\chi^2(y_{mod}) = -2\ln(\mathcal{L}(y_{mod}))\,. \tag{3.64}$$

Here the experimental likelihood $\mathcal{L}_{exp}$ expresses the agreement between the measured observables and their theoretical expressions, while the theoretical likelihood encodes the information about the QCD parameters.

Because of the non-gaussian structure of $\mathcal{L}_{theo}$ (and to a lesser extend of $\mathcal{L}_{exp}$, due to experimental systematics), it is in general *not possible* to infer a confidence level using the common function $\mathrm{Prob}(\chi^2(y_{mod}), N_{dof})$, defined in equation (3.72).

### Likelihood definitions

Given independent measurements, the experimental likelihood is given as

$$\mathcal{L}_{exp}\left(x_{exp} - x_{theo}(y_{mod})\right) = \prod_{i=1}^{N_{exp}} \mathcal{L}^i_{exp}\,, \tag{3.65}$$

where the individual components were ideally given as pure gaussians[4],

$$\mathcal{L}^i_{exp} = \frac{1}{\sqrt{2\pi}\sigma^i_{exp}} \exp\left[-\frac{1}{2}\left(\frac{x^i_{exp} - x^i_{theo}}{\sigma^i_{exp}}\right)^2\right]. \tag{3.66}$$

However, in many cases there are systematical errors in the measurements as well. For systematical errors, one cannot assume a gaussian distribution, which would lead to the procedure of adding the statistical and systematical errors in quadrature. They might rather be assumed to take the form of an unknown offset $x_0$. For this offset the *range* $[-\sigma_0, \sigma_0]$ is defined: the $\chi^2$ contribution of the offset is set to zero if $x_0$ lies within this range and it set to infinity if it lies outside. Minimizing $\chi^2$ with respect to $x_0$ then leads to the following prescription:

$$\chi^2_{min,x_0} = \begin{cases} 0 & \text{if } |x_{exp} - x_{theo}| \leq \sigma_0 \\ \left(\frac{|x_{exp} - x_{theo}| - \sigma_0}{\sigma_{exp}}\right)^2 & \text{if } |x_{exp} - x_{theo}| > \sigma_0 \end{cases}, \tag{3.67}$$

for which an example distribution is depicted in figure 3.6.

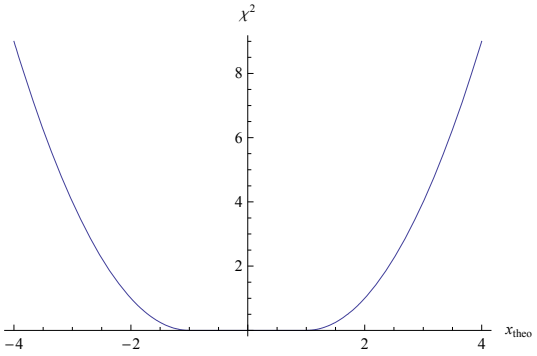


**Figure 3.6:** $\chi^2$-distribution corresponding to equation (3.67) for $x_{exp} = 0 \pm 1 \pm 1$

[4]The normalization factor is *not* used in the implementation, so if the fit is in best possible agreement with the measurement, it does not contribute to $\chi^2$.

Considering errors of theoretical quantities the situation is similar to that of experimental systematics, but the problem is more severe, because often the uncertainties involve large effects. In many cases, the knowledge on theoretical parameters is *educated guesswork*, that is, one might be able to exclude some ranges for the parameter values, but a large range still survives, in which no particular value is preferred. An example for such an unknown quantity is given by the first inverse moment of the $B$ meson distribution amplitude, $\lambda_B$. The way this situation is treated in the RFit scheme (and implemented in CKMfitter) is to define allowed ranges for these parameters, in the same way described before for the experimental systematics: the $\chi^2$ for the corresponding parameter is set to zero within the allowed range and infinity outside[5]. Here lies the one assumption one needs in order to deal with this ill-defined problem: *One assumes that the theoretical parameters take values inside their ranges.* Therefore, if one uses too small ranges one might get simply false results. On the other hand, one might miss a discovery if one uses too large ranges. Obviously choosing the right ranges is a delicate subject, and should be documented in detail.

### Metrology

As stated above, in metrology one assumes the theory to be correct and wants to find the best fit values of the parameters under consideration. For that purpose, one uses the offset-corrected $\chi^2$,

$$\Delta\chi^2(y_{mod}) = \chi^2(y_{mod}) - \chi^2_{min;y_{mod}}\,, \tag{3.68}$$

where $\chi^2_{min;y_{mod}}$ denotes the minmal $\chi^2$-value when all $y_{mod}$ parameters are allowed to vary.

In most cases, one is not interested in all of the $y_{mod}$ parameters the same way: For example, in a CKM-analysis, the interesting parameters are $\{\bar{\rho},\bar{\eta}\}$, while $\lambda$ and $A$ are less relevant. Denoting the parameters under consideration $a$ and the less relevant ones $\mu$, the aim is to *set confidence levels in the a space, irrespective of the $\mu$ values* [98]. In the RFit scheme, this is done by scanning the $a$ space, and finding for every point there the point in $\mu$ space which maximises the agreement between theory and data. The confidence level of that point is set

[5]This does not correspond to a uniform PDF for the parameter. For example, an allowed range in $\phi$ of $[0,\pi/2]$ leads to an allowed range of $\sin\phi$ of $[0,1]$, every value of $\sin\phi$ treated equally - which is not true if one assumes a uniform PDF for $\phi$.

to this maximum, that is

$$CL(a) = \mathrm{Max}_{\mu}\{CL(a,\mu)\}\,. \tag{3.69}$$

A given point is excluded only, if this maximal confidence level is beneath a given cut, e.g. $CL_{cut} = 0.05$. In that way one receives the most conservative estimate for a given $a$ point. The extracted distribution is therefore

$$\Delta\chi^2(a) = \chi^2_{min;\mu}(a) - \chi^2_{min;y_{mod}}\,. \tag{3.70}$$

If there were neither a component from $\mathcal{L}_{theo}$ in the combined likelihood nor significant experimental systematic errors, one would obtain the confidence level as

$$\mathcal{P}(a) = \mathrm{Prob}(\Delta\chi^2(a), N_{dof})\,, \tag{3.71}$$

using

$$\mathrm{CL} = \mathrm{Prob}(\chi^2(y_{mod}), N_{dof}) = \frac{1}{\sqrt{2^{N_{dof}}}\Gamma(N_{dof}/2)} \int_{\chi^2(y_{mod})}^{\infty} dt\, \left\{e^{-t/2}\, t^{N_{dof}/2-1}\right\}\,. \tag{3.72}$$

Actually, for the sake of simplicity, this expression *is* used in the present work, as it is in CKMfitter generally, which is clearly an approximation. The correct treatment were to use a Monte Carlo simulation to obtain the expected distribution of $\Delta\chi^2(a)$, which is however beyond the scope of this work.

# Chapter 4

# Applications

In this chapter, the methods developed in the last sections are applied to non-leptonic $B$ decays. The first two sections deal with NP in $b \to s$ transitions, discussing separately the possiblility of NP in the decay amplitude (section 4.1) and NP in mixing (section 4.2) by considering prominent example decays, in which the data seem to deviate from the SM expectations. In the last section, the formalism of $U$-spin including breaking corrections is applied to a couple of decays which already have been measured, and strategies are proposed how to exploit with aid of this method the expected precision from future experiments, prominently LHCb and a Super-$B$ factory.

## 4.1 New Physics in b $\to$ s Transition Amplitudes

$b \to s$ transitions tend to be a good ground for NP searches, because due to the hierarchy in the relevant CKM matrix elements part of the amplitude structure can be understood without having to deal with non-perturbative effects. In this section, three groups of decays are discussed:

- $B \to J/\psi K$,
- $B \to \phi K$, and
- $B \to \pi K$.

They are related by three observations:

- They all involve a $b \to s$ transition.

- All of them are "puzzling", i.e. tensions with the SM expectations are found.

- The data for these decays are relatively precise.

The first two points motivate to introduce NP contributions by operators of the form $\mathcal{O}_q^{b\to s} = (\bar{s}b)(\bar{q}q)$; the alternative possibility of NP in mixing, together with large non-factorizable SM effects will be discussed in the next section. The last point explains the absence of several other possible decay modes in the analysis, in which in principle effects should be seen as well. As discussed before, even when only considering operators of the type $\mathcal{O}_q^{b\to s}$, there could be several of these operators with in general different weak phases. In the following the assumption will be made, that one operator dominates the NP contributions, leading to a single weak phase for the corresponding matrix elements. In the whole analysis, colour and Dirac structure of the operators will not be specified, considering only their flavour structure. The different options regarding the quark pair $(\bar{q}q)$ are then discussed separately for each class of decays. Therefore, always the hamiltonian $\mathcal{H} = \mathcal{H}_{SM} + \mathcal{O}_q^{b\to s}$ is considered, and the corresponding isospin analysis leads to matrix elements which can be parametrized in an obvious way as modulus, strong phase, and weak phase.

While the operator under consideration is expected to contribute to all the decays discussed below, it is generally not possible to relate the contributions directly, as the final states are not connected by flavour symmetry. More importantly, two of the final states consist of one pseudoscalar and one vector meson, while in $B \to \pi K$ both final state particles are pseudoscalar. However, one might speculate that the matrix elements for $\phi K$ and $J/\psi K$ are in some way similar, as they have the same quantum numbers. However, this is considered only a crude estimate.

The analysis presented in this section has been published in [63]. However, some of the data changed significantly since then, therefore here an update of that analysis is presented. The differences are pointed out correspondingly.

As the prerequisites for this analysis have already presented in the previous chapters, this section proceeds directly by discussing the three considered classes of decays separately in some detail. Finally some concluding remarks are given.

### 4.1.1 $\mathbf{B \to J/\psi K}$

This decay, often referred to as the *Golden Mode*, plays a special role in the SM, because it is dominated to very good approximation by only one isospin amplitude. The reason for that is twofold:

- Cabibbo suppression: As noted in section 2.2, the relevant CKM parameter combinations in $b \to s$ transitions exhibit a strong hierarchy:

$$|\lambda_{us}/\lambda_{cs}| \sim \lambda^2 \sim 2\% \ll 1\,. \tag{4.1}$$

- Penguin suppression: (i) The operators $O_{1,2}^{(u)}$ do not contain charm quarks, therefore the hadronic matrix elements $\langle J/\psi K|O_{1,2}^{(u)}|B\rangle$ are suppressed.
  (ii) The coefficients of the loop-induced penguin operators $C_{3-6}$ are small with respect to those of the operators $C_{1,2}$.

Furthermore, the electroweak penguin operators have even smaller Wilson coefficients. Those with the potentially largest effect — that is, the ones proportional to the large CKM element combination and including charm quarks — are included in the leading amplitude. Consequently, in the SM the $B \to J/\psi K$ decay amplitude is expected to be completely dominated by

$$\mathcal{A}_0(\bar{B} \to J/\psi \bar{K}) = \frac{G_F}{\sqrt{2}}\, V_{cb}V_{cs}^*\, \langle J/\psi \bar{K}|C_{1,2}\,\mathcal{O}_{1,2}^{(c)} + \sum_{i=3}^{10} C_i \mathcal{O}_i^{(c)}|\bar{B}\rangle\,, \tag{4.2}$$

where $\bar{B} = \{\bar{B}_d^0,\, B^-\}$, and the leading $[\bar{s}b\bar{c}c]$ component in every operator has been projected out, denoted by $\mathcal{O}_i \to \mathcal{O}_i^{(c)}$. In particular, the amplitude is dominated by a single weak phase, and consequently the time-dependent CP asymmetry in $B^0 \to J/\psi K_S$ is completely determined by the $B^0 - \bar{B}^0$ mixing amplitude, involving the CKM angle $\beta$. Corrections from the subleading operators have been estimated by perturbative methods at the $b$-quark scale, and found to give only effects of the order of $10^{-3}$ [103, 104]. However, purely perturbative methods are clearly not suited for this kind of computation and tend to underestimate hadronic effects per construction. Long-distance penguin contributions have been estimated on the basis of experimental data to be not larger than $10^{-2}$ [105]. This ansatz will be used in the next section as well with the present data, in order to (i) estimate the influence of subleading SM amplitudes and (ii) to determine the influence of a possible NP weak phase in these decays.

Taking in a first step the SM picture seriously implies the following pattern of observables:

$$\begin{aligned} S(\bar{B}^0 \to J/\psi K_S) &= \sin 2\beta\,, \\ \bar{\Gamma}(\bar{B}^0 \to J/\psi \bar{K}^0) &= \bar{\Gamma}(B^- \to J/\psi K^-) \text{ and} \\ A_{\rm CP}(\bar{B}^0 \to J/\psi K_S) &= A_{\rm CP}(B^- \to J/\psi K^-) = 0\,. \end{aligned} \tag{4.3}$$

From the data, the following small deviations from this pattern are observed, see table 4.1:

- The direct CP asymmetry in the charged decay is measured different from zero, $A_{\rm CP}(B^- \to J/\psi K^-) \neq 0 \,@\, \sim 1\sigma$.

- The rate difference is non-vanishing,

$$\bar{\Gamma}(\bar{B}^0 \to J/\psi \bar{K}^0) \neq \bar{\Gamma}(B^- \to J/\psi K^-) @ \sim 1\sigma\,. \tag{4.4}$$

- Finally, depending on the interpretation of $B \to \tau\nu$, there is a deviation in $S(\bar{B}^0 \to J/\psi K_S)$ from $\sin 2\beta$:

$$\eta_{\rm CP} S(B \to J/\psi K_S) + \sin 2\beta_{B\to\tau\nu} = 0.16^{+0.04}_{-0.06}\,, \tag{4.5}$$

  which includes an enhanced error for $\sin 2\beta_{B\to\tau\nu}$ due to the non-gaussian behaviour of the extracted value from [29], which stems from the global fit excluding $\sin 2\beta_{b\to s\bar{c}c}$. As noted in secion 2.2.2, this value will not be used in the fits.

Neither of these tensions is conclusive. But having all three of them in the *Golden Mode* is at least curious.

| Decay | BR/$10^{-4}$ | $A_{\rm CP}$ | $S_{\rm CP}$ |
|---|---|---|---|
| $B^- \to J/\psi K^-$ | $10.07 \pm 0.35$ [35] | $0.017 \pm 0.016(*)$ [35] | – |
| $\bar{B}^0 \to J/\psi \bar{K}^0$ | $8.71 \pm 0.32$ [35] | $0.002 \pm 0.020(**)$ [54] | $0.657 \pm 0.025$ [54] |

**Table 4.1:** Measurements for $B \to J/\psi K$ observables. $(*)$: Error enhanced by the PDG, due to inconsistent measurements. $(**)$: Error enhanced according to the PDG prescription, for the same reason.

Turning now to the hypothesis of NP in the decay amplitudes as described above, the general parametrization reads

$$\begin{aligned} \mathcal{A}(B^- \to J/\psi K^-) &= \mathcal{A}_0(\bar{B} \to J/\psi \bar{K}) \left[1 + r_0\, e^{i\theta_W} e^{i\phi_0} - r_1\, e^{i\theta_W} e^{i\phi_1}\right] , \\ \mathcal{A}(\bar{B}_d \to J/\psi \bar{K}^0) &= \mathcal{A}_0(\bar{B} \to J/\psi \bar{K}) \left[1 + r_0\, e^{i\theta_W} e^{i\phi_0} + r_1\, e^{i\theta_W} e^{i\phi_1}\right] , \end{aligned} \tag{4.6}$$

with $r_{0,1}$ denoting the moduli of NP amplitudes with $\Delta I = 0, 1$ respectively, $\phi_{0,1}$ the corresponding strong phases, and $\theta_W$ the NP weak phase.

It is convenient to discuss the following critical observables [106], which help discriminating the different contributions. All of them vanish in the limit of negligable subleading contributions, and are given here for small values of the parameters $r_{0,1}$, while in the fit the exact expressions are used:

$$\begin{aligned} A_{\rm CP}^{\rm avg} &\equiv \frac{A_{\rm CP}(\bar{B}^0 \to J/\psi \bar{K}^0) + A_{\rm CP}(B^- \to J/\psi K^-)}{2} \\ &\simeq -2\, r_0\, \sin\phi_0\, \sin\theta_W , \\ \Delta A_{\rm CP} &\equiv \frac{A_{\rm CP}(\bar{B}^0 \to J/\psi \bar{K}^0) + A_{\rm CP}(B^- \to J/\psi K^-)}{2} \\ &\simeq -2\, r_1\, \sin\phi_1\, \sin\theta_W , \\ A_I &\equiv \frac{\bar{\Gamma}[B_d \to J/\psi K_0] - \bar{\Gamma}[B^\pm \to J/\psi K^\pm]}{\bar{\Gamma}[B_d \to J/\psi K_0] + \bar{\Gamma}[B^\pm \to J/\psi K^\pm]} \\ &\simeq 2\, r_1\, \cos\phi_1\, \cos\theta_W , \text{ and} \\ \eta_{\rm CP}\, S + \sin 2\beta &\simeq 2\,(r_0\, \cos\phi_0 + r_1\, \cos\phi_1) \sin\theta_W\, \cos 2\beta . \end{aligned} \tag{4.7}$$

The following limits, which can be read off from equations (4.7), hold also for arbitrary values of $r_{0,1}$:

$$A_{\rm CP}^{\rm avg} \overset{r_0 \to 0}{\longrightarrow} 0 , \tag{4.8}$$

$$\Delta A_{\rm CP} \overset{r_1 \to 0}{\longrightarrow} 0 , \tag{4.9}$$

$$A_I \overset{r_1 \to 0}{\longrightarrow} 0 . \tag{4.10}$$

In addition, equations (4.7) are manifestly invariant under the approximate reparametrizations, following from equations (2.61), as long as the power-counting leading to these approximations is not violated, that is, in the limit $\xi = \mathcal{O}(r_{0,1}) \ll 1$:

$$\begin{aligned} \sin\theta_W &\to \sin\theta_W \left(1 + \xi\, \cos\theta_W + \mathcal{O}(\xi^2)\right) , \\ \cos\theta_W &\to \cos\theta_W - \xi\, \sin^2\theta_W + \mathcal{O}(\xi^2) , \end{aligned}$$

$$\begin{aligned} r_0 \cos\phi_0 + r_1 \cos\phi_1 &\to (r_0 \cos\phi_0 + r_1 \cos\phi_1)\left(1 - \xi \cos\theta_W + \mathcal{O}(\xi^2)\right) , \\ r_1 \cos\phi_1 &\to r_1 \cos\phi_1 \left(1 + \xi \sin\theta_W \tan\theta_W + \mathcal{O}(\xi^2)\right) , \\ r_{0,1} \sin\phi_{0,1} &\to r_{0,1} \sin\phi_{0,1} \left(1 - \xi \cos\theta_W + \mathcal{O}(\xi^2)\right) . \end{aligned} \tag{4.11}$$

The values for the critical observables, as following from the data in table 4.1, are given in table 4.2.

| Observable | $B \to J/\psi K$ |
|---|---|
| $\eta_{\rm CP} S_{\rm CP} + \sin 2\beta$ | $0.089^{+0.029}_{-0.032} \pm 0.081$ |
| $A_{\rm CP}^{\rm avg}$ | $0.010 \pm 0.013(*)$ |
| $\Delta A_{\rm CP}$ | $-0.008 \pm 0.013(*)$ |
| $A_I$ | $-0.038 \pm 0.025$ |

**Table 4.2:** The critical observables in $B \to J/\psi K$, computed from the data in table 4.1.

### Fit with $\Delta I = 0$ only (New Physics in $b \to s c \bar{c}$)

Among the different possible operators, the $b \to s c\bar{c}$ term is expected to give the dominating contributions to $B \to J/\psi K$ decays, because it has unsuppressed tree-level matrix elements with the hadronic final state, leading to a $\Delta I = 0$ contribution. Therefore, in the first fit it is assumed that $b \to s c\bar{c}$ gives the only relevant NP contribution in (4.6), which amounts to setting $r_1$ to zero. In order to keep track of the different effects determining the order of magnitude for different contributions, the following power-counting is introduced[1] [106–108]:

- The CKM elements are counted in the obvious manner, corresponding to their Wolfenstein hierarchy, with $R_u \sim 1$.
- Matrix elements stemming from penguin operators and penguin matrix elements of tree operators are counted with an additional factor of $\lambda$.
- Matrix elements stemming from electroweak penguin operators are assigned a factor of $\lambda^2$.

[1] Obviously the power-counting parameter $\lambda$ is *not* the same as the Wolfenstein parameter. However, it is taken to be of the same order, and for simplicity the two are not differentiated in the following.

- The relative "generic size" of NP contributions is estimated to be

$$\mathcal{A}_{\rm NP} \sim M_W^2/\Lambda_{\rm NP}^2 \langle \mathcal{O}_{\rm NP} \rangle \sim \lambda \times \mathcal{A}_0(\bar{B} \to J/\psi \bar{K}) \,. \tag{4.12}$$

While these are rough order of magnitude estimates, for the following considerations it is usually sufficient that the NP contribution is expected to be smaller than the leading, but larger than the suppressed SM contributions.

The isospin breaking between charged and neutral $B$ decays is not affected by this operator, and should not be part of the fit. Thus one is left with the time-dependent CP asymmetries in $\bar{B}^0 \to J/\psi \bar{K}^0$ and the direct CP asymmetry in $B^- \to J/\psi K^-$. Including the contribution from $r_0$ in equations (4.6), the explicit expressions for the CP asymmetries read

$$\begin{aligned} C_{J/\psi K_S} &= -A_{\rm CP}^{\rm dir}(B^- \to J/\psi K^-) \\ &= \frac{2 r_0 \, \sin\phi_0 \, \sin\theta_W}{1 + 2 r_0 \, \cos\phi_0 \, \cos\theta_W + r_0^2} \,, \end{aligned} \tag{4.13}$$

$$\eta_{\rm CP} \, S_{J/\psi K_S} = -\sin(2\beta) + \frac{2 r_0 \, \sin\theta_W \, (\cos(2\beta) \, \cos\phi_0 + r_0 \, \cos(2\beta - \theta_W))}{1 + 2 r_0 \, \cos\phi_0 \, \cos\theta_W + r_0^2} \,. \tag{4.14}$$

The NP amplitudes are expected to provide small corrections to the SM, $r_0 \ll 1$, and thus the expansion

$$\begin{aligned} \eta_{\rm CP} \, S_{J/\psi K_S} + \sin(2\beta) &\simeq 2 r_0 \, \sin\theta_W \, \cos\phi_0 \, \cos(2\beta) \,, \\ C_{J/\psi K_S} &\simeq 2 r_0 \, \sin\theta_W \, \sin\phi_0 \end{aligned} \tag{4.15}$$

should be a valid approximation for the full expressions. From this the following interesting parameter combinations are read off:

$$|r_0 \sin\theta_W| \simeq \frac{\sqrt{(\eta_{\rm CP} \, S_{J/\psi K_S} + \sin 2\beta)^2 + (C_{J/\psi K_S} \, \cos 2\beta)^2}}{2 \cos 2\beta} \,, \tag{4.16}$$

determining the *overall* size of the deviations from the SM limit, and

$$\tan\phi_0 \simeq \frac{C_{J/\psi K_S} \, \cos 2\beta}{\eta_{\rm CP} \, S_{J/\psi K_S} + \sin 2\beta} \,, \tag{4.17}$$

determining the *relative* size of the two effects. Given in terms of observables, these combinations should be reparametrization-invariant. This is indeed the case, as shown in figure 4.1, where $r_0 \, \sin\theta_W(\xi)$ (left) and $\tan\phi_0(\xi)$ (right) are

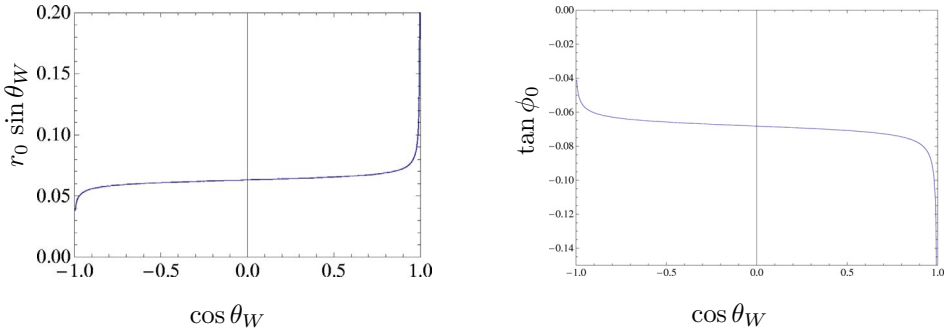


**Figure 4.1:** Illustration of approximate reparametrization invariance, as explained in the text.

plotted vs. $\cos\theta_W(\xi)$ for $\xi \in [-10, 10]$. As a reference point, the values of $|r_0 \sin\theta_W| \approx 0.07$ and $\tan\phi_0 \approx -0.07$ are taken, as calculated from equations (4.16),(4.17), with the data given in table 4.1. As can be seen, the approximate invariance holds. It is limited by two factors: it breaks down if the reparametrization leads to $r_0 \sim 1$, thereby violating the power-counting leading to the expressions (4.16),(4.17), and if $\theta_W \sim 0, \pi$, because at these points the CP asymmetries vanish for all values of $r_0, \phi_0$.

As a consequence of the reparametrization invariance, the fit to the experimental data will generally allow for "unphysical" solutions, where the strong and weak phases are tuned in such a way that the absolute size of the NP contribution $r_0$ can be unreasonably large. In order to suppress such effects, additional constraints are implemented in different scenarios: (i) For small NP contributions, the fit should not depend on the parameter combination $|r_0 \cos\theta_W|$; constraining $|r_0 \cos\theta_W| < 0.4$ should therefore only affect the unphysical solutions. (ii) If the phase $\theta_W$ of the NP operator is close to the one from the leading contribution in the SM, it is not expected to be sensitive to NP in CP asymmetries in any case; therefore one may concentrate on $30° \leq \theta_W \leq 150°$. (iii) For $\theta_W = \pi - \gamma_{\rm SM}$ the fit can also be interpreted as a determination of the size of subleading SM contributions from Cabibbo- and penguin-suppressed amplitudes, which possibly may have been underestimated in [103, 104].

Using the experimental values for the CP asymmetries together with the value for $\sin 2\beta$ from the indirect determination in figure 2.3, it is fitted for the preferred ranges for the NP parameters, applying the different constraints as discussed above. The results are shown in table 4.3 and figure 4.2. Note that there is

no degree of freedom left, having two independent measurements and the same or even larger number of parameters. Therefore, there is no measure for the quality of the fit, apart from the question if the resulting parameter ranges are theoretically acceptable or not.

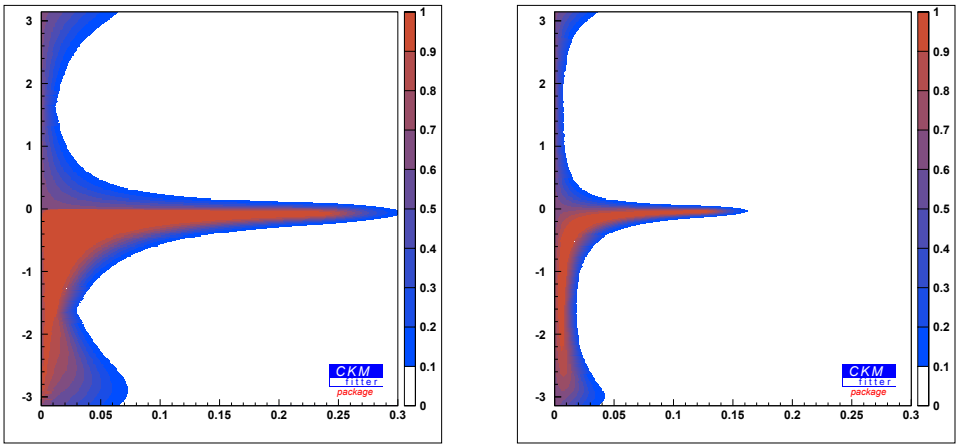


**Figure 4.2:** Fit results $\phi_0$ vs. $r_0 \sin\theta_W$ for different scenarios, see also table 4.3. In the plot on the left only the constraint $|r_0 \cos\theta_W| \leq 0.4$ is imposed. The plot on the right is for fixed $\theta_W = \pi - \gamma_{\rm SM}$.

Since the value for $S_{\rm CP}$ in $B \to J/\psi K_S$ is close to the indirect determination of $\sin 2\beta$ as long as $B \to \tau\nu$ is not taken into account, the fitted range for $r_0 \sin\theta_W$ is consistent with zero, and the related strong phase $\phi_0$ is unconstrained. Still, for sufficiently small strong phases, NP contributions of the order 20% are not excluded either. Inclusion of $B \to \tau\nu$ in the indirect determination would obviously exclude $r_0 = 0$ significantly; the small value for $A_{\rm CP}^{\rm avg}$ then implies a relatively small strong phase. Notice that small strong phases are generally expected within QCDF, as explained in detail in section 3.2, together with the limitations of this statement. Compared to the estimate of SM corrections in [103, 104], the typical order of magnitude for $r_0$ is significantly larger, taking into account that $r_0$ includes a factor of $|\lambda_{us}/\lambda_{cs}|$ in the SM. Although the present experimental situation is not conclusive, the analysis shows that an improvement of the experimental precision for $B \to J/\psi K$ observables on the one hand, or the theoretical precision in the $|V_{ub}/V_{cb}|$ determination on the other, may still lead to interesting conclusions. Furthermore, a reliable determination of $f_B$ would imply

| Scenario | | $\lvert r_0 \sin\theta_W\rvert$ |
|---|---|---|
| $\theta_W$ free | $\lvert r_0 \cos\theta_W\rvert \leq 0.4$ | [0 to 0.28] |
| $30° \leq \theta_W \leq 150°$ | $\lvert r_0 \cos\theta_W\rvert$ free | [0 to 0.20] |
| $30° \leq \theta_W \leq 150°$ | $\lvert r_0 \cos\theta_W\rvert \leq 0.4$ | [0 to 0.20] |
| $\theta_W = \pi - \gamma_{\rm SM}$ | $\lvert r_0 \cos\theta_W\rvert$ free | [0 to 0.14] |

**Table 4.3:** Fit to direct and mixing-induced CP asymmetries in $B \to J/\psi K$, using the indirect determination of $\sin 2\beta$ and including the $\Delta I = 0$ NP contribution $r_0$, only. Shown are the ranges for the relevant parameter combination $|r_0 \sin\theta_W|$, using different additional constraints to suppress "unphysical" solutions (see text). As $r_0 = 0$ is allowed in all cases, the strong phase is unconstrained.

an interesting additional constraint, especially in the light of the high precision expected from LHCb and a possible Super-$B$ factory.

### Fit with $\Delta I = 0, 1$ (New Physics in $b \to s\bar{u}u$ or $b \to s\bar{d}d$)

While the contributions from operators $(\bar{s}b)(\bar{u}u)$ or $(\bar{s}b)(\bar{d}d)$ are expected to be suppressed in $B \to J/\psi K$ with respect to those from $(\bar{s}b)(\bar{c}c)$, they induce a $\Delta I = 1$ amplitude, which contributes to $A_I$ and $\Delta A_{\rm CP}$ in equations (4.7). Taking the data at face value, the observed $A_I \neq 0$ implies a $\Delta I = 1$ amplitude, which has to have a different weak and strong phase because of $\Delta A_{\rm CP} \neq 0$, too. This to be accomodated for in the SM would require a large penguin matrix element of the doubly Cabibbo-suppressed tree operators $\mathcal{O}^u_{1,2}$ (or a gigantic contribution from electroweak penguins). In the following, the weak phase is set to $\pi - \gamma$ for simplicity, the solutions for other values of $\theta_W$ can be obtained from equations (4.11).

Including a NP operator $(\bar{s}b)(\bar{u}u)/(\bar{d}d)$, one can again trivially fit all observables. The fit result is plotted in figure 4.3. The $1\sigma$ parameter ranges are given by

$$\begin{aligned} r_0 \cos\phi_0 &= [-0.074 \text{ to } 0.118]\,, & r_0 \sin\phi_0 &= [-0.015 \text{ to } 0.003]\,, \\ r_1 \cos\phi_1 &= [\ \ 0.014 \text{ to } 0.089]\,, & r_1 \sin\phi_1 &= [-0.002 \text{ to } 0.013]\,. \end{aligned} \quad (4.18)$$

Notice that again the preferred values for the strong phases turn out to be small.

As a result, the small deviations from the SM expectations in $B \to J/\psi K$ can be explained by NP in either $b \to su\bar{u}$ or $b \to sd\bar{d}$, alone. However, as

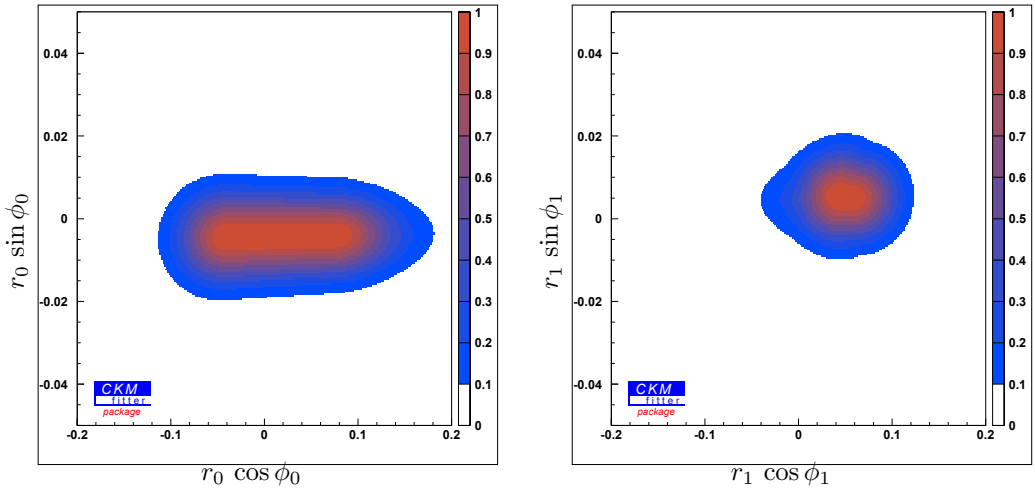


**Figure 4.3:** The result for $r_0\, e^{i\phi_0}$ (left) and $r_1\, e^{i\phi_1}$ (right) in the complex plane from the fit to $J/\psi K$ observables, with isospin-breaking NP contributions $b \to su\bar{u}$ or $b \to sd\bar{d}$. The NP weak phase has been fixed to $\theta_W = \pi - \gamma_{\rm SM}$.

noted above, one has to keep in mind that, compared to the contributions from $b \to sc\bar{c}$, the $b \to su\bar{u}$ or $b \to sd\bar{d}$ only contribute via penguin ($r_0$) or annihilation ($r_1$) diagrams to hadronic matrix elements. Thus, an additional suppression with respect to the tree-level matrix elements fitted in the last section (see table 4.3) is expected for the isospin breaking part, while in the isospin conserving amplitude contributions from the different operators cannot be separated. Notice that, depending on the actual size of these suppression factors, the result for $r_0$ and $r_1$ may also be interpreted as due to unexpectedly large effects from subleading SM operators.

### 4.1.2 $\mathbf{B \to \phi K}$

The analysis of this decay proceeds in many respects along the same lines as that for $B \to J/\psi K$. The main difference is the fact that, as a tree-operator $(\bar{s}b)(\bar{s}s)$ is absent in the SM, the tree operators contribute only via penguin matrix elements in the SM. Therefore the leading amplitude consists of tree level matrix elements of penguin operators and penguin matrix elements of tree operators, which is why this kind of mode is called *penguin dominated*. As a consequence, the subleading contributions in the SM are suppressed only by the a relative factor of $\lambda^2$ in the power-counting described above, stemming either from the Cabibbo

suppression factor or the smallness of the Wilson coefficients for electroweak penguin operators. Estimates within the SM of these subleading contributions usually give small effects [109–112]. However, the relative importance of the NP contributions is increasing as well, as they may include a matching tree operator. Therefore one expects from the power-counting analogous to the one described for $B \to J/\psi K$ (see for instance [113]):

$$\frac{A_{\rm NP}(\Delta I = 0)}{\lambda_{cs} A_c^0} \lesssim \mathcal{O}(1)\,, \quad \frac{A_{\rm NP}(\Delta I = 1)}{\lambda_{cs} A_c^0} \lesssim \mathcal{O}(\lambda)\,. \tag{4.19}$$

The parametrization is completely analogous to the one of $B \to J/\psi K$. Note that for simplicity the same symbols are used:

$$\mathcal{A}(\bar{B} \to \phi \bar{K}) \;=\; \mathcal{A}_0(\bar{B} \to \phi \bar{K}) \left[1 + r_0\, e^{i\theta_W} e^{i\phi_0} \mp r_1\, e^{i\theta_W} e^{i\phi_1}\right]\,. \tag{4.20}$$

Correspondingly, the expressions for the observables are the same; their experimental values are given in table 4.4. However, the matrix elements are independent, as both, the strong dynamics and the NP operators involved, are different. The corresponding critical observables can be found in table 4.5. Again, tensions with the naive SM expectations are found, much larger in magnitude of the central values than for $J/\psi K$, but with larger uncertainties as well, which results in only a slightly higher significance. While this increase is expected within the scenario considered here, it is expected for subleading SM contributions as well.

| Decay | BR/$10^{-6}$ | $A_{\rm CP}$ | $S_{\rm CP}$ |
|---|---|---|---|
| $B^- \to \phi K^-$ | $8.3 \pm 0.65$ | $0.034 \pm 0.044$ | – |
| $\bar{B}^0 \to \phi \bar{K}^0$ | $8.3^{+1.2}_{-1.0}$ | $0.23 \pm 0.15$ | $-(0.44^{+0.17}_{-0.18})$ |

**Table 4.4:** Measurements for observables in $B \to \phi K$, averaged by the HFAG [54].

### Fit with $\Delta I = 0$ (New Physics in $b \to s\bar{s}s$)

Using the experimental values for the direct and mixing-induced CP asymmetries in $B \to \phi K$ together with the value for $\sin 2\beta$ from the indirect determination in figure 2.3, the preferred ranges for the NP parameters are fitted as shown in figure 4.4 and table 4.6. Again, only the result for a particular value for the NP weak phase, $\theta_W = \pi - \gamma_{\rm SM}$, is quoted. Other solutions follow from the same

| Observable | $B \to \phi K$ |
|---|---|
| $\eta_{\rm CP} S_{\rm CP} + \sin 2\beta$ | $0.31^{+0.18}_{-0.17} \pm 0.08$ |
| $A_{\rm CP}^{\rm avg}$ | $0.13 \pm 0.08$ |
| $\Delta A_{\rm CP}$ | $0.10 \pm 0.08$ |
| $A_I$ | $0.04^{+0.08}_{-0.07}$ |

**Table 4.5:** The critical observables in $B \to \phi K$, computed from the data in table 4.4.

reparametrization invariance as given in equations (4.11). Comparison with the $B \to J/\psi K$ case in figure. 4.2 shows:

- The effect is more pronounced, the shape of the allowed region similar to the one in $J/\psi K$.
- Again, the fit tends to prefer small strong phases $\phi_0$.
- The preferred value for $r_0$ in $B \to \phi K$ is by a factor of 2-3 larger than the one in the corresponding fit in $B \to J/\psi K$. After correcting for the penguin suppression factor, phase space and normalization, this implies that the coefficients of the involved NP operators in both cases may be of similar size.

| Quantity | Value |
|---|---|
| $\lvert r_0 \sin\theta_W \rvert$ | [ 0.03 to 0.32 ] ($1\sigma$) |
| $\phi_0$ | [-0.76 to -0.01 ] ($1\sigma$) |

**Table 4.6:** Results for the fit to the CP asymmetries in $B \to \phi K$, allowing for a NP contribution with $\Delta I = 0$, only.

It should be emphasized, that the latter observation also implies that unusually large hadronic penguin matrix elements in the SM could simultaneously explain the $B \to J/\psi K$ and $B \to \phi K$ discrepancies.

### Including $\Delta I = 1$ operators

Since the publication [63], the data of the time-dependent CP asymmetries changed significantly. At that time there were no signs for isospin breaking effects, there-

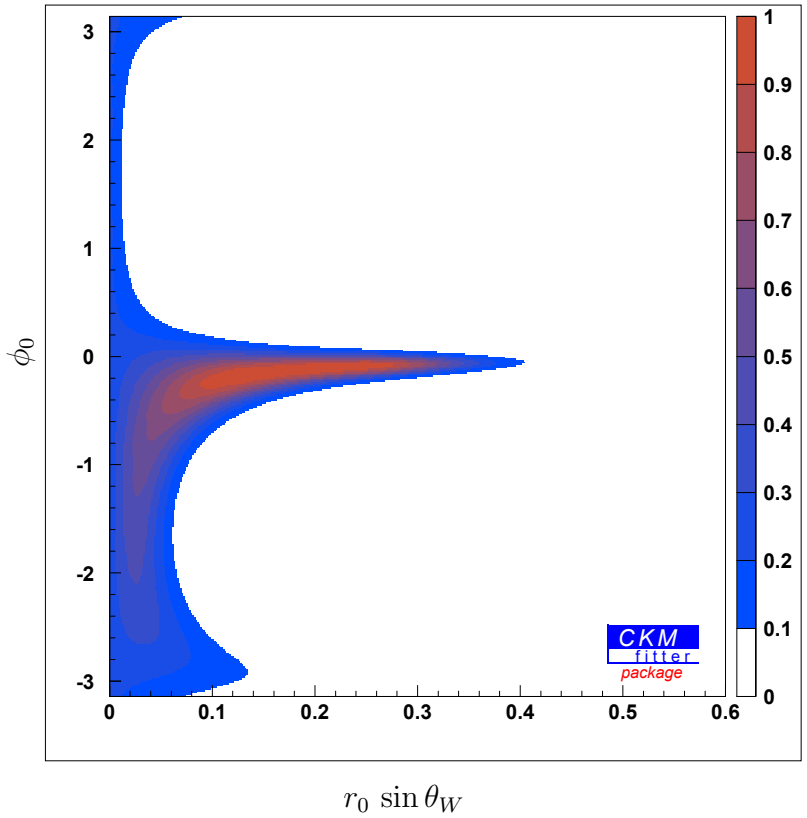


**Figure 4.4:** Fit to CP asymmetries in $B \to \phi K$, using the indirect determination of $\sin 2\beta$ and including the contribution of a NP operator with $\Delta I = 0$, i.e. $(\bar{s}b)(\bar{s}s)$. The NP weak phase is set to $\theta_W = \pi - \gamma_{\rm SM}$. Shown are confidence levels in the plane of the two relevant parameter combinations $|r_0 \sin\theta_W|$ and $\phi_0$.

fore instead of performing a fit, we roughly estimated the ranges, in which the critical observables in $B \to \phi K$ should lie, by scaling the results from $B \to J/\psi K$, yielding

$$\begin{aligned} \Delta A_{\rm CP}(B \to \phi K) &\stackrel{?}{\sim} (0 \text{ to } 0.14)\,, \\ A_I(B \to \phi K) &\stackrel{?}{\sim} -(0.17 \text{ to } 0.01)\,. \end{aligned} \tag{4.21}$$

The data in table 4.2 now shows a non-vanishing $\Delta A_{\rm CP}$ in the estimated range, while the data for the branching ratios has not been updated since then. While the tension is again only at the level of $1-2\sigma$ and therefore far from conclusive, it is interesting to note that the prediction is now confirmed by data. However, as there are now signs for an isospin breaking amplitude in the critical observables

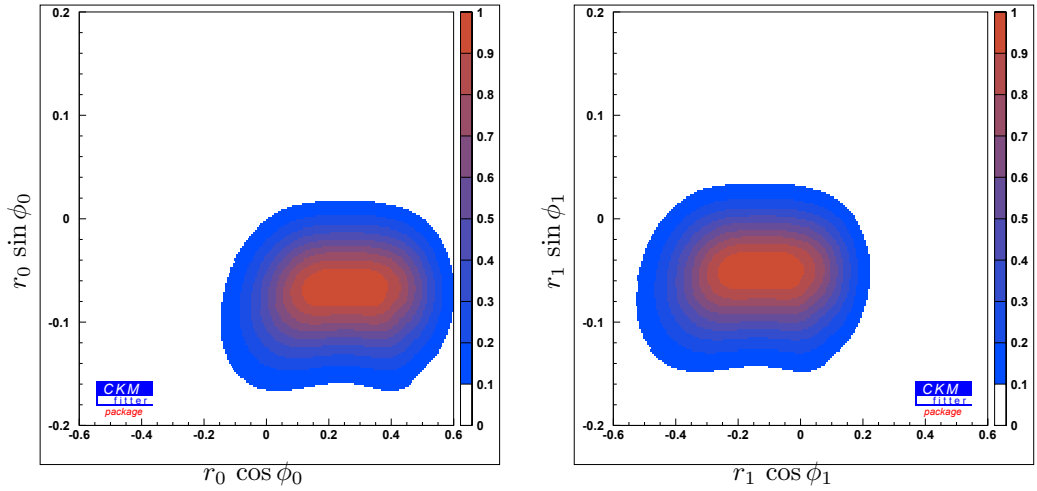


**Figure 4.5:** The result for $r_0\, e^{i\phi_0}$ (left) and $r_1\, e^{i\phi_1}$ (right) in the complex plane from the fit to $\phi K$ observables, with isospin-breaking NP contributions $(\bar{s}b)(\bar{u}u)$ or $(\bar{s}b)(\bar{d}d)$. The new weak phase has been fixed to $\phi_W = \pi - \gamma_{\mathrm{SM}}$.

for $\Delta I = 0$ and $\Delta I = 1$, the corresponding fit is performed. The results are shown in figure 4.5, yielding the $1\sigma$-ranges

$$\begin{aligned} r_0 \cos\phi_0 &= [\ \ 0.03 \text{ to } 0.48]\ , & r_0 \sin\phi_0 &= [-0.11 \text{ to } -0.03]\ , \\ r_1 \cos\phi_1 &= [-0.35 \text{ to } 0.10]\ , & r_1 \sin\phi_1 &= [-0.09 \text{ to } -0.01]\ . \end{aligned} \quad (4.22)$$

Also in this case small phases are preferred. In addition, the fit yields non-vanishing values for both contributions, with the contribution to $\Delta I = 0$ tending to be larger.

Again, there are signs for contributions considerably larger than those expected from the SM, and an increased experimental precision would render this effect even more interesting. Especially an update on the branching fractions would be desirable. Importantly, also here an operator with the structure $(\bar{s}b)(\bar{u}u/\bar{d}d)$ is needed to explain all deviations, and the relative size of the effects in $B \to J/\psi K$ and $B \to \phi K$ corresponds to naive expectations, when assigning the deviations to the same source.

### 4.1.3 $\mathbf{B \to \pi K}$

$B \to \pi K$ decays are also penguin dominated, similarly to $B \to \phi K$. While in contrast to $B \to \phi K$ in this case a tree level operator with tree level matrix

elements exists, it is doubly Cabibbo suppressed and contributes therefore with a relative magnitude of $\lambda$ when using again the power-counting discussed before. Interestingly at this order also electroweak penguin operators contribute, to which this class of decays therefore is sensitive. Apart from decays containing $\eta'$, whose treatment is difficult theoretically, these decays have the largest branching ratios under the charmless $B$ decays, and are therefore known with the highest precision. Specifically, in the decay $B \to \pi^+ K^-$ direct CP violation has been observed for the first time in the $B$ system.

In the SM, the general isospin decomposition for $B \to K\pi$ decays can be parametrized as [69, 114]

$$\begin{aligned} \mathcal{A}(B^- \to \pi^- \bar{K}^0) &= P\left(1 + \epsilon_a\, e^{i\phi_a}\, e^{-i\gamma}\right), \\ -\sqrt{2}\,\mathcal{A}(B^- \to \pi^0 K^-) &= P\left(1 + \epsilon_a\, e^{i\phi_a}\, e^{-i\gamma} - \epsilon_{3/2}\, e^{i\phi_{3/2}}\left(e^{-i\gamma} - q e^{i\omega}\right)\right), \\ -\mathcal{A}(\bar{B}_d \to \pi^+ K^-) &= P\left(1 + \epsilon_a\, e^{i\phi_a}\, e^{-i\gamma} - \epsilon_T\, e^{i\phi_T}\left(e^{-i\gamma} - q_C e^{i\omega_C}\right)\right) \end{aligned} \tag{4.23}$$

and

$$\sqrt{2}\,\mathcal{A}(\bar{B}_d \to \pi^0 \bar{K}^0) = \mathcal{A}(B^- \to \pi^- \bar{K}^0) + \sqrt{2}\,\mathcal{A}(B^- \to \pi^0 K^-) - \mathcal{A}(\bar{B}_d \to \pi^+ K^-) \tag{4.24}$$

fixed by isospin symmetry (i.e. neglecting QED and light quark-mass corrections in the hadronic matrix elements). Here $P$ is the dominating penguin amplitude, whereas the quantities $\epsilon_{T,3/2} e^{i\phi_{T,3/2}}$ contain contributions from tree-operators but are doubly CKM-suppressed, and $q e^{i\omega}$ and $q_C e^{i\omega_C}$ parametrize contributions from electroweak penguin operators relative to those from the tree operators. $\epsilon_a e^{i\phi_a}$ finally is doubly CKM-suppressed and receives only contributions from penguin operators. Without any assumptions on strong interaction dynamics, in the isospin limit one is left with 11 independent hadronic parameters for 9 observables.

The experimental data is given in table 4.7. Compared with the situation in [63], most of the data is essentially unchanged, but the uncertainties slightly decreased. This leads to

$$\Delta A_{\rm CP}^{\pi K} = A_{\rm CP}(\bar{B}^0 \to \phi \bar{K}^0) - A_{\rm CP}(\bar{B}^0 \to \pi^+ K^-) \neq 0 @ \gtrsim 5\sigma\,, \tag{4.25}$$

which is widely discussed in the literature and to be commented on later. The only significant shift has taken place in the time-dependent CP asymmetries, which shifted by $\sim 1\sigma$ each, due to new results from both $B$ factories.

In order to test the SM against possible NP effects in these decays, one needs additional dynamical input. This of course implies a stronger model dependence

than before, therefore results of this kind of analysis have to be taken with care. Qualitative results from QCDF [70] include:

- The $SU(3)_F$ symmetry prediction [91]

$$q\, e^{i\omega} \simeq -\frac{3}{2}\frac{|V_{cb}V_{cs}^*|}{|V_{ub}V_{us}^*|}\frac{C_9 + C_{10}}{C_1 + C_2} \tag{4.26}$$

  only receives small corrections. This relation is the $b \to s$ equivalent of equation (3.48), related to it by $SU(3)$ symmetry.

- The parameter $\epsilon_a\, e^{i\phi_a}$ is negligible in QCDF. Consequently the direct CP asymmetry in $B^- \to \pi^- K^0$ is tiny (in accord with experiment).

- The parameter $q_C\, e^{i\omega_C}$ is of minor numerical importance. This is true for QCDF as well as the diagrammatic analysis, as used for example in [115][2], where this parameter corresponds to the strength of the colour suppressed electroweak penguin amplitude relative to the tree amplitude. There exists an $SU(3)$ relation similar to relation (4.26) for this contribution. However, this is known to receive large corrections already in QCDF from annihilation processes.

- The parameters $\epsilon_T$ and $\epsilon_{3/2}$ are expected to be of the order 20-30%, with the related strong phases of the order 10°. Furthermore, at least at NLO accuracy, the difference between $\epsilon_T\, e^{i\phi_T}$ and $\epsilon_{3/2}\, e^{i\phi_{3/2}}$ is a subleading effect proportional to the small coefficients $a_{2,7,9}$ in QCDF. In the diagrammatical approach the difference is corresponding to the ratio $C/P$.

In the subsequent fits, $\epsilon_a$ is set to zero and the values from [69],

$$q = 0.59 \pm 0.12 \pm 0.07\,, \qquad \omega = -0.044 \pm 0.049\,, \tag{4.27}$$

$$q_C = 0.083 \pm 0.017 \pm 0.045\,, \qquad \omega_C = -1.05 \pm 0.86\,, \tag{4.28}$$

are used in order to reduce the number of independent hadronic parameters within the SM to 5. Notice that the overall penguin amplitude parameter $P$ in equations (4.24) will not be constrained from theory, but will essentially be fixed by the experimental data for the $B^\pm \to \pi^\pm K^0$ branching fractions. Tensions in the fit, or incompatible values for the parameters $\epsilon_{T,3/2}$ and $\phi_{T,3/2}$ then may be taken as indication for possible NP contributions.

[2] This parametrization and its relation to the one used here is given in the appendix 6.1.

| Observable | HFAG [54] | SM fit | NP ($I = 0, 1$) |
|---|---|---|---|
| $\overline{\text{BR}}(\pi^0 K^-) \cdot 10^6$ | $12.9 \pm 0.6$ | 12.4 | 12.8 |
| $\overline{\text{BR}}(\pi^- \bar{K}^0) \cdot 10^6$ | $23.1 \pm 1.0$ | 23.7 | 23.3 |
| $\overline{\text{BR}}(\pi^+ K^-) \cdot 10^6$ | $19.4 \pm 0.6$ | 19.7 | 19.5 |
| $\overline{\text{BR}}(\pi^0 \bar{K}^0) \cdot 10^6$ | $9.8 \pm 0.6$ | 9.3 | 9.7 |
| $\mathcal{A}_{\text{CP}}(\pi^- \bar{K}^0)$ | $0.009 \pm 0.025$ | $0^*$ | $0^*$ |
| $\mathcal{A}_{\text{CP}}(\pi^0 K^-)$ | $0.050 \pm 0.025$ | 0.043 | 0.047 |
| $\mathcal{A}_{\text{CP}}(\pi^+ K^-)$ | $-0.098^{+0.012}_{-0.011}$ | $-0.098$ | $-0.092$ |
| $\eta_{\text{CP}}\, S_{\pi^0 K_S}$ | $-0.57 \pm 0.17$ | $-0.62$ | $-0.78$ |
| $C_{\pi^0 K_S}$ | $0.01 \pm 0.10$ | 0.14 | 0.10 |
| $R_c$ | $1.12 \pm 0.07$ | 1.05 | 1.09 |
| $R_n$ | $0.99 \pm 0.07$ | 1.06 | 1.01 |
| $\Delta A$ | $0.148 \pm 0.028$ | 0.141 | 0.141 |

**Table 4.7:** Experimental data for $B \to \pi K$ decays vs. various best fit results. The third column shows the SM fit with $\Delta\epsilon \neq 0$, which corresponds to $\chi^2/\text{d.o.f.} = 3.8/3$. The fourth column shows the best fit result for $\Delta\epsilon = 0$ (with $\epsilon_T\, e^{i\phi_T} = \epsilon_{3/2}\, e^{i\phi_{3/2}}$ varied according to their QCDF ranges, see text) and a NP contribution from (essentially) $b \to s\bar{u}u$ and $\theta_W = \pi - \gamma_{\text{SM}}$, yielding $\chi^2/\text{d.o.f.} = 2.6/3$.

**New Physics in $\mathbf{B \to \pi K}$?**

The critical observables in $B \to \pi K$ transitions are [116]:

$$\begin{aligned}
R_c &= 2\left[\frac{\text{BR}(B^- \to \pi^0 K^-) + \text{BR}(B^+ \to \pi^0 K^+)}{\text{BR}(B^- \to \pi^- \bar{K}^0) + \text{BR}(B^+ \to \pi^+ K^0)}\right] = 1.12 \pm 0.07\,, \\
R_n &= \frac{1}{2}\left[\frac{\text{BR}(\bar{B}_d \to \pi^+ K^-) + \text{BR}(B_d \to \pi^- K^+)}{\text{BR}(\bar{B}_d \to \pi^0 \bar{K}^0) + \text{BR}(B_d \to \pi^0 K^0)}\right] = 0.99 \pm 0.07\,, \\
\Delta A &= A_{\text{CP}}^{\text{dir}}(B^\pm \to \pi^0 K^\pm) - A_{\text{CP}}^{\text{dir}}(B_d \to \pi^\mp K^\pm) = 0.148 \pm 0.028\,, \\
C_{\pi^0 K_S} &= 0.01 \pm 0.10\,, \qquad \eta_{\text{CP}}\, S_{\pi^0 K_S} = -0.57 \pm 0.17\,,
\end{aligned} \tag{4.29}$$

where in the limit of vanishing corrections to the leading penguin amplitude $R_c = R_n = 1, \Delta A = C_{\pi^0 K_S} = 0$, and $\eta_{\text{CP}} S_{\pi^0 K_S} = -\sin 2\beta$ holds. Within the SM

| | $\epsilon_T$ | $\phi_T$ | $\epsilon_{3/2}$ | $\phi_{3/2}$ | $\mathrm{Re}\,\Delta\epsilon$ | $\mathrm{Im}\,\Delta\epsilon$ |
|---|---|---|---|---|---|---|
| Best: | 0.18 | 0.25 | 0.14 | -0.18 | 0.04 | 0.07 |
| $1\sigma$: | [0.11,0.28] | [0.13,0.44] | [0.04,0.31] | [-0.67,-0.06] | [-0.12,0.16] | [0.05,0.08] |
| $2\sigma$: | [0.06,0.50] | [0.04,0.90] | [0.01,0.59] | [-2.72, 0.05] | [-0.30,0.25] | [0.04,0.10] |
| | $r$ | $\delta$ | $r_c$ | $\delta_c$ | $-\rho_n \cos\theta_n$ | $-\rho_n \sin\theta_n$ |
| [118] | 0.12 | 0.44 | 0.20 | 0.02 | −0.10 | 0.04 |

**Table 4.8:** SM fit results for $\epsilon_T$, $\phi_T$, $\epsilon_{3/2}$, $\phi_{3/2}$, with $\epsilon_a = 0$ and $q\,e^{i\omega}$ and $q_C\,e^{i\omega_C}$ varied according to (4.27),(4.28) from [70]. The best fit values for the latter parameter are obtained as $q = 0.51$, $\omega = 0.005$, $q_C = 0.13$, $\omega_C = -1.91$. For comparison, in the last line estimates for the corresponding hadronic parameters from [118] are shown, which have been obtained by relating $B \to \pi K$ to $B \to \pi\pi$ via $SU(3)$ relations and dynamical assumptions, using the strategy developed in [119] (central values only).

approximation given above, the following relations are expected to hold [117]:

$$R_c - R_n \simeq -2\,\epsilon_{3/2}\left(\epsilon_T - \epsilon_{3/2}\left(1-q^2\right)\right) + \mathcal{O}(\lambda^3)\,, \tag{4.30}$$

$$\eta_{\mathrm{CP}}\,S_{\pi^0 K_S} \simeq -\sin 2\beta + 2\,\cos 2\beta\left(\epsilon_T - \epsilon_{3/2}\right) + \mathcal{O}(\lambda^2)\,, \tag{4.31}$$

$$\Delta A \simeq C_{\pi^0 K_S} \simeq 2\left(\epsilon_T\,\sin\phi_T - \epsilon_{3/2}\,\sin\phi_{3/2}\right) + \mathcal{O}(\lambda^3)\,, \tag{4.32}$$

where it has been used that $\epsilon_{T,3/2} \sim \lambda$, $\phi_{T,3/2} \sim \lambda$, $q_c \simeq 0$, $\omega \simeq 0$, and $\cos\gamma \sim \lambda$ in the SM. Considering the recent experimental data, now the first two relations turn out to be well fulfilled within experimental uncertainties, whereas the third relation shows a tension. Note that the mentioned shift of the data on the time-dependent CP asymmetries moved both coefficients towards the SM expectations, thereby reducing the tensions present before. However, note also that the small value for $C_{\pi^0 K_S}$ is a result of two measurements with opposite signs from BaBar and Belle. The precisely measured value for $\Delta A$ still requires a sizeable difference between $\epsilon_T\,e^{i\phi_T}$ and $\epsilon_{3/2}\,e^{i\phi_{3/2}}$, which is at odds with the expection from QCDF as noted above.

To quantify these observations, this scenario ($\epsilon_a \equiv 0$, $q, q_C$ taken from QCDF) is fitted to the data, leaving $\epsilon_T$ and $\epsilon_{3/2}$ uncorrelated. The results, given in table 4.8, show clearly the reduction of $B \to \pi K$ puzzle for the new data. Especially the key parameter $\Delta\epsilon$ is estimated to be smaller; it corresponds to

$$|C/T| = |\Delta\epsilon/\epsilon_T| = 0.43\,,\ [0.22, 1.00](1\sigma)\,, \tag{4.33}$$

which does not seem unreasonable. This led the authors of [120] to the conclusion that the $B \to \pi K$ data now is compatible with the SM. On the other hand, in another paper [121] it has been concluded that the pattern of the measured time-dependent CP asymmetries shows a tension with the values predicted from $B^- \to \pi^-\pi^0$ with aid of $SU(3)$ arguments (fixing mainly $\epsilon_{3/2}$). As a result they have $S_{\pi^0 K_S} \sim 1$ and essentially $C_{\pi^0 K_S} = \Delta A$ as above, and they point out that a modified electroweak penguin sector with a large weak phase could resolve this tension. In [122] an analysis along similar lines was performed, pointing out that (i) $C_{\pi^0 K_S} \simeq \Delta A$ is an approximate result of a model-independent sumrule [123], holding at the percent level, namely

$$\Delta(K^+\pi^-) + \Delta(K^0\pi^+) = 2\Delta(K^+\pi^0) + 2\Delta(K^0\pi^0)\,, \tag{4.34}$$

where

$$\Delta(f) = \Gamma(\bar{B} \to \bar{f}) - \Gamma(B \to f)\,, \tag{4.35}$$

and (ii) that $S_{\pi^0 K_S} \sim 1$ is extremely sensitive to $\mathrm{BR}(B \to \pi^0 K^0)$. Finally, the authors of [115] find a reduced puzzle, using relation (4.26) and its counterpart for colour-suppressed penguins. They find the tension not significantly relaxed by introducing modified electroweak penguins. Obviously the interpretation of this data stays difficult within the SM. These different results show a model-dependence, which clearly has to be clarified before any reliable conclusions are possible. The value for $\Delta A$ still implies large non-factorizable contributions, when interpreted in SM terms. In addition, as shown above, the fits for $B \to J/\psi K$ and $B \to \phi K$ data prefer the presence of an operator $(\bar{s}b)(\bar{u}u/\bar{d}d)$, which should have an even more pronounced effect in $B \to \pi K$. This motivates the inclusion of NP operators along similar lines as in $B \to J/\psi K$ and $B \to \phi K$, despite the unclear situation in the SM. This is discussed in the following.

### New Physics contributions with $\Delta I = 0$ only

The presence of a NP contribution with $\Delta I = 0$ (this includes the "charming penguin" $b \to sc\bar{c}$, as well as $b \to ss\bar{s}$ and $b \to s(u\bar{u} + d\bar{d})$) has the same impact as the SM parameter $\epsilon_a$ in equations (4.24), except for a possibly different weak phase. Within the adopted approximation one thus obtains

$$\begin{aligned}
-\mathcal{A}(\bar{B}_d \to \pi^+ K^-) &\simeq P\left(1 + r_0\, e^{i\phi_0}\, e^{i\theta_W} - \epsilon_T\, e^{i\phi_T}\left(e^{-i\gamma} - q_C\, e^{i\omega_C}\right)\right)\,, \\
-\sqrt{2}\,\mathcal{A}(B^- \to \pi^0 K^-) &\simeq P\left(1 + r_0\, e^{i\phi_0}\, e^{i\theta_W} - \epsilon_{3/2}\, e^{i\phi_{3/2}}\left(e^{-i\gamma} - q e^{i\omega}\right)\right)\,, \\
\mathcal{A}(B^- \to \pi^- \bar{K}^0) &\simeq P\left(1 + r_0\, e^{i\phi_0}\, e^{i\theta_W}\right)\,,
\end{aligned} \tag{4.36}$$

where $r_0\, e^{i\phi_0}\, e^{i\theta_W}$ parametrizes the NP amplitude. As explained above, the QCDF approach predicts small values $\Delta\epsilon \approx 0$. In the following NP fits to $B \to \pi K$ decays, therefore $\Delta\epsilon = 0$ will be fixed for simplicity, and the common values varied in the ranges

$$\epsilon_T = \epsilon_{3/2} = 0.23 \pm 0.06_{\text{flat}} \pm 0.05_{\text{gauss}}\,, \qquad \phi_T = \phi_{3/2} = -0.13 \pm 0.11_{\text{flat}}\,, \quad (4.37)$$

which have been determined by combining the errors from QCDF [70] on the individual parameters (flat errors are combined linearly, and the larger of the Gaussian errors is chosen). As in the $B \to \phi K$ example, since the leading SM amplitudes are already penguin-suppressed, $r_0 \lesssim \mathcal{O}(1)$ and $\phi_0 \lesssim \mathcal{O}(\lambda)$ is expected. Generically, this implies a sizeable direct CP asymmetry in $B^- \to \pi^- \bar{K}^0$ of the order $\lambda$. The experimental value for that asymmetry should therefore be included in the fit and will essentially constrain the parameter combination $r_0 \sin\phi_0$. On the other hand, using the power-counting $\epsilon_i, q_C, \omega, \phi_i \sim \lambda$, a $\Delta I = 0$ NP operator does not contribute to the critical observable $\Delta A_{\text{CP}}$ in equation (4.29) at order $\lambda$, either. As explained in [118] and references therein, these observables are sensitive to $\Delta I = 1$ operators which, in the SM, are represented by electroweak penguin and tree operators which contain light quarks.

As a result, the NP fit with $\Delta I = 0$ contributions generally leads to a bad description of the experimental data[3], $\chi^2/\text{d.o.f.} = 12.4/5$. It is thus confirmed on a quantitative level that $\Delta I = 0$ NP contributions alone cannot resolve the $B \to K\pi$ puzzles.

### New Physics with $\Delta I = 0, 1$ ($b \to s\bar{u}u$ or $b \to s\bar{d}d$)

Considering now isospin changing operators, the fit becomes more complicated than in the previous cases, because NP contributions with $\Delta I = 1$ induce two new isospin amplitudes

$$r_1^{(1/2)}\, e^{i\theta_W}\, e^{i\phi_1^{(1/2)}}\, P \quad \text{and} \quad r_1^{(3/2)}\, e^{i\theta_W}\, e^{i\phi_1^{(3/2)}}\, P\,,$$

corresponding to final $|K\pi\rangle$ states with $I = 1/2$ or $I = 3/2$. Using the connection between equations (4.24) and isospin amplitudes (see e.g. [124]), this leads —

[3] Notice, that contrary to the $B \to \phi K$ and $B \to J/\psi K$ analyses, reparameterization invariance cannot be exploited here, because certain hadronic input values from QCDF are used. As a consequence, the fit results will explicitly depend on the value of the NP weak phase. Given is the minimum for $\chi^2$.

again within the adopted approximation — to

$$\begin{aligned}
\mathcal{A}(B^- \to \pi^- \bar{K}^0) &\simeq P\Big(1 + \Big[r_0\, e^{i\phi_0} + r_1^{(1/2)}\; e^{i\phi_1^{(1/2)}} + r_1^{(3/2)}\, e^{i\phi_1^{(3/2)}}\Big]\, e^{i\theta_W}\Big)\,, \\
-\sqrt{2}\,\mathcal{A}(B^- \to \pi^0 K^-) &\simeq P\Big(1 + r_0\, e^{i\phi_0}\, e^{i\theta_W} - \epsilon_{3/2}\, e^{i\phi_{3/2}}\left(e^{-i\gamma} - q\, e^{i\omega}\right) \\
&\qquad + \Big[r_1^{(1/2)}\; e^{i\phi_1^{(1/2)}} - 2r_1^{(3/2)}\, e^{i\phi_1^{(3/2)}}\Big]\, e^{i\theta_W}\Big)\,, \\
-\mathcal{A}(\bar{B}_d \to \pi^+ K^-) &\simeq P\Big(1 + r_0\, e^{i\phi_0}\, e^{i\theta_W} - \epsilon_T\, e^{i\phi_T}\left(e^{-i\gamma} - q_C\, e^{i\omega_C}\right) \\
&\qquad - \Big[r_1^{(1/2)}\; e^{i\phi_1^{(1/2)}} + r_1^{(3/2)}\, e^{i\phi_1^{(3/2)}}\Big]\, e^{i\theta_W}\Big)\,. \qquad (4.38)
\end{aligned}$$

Note that in this case, the contributions with $\Delta I = 1$ are not expected to be suppressed with respect to the isospin conserving ones, because the final states contain up quarks. In order to reduce the number of free parameters in the fit, and to avoid unphysical solutions, the following additional assumptions/approximations are applied:

- Following the experimental observation, the direct CP asymmetry in the decay $B^- \to \pi^- \bar{K}^0$ is forced to vanish identically, which yields the relation

  $$r_0\, e^{i\phi_0} + r_1^{(1/2)}\; e^{i\phi_1^{(1/2)}} + r_1^{(3/2)}\, e^{i\phi_1^{(3/2)}} = 0\,.$$

  This is used to eliminate the parameters $r_0$ and $\phi_0$ and effectively implies dealing with a $b \to s\bar{u}u$ operator which does not contribute to $B^- \to \pi^- \bar{K}^0$ in the naive factorization approximation.

- Again, the amplitude parameters $\epsilon_{T,3/2}$ and $\phi_{T,3/2}$ are chosen to be equal and lie within the QCDF ranges, see equation (4.37).

Figure 4.6 displays the results for the NP parameters $r_1^{(1/2)}\, e^{i\phi_1^{(1/2)}}$ and $r_1^{(3/2)}\, e^{i\phi_1^{(3/2)}}$ in the complex plane, for different values of the NP weak phase $\theta_W$. The corresponding $1\sigma$ ranges are collected in Table 4.9. The resulting central values for the observables in the case $\theta_W = \pi - \gamma_{\rm SM}$ are listed in the last column of Table 4.7.

One observes that the fit depends on the value of the NP weak phase $\theta_W$ in an essential way. In particular, depending on whether $\theta_W$ is less or greater than $\pi/2$, disjunct regions in parameter space are encountered. One of the regions always corresponds to relatively small values of $r_1^{(1/2,3/2)} \lesssim 10\%$, whereas for values of $\theta_W$ closer to 0 or $\pi$ solutions with $r_1^{(1/2,3/2)}$ as large 50% are possible. Notably, also in this scenario the measured values for the time-dependent CP asymmetry in $B \to \pi^0 K_S$ are difficult to accomodate, as can be seen in table 4.7. With a phase

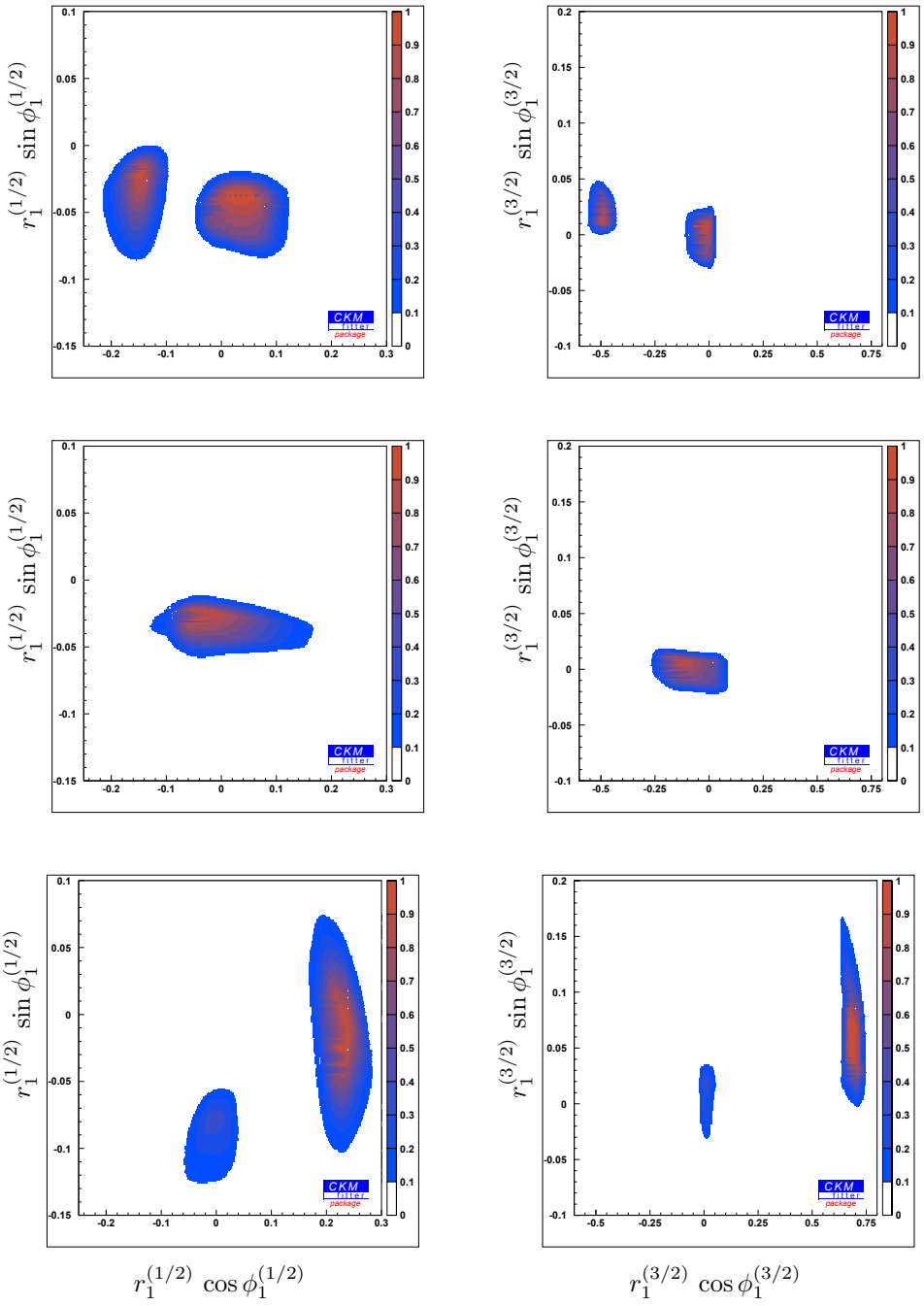


**Figure 4.6:** Fit results for $\Delta I = 1$ NP contributions $r_1^{1/2}\, e^{i\phi_1^{1/2}}$ (left) and $r_1^{3/2}\, e^{i\phi_1^{3/2}}$ (right), with $\epsilon_a = 0$, $\Delta\epsilon = 0$ and $\mathcal{A}_{\rm CP}^{\rm dir}(\pi^-\bar{K}^0) = 0$, see also text. The plots in the upper row refer to a weak phase $\theta_W = 5\pi/6$, the ones in the middle row to $\theta_W = \pi - \gamma_{\rm SM}$, and the lower ones to $\theta_W = \pi/6$.

| $\theta_W$ | $r_1^{(1/2)}$ | $\phi_1^{(1/2)}$ | $r_1^{(3/2)}$ | $\phi_1^{(3/2)}$ | $\chi^2$/d.o.f. |
|---|---|---|---|---|---|
| $5\pi/6$ | [0.03 to 0.09]$\vee$ | [-2.05 to -0.42] | [0.00 to 0.08]$\vee$ | unconstr. | 2.4/3 |
| | [0.12 to 0.17] | | [0.47 to 0.52] | | |
| $\pi - \gamma_{\rm SM}$ | [0.02 to 0.08] | [-2.84 to -0.52] | [0.00 to 0.23] | unconstr. | 2.6/3 |
| $\pi/2$ | [0.03 to 0.09] | [-2.74 to -0.65] | [0.08 to 0.21] | [-0.35 to 3.04] | 1.5/3 |
| $\pi/3$ | [0.15 to 0.21] | [-0.25 to -0.07] | [0.41 to 0.51] | [-0.04 to 0.02] | 0.4/3 |
| $\pi/6$ | [0.20 to 0.26] | [-0.24 to 0.13] | [0.66 to 0.72] | [ 0.03 to 0.15] | 2.5/3 |

**Table 4.9:** Results for the NP parameters in the fit with a $\Delta I = 0, 1$ NP contribution in $B \to \pi K$, for different values of the NP weak phase $\theta_W$. Given are the $1\sigma$ ranges.

differing strongly from the SM one that is possible (for example with $\theta_W \sim \pi/3$), however only with rather large NP contributions. While this is a first hint on a genuine NP phase, it is paid by the model-dependence mentioned before.

### 4.1.4 Conclusions

While within concrete NP models the chiral, flavour and colour structure of new operators could be completely specified, the work presented in this section pursues a model-independent approach. Assuming the dominance of an individual NP operator, the analysis of $B \to J/\psi K$, $B \to \phi K$ and $B \to K\pi$ observables allows for infering semi-quantitative information about the relative size of NP contributions to $b \to s\, c\bar{c}$, $b \to s\, s\bar{s}$, $b \to s\, d\bar{d}$, and $b \to s\, u\bar{u}$ operators. The main conclusions to be drawn are:

- All three modes discussed above prefer the inclusion of an operator transforming non-trivial under isospin, namely an operator with the structure $\mathcal{O}_{\rm NP} \sim (\bar{s}b)(\bar{u}u)$ provides a solution for all observed tensions. Contributions from $(\bar{s}b)(\bar{s}s)/(\bar{c}c)$ might however contribute as well in the fitted contributions, because only isospin amplitudes can be identified. However, $\Delta I = 0$-contributions alone do not explain the observed pattern of observables, unless most of the observed tensions are statistical fluctuations.

- From the comparison of isospin-averaged $B \to J/\psi K$ and $B \to \phi K$ observables it is found that — after correcting for relative penguin, phase-space and normalization factors — NP contributions to $b \to sc\bar{c}$ and $b \to ss\bar{s}$

operators may be of similar size (order 10% relative to a SM tree operator).

- In a scenario, where $b \to sd\bar{d}$ is the *only* source for NP contributions in $B \to \pi K$ observables, while the SM contributions are estimated in QCDF, one cannot simultaneously explain the individual CP asymmetries. In particular, the experimental value for $A_{\rm CP}(\pi^+K^-)$, which does not receive leading NP contributions from $b \to sd\bar{d}$, cannot be reproduced in a scenario with negative strong phase $\phi_T$.

  Moreover, the small direct CP asymmetry for $B^- \to \pi^-\bar{K}^0$ requires the matrix element of a $b \to sd\bar{d}$ NP operator to have either a small coefficient or a small phase.

In all cases, in order to explain the tensions with SM expectations for CP asymmetries without fine-tuning of hadronic parameters, one has to require non-trivial weak phases ($\theta_W \neq 0, \pi$), which could be due to NP, albeit the case $\theta_W = \pi - \gamma_{\rm SM}$ is always allowed, too. A different weak phase is only preferred in $B \to \pi K$, which is however only a very weak indication of a genuine NP phase. Consequently, these findings are still compatible with a SM scenario where non-factorizable QCD dynamics in matrix elements of subleading operators is unexpectedly large.

In the future, an improvement of experimental accuracy, in particular on the isospin-violating observables, could lead to even more interesting constraints on the relative importance of different $b \to sq\bar{q}$ operators and their interpretation within particular NP models. Interestingly, already an update for the branching ratios in the various decays might change the picture.

## 4.2 NP in Mixing: the Golden Mode revisited

Up to now only NP contributions in the decay amplitude have been considered. In the following the opposite assumption will be made, namely that NP affects only the mixing amplitude, while the decay amplitudes stay unaffected. This can be simply parametrized by

$$\phi_d = 2\beta + \phi_{\rm NP}\,. \tag{4.39}$$

On the other hand, the suppressed SM amplitudes have been neglected in the last section. However, it has been noted that the NP contributions fitted for could also represent SM contributions which are larger than expected. If this

interpretation holds, the effects examined in $b \to s$ transitions should show up in $b \to d$ decays as well, as they are related by $SU(3)$ symmetry. Importantly, they should be even more pronounced there, as the Cabibbo suppression is absent — which in most cases renders these decays less useful for NP searches, since the large SM contributions are difficult to disentangle from possible NP ones.

Concentrating on the modes discussed in the last section, the situation is as follows:

- For $B \to \pi K$, numerous studies exist, which use $SU(3)$ to relate these decays to $B \to \pi\pi$. For recent analyses along these lines, see [118, 121, 122]. In addition, first measurements of $B_s \to \pi K$ observables allow by now for an analysis of another set of $SU(3)$ relations [125]. The results are not conclusive, but point to a tension between $B \to \pi K$ and $B \to \pi\pi$. This kind of analysis will not be repeated here.

- For $B \to \phi K$, no simple $SU(3)$ relation exists, as $\phi$ transforms as a sum of $SU(3)$-singlet and -octet, which is why it is not discussed in the following as well.

- The remaining decay, $B^0 \to J/\psi K^0$, is, as pointed out before, also the most interesting, because of its important role in determining $\sin 2\beta$. In light of the discussion in section 4.3, the obvious partner with a $b \to d$ transition would be $B_s \to J/\psi \bar{K}^0$. This process has not been measured so far. However, $\bar{B}^0 \to J/\psi \bar{K}^0$ is also approximately related to the decay $\bar{B}^0 \to J/\psi \pi^0$ [126]; this relation will be discussed in the following.

The work presented below has been published in [127]. Since then, the data mainly for $|V_{ub}/V_{cb}|$ changed slightly. This results in $\eta_{\rm CP} S + \sin 2\beta$ now being compatible with zero as discussd already in section 2.2.2. However, as also noted before, $B \to \tau\nu$ points towards a discrepancy even larger than the one discussed here. Therefore, the analysis with the old values is presented below, and the results are considered to be still valid. In addition, the inclusion of the updated value for $\sin 2\beta$ would only change the extracted range for $\phi_{\rm NP}$, as will be seen from the analysis below, which is compatible with zero anyway. The other observables are given explicitly, where they differ, otherwise they are listed in tables 4.1 and 4.4.

Starting point of the analysis is again the extraction of the CKM parameters $\beta, \gamma$ independent from NP in mixing, as discussed in section 2.2.2. From that fit,

$$(\phi_d)_{J/\psi K^0} - 2\beta_{\text{true}} = -(8.7^{+2.6}_{-3.6} \pm 3.8)^\circ \tag{4.40}$$

is obtained.

The amplitude for $B \to J/\psi K$ is written similarly to equation (4.2) as

$$A(B^0 \to J/\psi K^0) = \left(1 - \lambda^2/2\right) \mathcal{A} \left[1 + \epsilon a e^{i\theta} e^{i\gamma}\right], \tag{4.41}$$

where

$$\mathcal{A} \equiv \lambda^2 A \left[A_{\text{T}}^{(c)} + A_{\text{P}}^{(c)} - A_{\text{P}}^{(t)}\right] \tag{4.42}$$

and

$$a e^{i\theta} \equiv R_u \left[\frac{A_{\text{P}}^{(u)} - A_{\text{P}}^{(t)}}{A_{\text{T}}^{(c)} + A_{\text{P}}^{(c)} - A_{\text{P}}^{(t)}}\right] \tag{4.43}$$

are CP-conserving parameters, with $A_{\text{T}}^{(c)}$ and $A_{\text{P}}^{(j)}$ denoting strong amplitudes that are related to tree-diagram-like and penguin topologies (with internal $j \in \{u, c, t\}$ quarks), respectively. As the charged counterparts of the decays will not be used in the analysis below, the isospin classification discussed in previous chapters is not relevant here.

The Cabibbo suppressed part of the amplitude is usually neglected as discussed in the last section. However, $a e^{i\theta}$ suffers from large hadronic uncertainties, and may be enhanced through long-distance effects. The generalization of equations (4.3) to take also the penguin effects into account can be written as

$$\frac{-\eta_{\text{S,L}} S(J/\psi K_{\text{S,L}})}{\sqrt{1 - C(J/\psi K_{\text{S,L}})^2}} = \sin(\phi_d + \Delta\phi_d), \tag{4.44}$$

where

$$\sin\Delta\phi_d = \frac{2\epsilon a \cos\theta \sin\gamma + \epsilon^2 a^2 \sin 2\gamma}{N\sqrt{1 - C(J/\psi K_{\text{S,L}})^2}}, \tag{4.45}$$

$$\cos\Delta\phi_d = \frac{1 + 2\epsilon a \cos\theta \cos\gamma + \epsilon^2 a^2 \cos 2\gamma}{N\sqrt{1 - C(J/\psi K_{\text{S,L}})^2}}, \tag{4.46}$$

with $N \equiv 1 + 2\epsilon a \cos\theta \cos\gamma + \epsilon^2 a^2$, so that

$$\tan\Delta\phi_d = \frac{2\epsilon a \cos\theta \sin\gamma + \epsilon^2 a^2 \sin 2\gamma}{1 + 2\epsilon a \cos\theta \cos\gamma + \epsilon^2 a^2 \cos 2\gamma}. \tag{4.47}$$

Concerning direct CP violation, the present measurement reads

$$C(J/\psi K^0) = -0.003 \pm 0.019, \tag{4.48}$$

which is again an average over the $J/\psi K_{\rm S}$ and $J/\psi K_{\rm L}$ final states [128, 129]. Consequently, the deviation of the terms $\sqrt{1 - C(J/\psi K_{\rm S,L})^2}$ from one is at most at the level of 0.0002, and is hence completely negligible.

In the following, the decay $B^0 \to J/\psi\pi^0$ will be used to constrain the penguin contributions from data. As can be seen in [130], it is related to $B^0 \to J/\psi K^0$ via $SU(3)$ in the approximation that isospin symmetry holds and that the emission-annihilation parameter $EA_2$ can be neglected. This can be checked from data by considering the decay $B \to \bar{D}^0\phi$ [130], which proceeds only via this diagram. This decay has not been measured yet, the upper limit is given by [35]

$$\mathrm{BR}(B^0 \to \bar{D}^0\phi) \leq 1.16 \times 10^{-5}\,. \tag{4.49}$$

However, in this decay the amplitude enters with the CKM parameter combination $V_{cb}^* V_{ud}$, i.e. it is enhanced by a factor of $1/\lambda$ in the amplitude with respect to $B^0 \to J/\psi\pi^0$. In light of this and $\mathrm{BR}(B^0 \to J/\psi\pi^0) = 2 \times 10^{-5}$ the assumption $EA_2 \to 0$ therefore seems justified, even if this is only an order-of-magnitude estimate, because the hadronization will obviously differ in the two channels. A combination of the neglected amplitudes can also be measured via $B_s \to J/\psi\pi^0$, but the corresponding upper limit is not restrictive at the moment [35]: $\mathrm{BR}(B_s \to J/\psi\pi^0) \leq 1.2 \times 10^{-3}$.

In reference [126], this ansatz was used to constrain the penguin effects in the golden mode. However, the quality of the data has improved such that it is possible to go beyond this paper by allowing for $\phi_d^{\rm NP} \neq 0^\circ$. Moreover, as will be seen below, the current $B$ factory data point already towards a *negative* value of $\Delta\phi_d$, where mixing-induced CP violation in $B^0 \to J/\psi\pi^0$ is the driving force, thereby reducing the tension (4.40) in the fit of the UT.

In the SM, the amplitude for $B \to J/\psi\pi^0$ is given by

$$\sqrt{2}A(B^0 \to J/\psi\pi^0) = \lambda\mathcal{A}'\left[1 - a' e^{i\theta'} e^{i\gamma}\right], \tag{4.50}$$

where the $\sqrt{2}$ factor is associated with the $\pi^0$ wavefunction, while $\mathcal{A}'$ and $a' e^{i\theta'}$ are the counterparts of the parameters defined in equations (4.42) and (4.43), respectively. The CP asymmetry $a_{\rm CP}(t; J/\psi\pi^0)$ (see equation (2.52)) has recently

been measured by the BaBar [131] and Belle [132] collaborations, yielding the following averages [54]:

$$C(J/\psi\pi^0) = -0.10 \pm 0.13, \tag{4.51}$$

$$S(J/\psi\pi^0) = -0.93 \pm 0.15\,. \tag{4.52}$$

Note that the error of $S(J/\psi\pi^0)$ is that of the HFAG, which is not inflated due to the inconsistency of the data.

These measurements allow for calculating $a'$ as functions of $\theta'$. The following two relations are obtained from $C(J/\psi\pi^0)$ and $S(J/\psi\pi^0)$ ($\mathcal{O} = C$ and $S$, respectively):

$$a' = U_{\mathcal{O}} \pm \sqrt{U_{\mathcal{O}}^2 - V_{\mathcal{O}}}, \tag{4.53}$$

where

$$U_C \equiv \cos\theta' \cos\gamma + \frac{\sin\theta' \sin\gamma}{C(J/\psi\pi^0)}, \quad V_C \equiv 1, \tag{4.54}$$

and

$$U_S \equiv \left[\frac{\sin(\phi_d+\gamma) + S(J/\psi\pi^0)\cos\gamma}{\sin(\phi_d+2\gamma) + S(J/\psi\pi^0)}\right]\cos\theta'\,, \tag{4.55}$$

$$V_S \equiv \frac{\sin\phi_d + S(J/\psi\pi^0)}{\sin(\phi_d+2\gamma) + S(J/\psi\pi^0)}. \tag{4.56}$$

The intersection of the $C(J/\psi\pi^0)$ and $S(J/\psi\pi^0)$ contours fixes then the hadronic parameters $a'$ and $\theta'$ in the SM; when allowing for an additional NP phase, one has to take into account $S(J/\psi K^0)$ together with $S(J/\psi\pi^0)$ in order to have a constraint in the $a'$–$\theta'$ plane. From $C(J/\psi K^0)$ comes another constraint, which is also of the form (4.53) with the replacements $a' \to \epsilon a$ and $\theta' \to 180^\circ + \theta$. It should be stressed that equations (4.53)–(4.55) are valid exactly as these expressions follow from the SM structure of $B^0 \to J/\psi\pi^0$.

Within the approximation discussed above, the $SU(3)$ limit now leads to

$$a' = a, \quad \theta' = \theta\,. \tag{4.57}$$

Thanks to these relations, the shift $\Delta\phi_d$ can be determined by means of equations (4.44)–(4.48) from the data. They are subject to $SU(3)$ breaking corrections, due to sizable non-factorizable effects expected in these decays. Their impact on the determination of $\Delta\phi_d$ can be easily inferred from equation (4.47). Neglecting terms of order $\epsilon^2$, there is a linear dependence on $a\cos\theta$. Consequently, corrections to the left-hand side of equation (4.57) propagate linearly,

while $SU(3)$-breaking effects in the strong phases will generally lead to an asymmetric uncertainty for $\Delta\phi_d$.

There is another constraint, which follows from the CP-averaged branching ratios. It is introduced by

$$\begin{aligned} H &\equiv \frac{2}{\epsilon}\left[\frac{\mathrm{BR}(B_d \to J/\psi\pi^0)}{\mathrm{BR}(B_d \to J/\psi K^0)}\right]\left|\frac{\mathcal{A}}{\mathcal{A}'}\right|^2 \frac{\Phi_{J/\psi K^0}}{\Phi_{J/\psi\pi^0}} \\ &= \frac{1-2a'\cos\theta'\cos\gamma+a'^2}{1+2\epsilon a\cos\theta\cos\gamma+\epsilon^2 a^2}, \end{aligned} \tag{4.58}$$

where the $\Phi_{J/\psi P} \equiv \Phi(M_{J/\psi}/M_{B^0}, M_P/M_{B^0})$ are phase-space factors [133]. In order to extract $H$ from the data, one has to analyze the $SU(3)$-breaking corrections to $|\mathcal{A}/\mathcal{A}'|$. Assuming them to be naively factorizable, they are given by the ratio of two form factors, evaluated at $q^2 = M^2_{J/\psi}$. This ratio has been studied in detail using QCD light-cone sum rules (LCSR) [134]. Here, the result for the form factor ratio at $q^2 = 0$ from [135, 136],

$$\frac{f^+_{B\to K}(0)}{f^+_{B\to\pi}(0)} = 1.38^{+0.11}_{-0.10}, \tag{4.59}$$

is used and the extrapolation to $q^2 = M^2_{J/\psi}$ by using a simple BK parametrization [137],

$$f^+(q^2) = f^+(0)\left[\frac{M_B^2\, M_*^2}{(M_*^2-q^2)(M_B^2-\alpha q^2)}\right], \tag{4.60}$$

is performed. Here $M_*$ denotes the mass of the ground state vector meson in the relevant channel and the pole at $q^2 = M^2/\alpha$ models the contribution of the hadronic continuum for $q^2 > M_*^2$. The BK parameter $\alpha$ has been fitted to the $B \to \pi$ lattice data to be $\alpha_\pi = 0.53 \pm 0.06$. Nothing is known about the value of $\alpha$ for the $B \to K$ form factor and the simple assumption will be used that the main $SU(3)$ breaking effect is due to the shift of the continuous part of the spectral function from the $B\pi$ to the $BK$ threshold. This leads to $\alpha_K = 0.49 \pm 0.05$, and – extrapolating in this way to $q^2 = M^2_{J/\psi}$ – finally to

$$\frac{f^+_{B\to K}(M^2_{J/\psi})}{f^+_{B\to\pi}(M^2_{J/\psi})} = 1.34 \pm 0.12. \tag{4.61}$$

Using [54]

$$\mathrm{BR}(B^0 \to J/\psi K^0) = (8.63 \pm 0.35) \times 10^{-4} \tag{4.62}$$

and

$$\mathrm{BR}(B^0 \to J/\psi\pi^0) = (0.20 \pm 0.02) \times 10^{-4}, \tag{4.63}$$

the obtained value is

$$H = 1.53 \pm 0.16_{\mathrm{BR}} \pm 0.27_{\mathrm{FF}}\,, \tag{4.64}$$

where the errors given are induced by the branching ratios and the form-factor ratio respectively.

Using the $SU(3)$-assumption (4.57), the following relation [133]

$$C(J/\psi K^0) = -\epsilon H C(J/\psi \pi^0), \tag{4.65}$$

can be obtained, which corresponds to equation (3.62) for this case. This would in principle offer an interesting probe for $SU(3)$ breaking, however, the value of $H$ given above yields $C(J/\psi K^0) = 0.01 \pm 0.01$, which is consistent with (4.48), but obviously too small for a powerful test. For such a test to be effective, at least one of the CP asymmetries has be measured significantly different from zero.

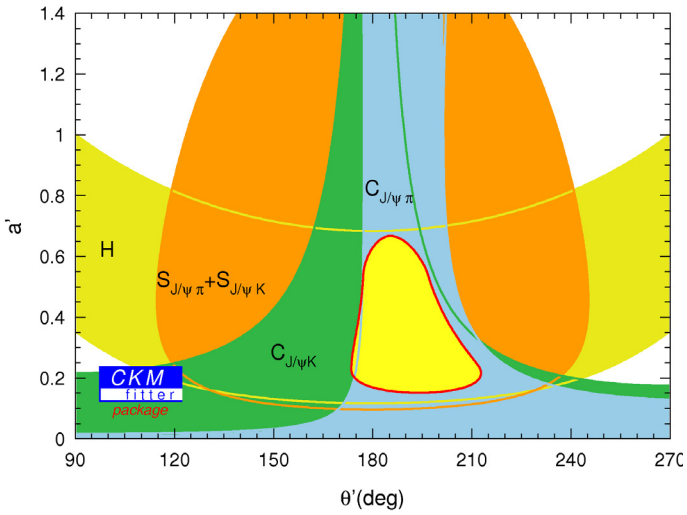


**Figure 4.7:** The $1\,\sigma$ ranges (corresponding to 39% CL) in the $\theta'$–$a'$ plane with current data.

Applying once more equation (4.53) with

$$U_H = \left(\frac{1+\epsilon H}{1-\epsilon^2 H}\right)\cos\theta'\cos\gamma\,, \tag{4.66}$$

$$V_H = (1-H)/(1-\epsilon^2 H), \tag{4.67}$$

i.e. $\mathcal{O} = H$, results in another constraint in the $a' - \theta'$ plane. In contrast to the

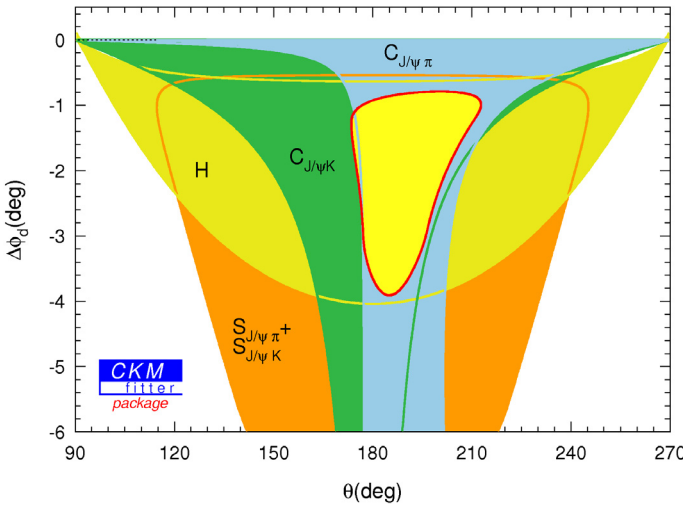


**Figure 4.8:** $\Delta\phi_d$ for the constraints shown in figure 4.7.

CP asymmetries of $B^0 \to J/\psi\pi^0$, here $SU(3)$ breaking effects enter implicitly through the determination of $H$.

In figure 4.7, $1\sigma$ ranges for the fits in the $\theta'$–$a'$ plane are shown for the current data. The major implication of $S(J/\psi\pi^0)$ is $\theta' \in [90°, 270°]$. Looking at equation (4.44), applied to $B \to J/\psi\pi$, this is actually expected. $S(J/\psi K^0)$ fixes the NP phase essentially to $(\phi_d)_{J/\psi K^0} - 2\beta_{\text{true}}$, as the NP phase is an $\mathcal{O}(1)$ effect in $S(J/\psi K^0)$, while the additional SM contribution is suppressed by $\epsilon$. The negative central value of $C(J/\psi\pi^0)$ prefers $\theta' > 180°$. The intersection of the $C(J/\psi\pi^0)$ and $H$ bands, which falls well into the $S(J/\psi\pi^0, J/\psi K^0)$ as well as the $C(J/\psi K^0)$ region, gives then

$$a' \in [0.15, 0.67] \quad \text{and} \quad \theta' \in [174, 213]° \quad (1\sigma)\,. \tag{4.68}$$

Note that all three constraints give finally an unambiguous solution for these parameters.

In figure 4.8 the constraints shown in figure 4.7 are converted into the $\theta$–$\Delta\phi_d$ plane with the help of equations (4.57) and (4.45)–(4.47). A negative value of $\Delta\phi_d$ emerges; the global fit to all observables yields

$$\Delta\phi_d \in [-3.9, -0.8]°\,, \tag{4.69}$$

mainly due to the constraints from $H$ and $C(J/\psi\pi^0)$, corresponding to a SM

mixing phase of $\phi_d = (42.4^{+3.4}_{-1.7})^\circ$. Furthermore, the fit gives

$$\phi_d^{\rm NP} \in [-13.8, 1.1]^\circ\,, \tag{4.70}$$

which includes the SM value $\phi_d^{\rm NP} = 0^\circ$. Consequently, the negative sign of the SM correction $\Delta\phi_d$ softens the tension in the fit of the UT. Performing the fit in a SM scenario, where $\phi_{\rm NP} \equiv 0$, yields

$$\Delta\phi_d^{\rm SM} \in [-4.1, -0.6]^\circ\,, \tag{4.71}$$

where only $B \to J/\psi\pi$ data and ${\rm BR}(B \to J/\psi K)$ have been used.

The impact of $SU(3)$-breaking corrections has been studied by setting $a = \xi a'$ in relation (4.57) and uncorrelating $\theta$ and $\theta'$. Even when allowing for $\xi \in [0.5, 1.5]$ and $\theta, \theta' \in [90, 270]^\circ$ in the fit, and using a 50% increased error for the form-factor ratio in view of non-factorizable contributions to $|\mathcal{A}/\mathcal{A}'|$, the global fit yields $\Delta\phi_d \in [-6.7, 0.0]^\circ$ and $\phi_d^{\rm NP} \in [-14.9, 4.0]^\circ$, determined now mostly by $C(J/\psi K^0)$ and $H$. Consequently, these $SU(3)$-breaking effects do not alter the conclusions from this analysis. It should be emphasized that the novel feature of this determination of $\phi_d^{\rm NP}$ in comparison with other analyses in the literature is, that the doubly Cabibbo-suppressed SM contributions are included, which is crucial in order to eventually detect or exclude such a NP effect.

In view of the relatively large experimental errors in $B \to J/\psi\pi$, again final conclusions cannot be drawn. However, the increasing experimental precision will further constrain the hadronic parameters. The final reach for a NP contribution to the $B_d^0$–$\bar{B}_d^0$ mixing phase will strongly depend on the measured values of the CP asymmetries of $B^0 \to J/\psi\pi^0$, which are challenging for LHCb because of the neutral pions (where, as noted above, a similar analysis could be performed with $B_s^0 \to J/\psi K_{\rm S}$ [133]), but can be measured at future Super-$B$ factories.

The possible impact is illustrated through two benchmark scenarios, assuming a future reduction of the experimental uncertainties of the CP asymmetries of $B^0 \to J/\psi K^0$ by a factor of 2, and errors of the branching ratios and $\gamma$ that are five times smaller; the scenarios agree in $C(J/\psi\pi^0) = -0.10 \pm 0.03$, but differ in $S(J/\psi\pi^0)$. In the high-$S$ scenario (a), $S = -0.98 \pm 0.03$ is assumed. As can be seen in figure 4.9, $\Delta\phi_d \in [-3.1, -1.8]^\circ$ (with $a' \sim 0.42$, $\theta' \sim 191^\circ$) would then come from the lower value of $S$ and $H$, which is assumed to be $H = 1.53 \pm 0.03 \pm 0.27$. In the low-$S$ scenario (b), $S = -0.85 \pm 0.03$ is assumed. In this case, $\Delta\phi_d \in [-1.2, -0.8]^\circ$ (with $a' \sim 0.18$, $\theta' \sim 201^\circ$) would be determined

by $S$ and $C$ alone, while $H$ would only be used to rule out the second solution. By the time the accuracies of these benchmark scenarios can be achieved, hopefully also a much better picture of $SU(3)$ breaking effects through data about $B_{s,d,u}$ decays will have been emerged. A step in that direction will be discussed in the following section.

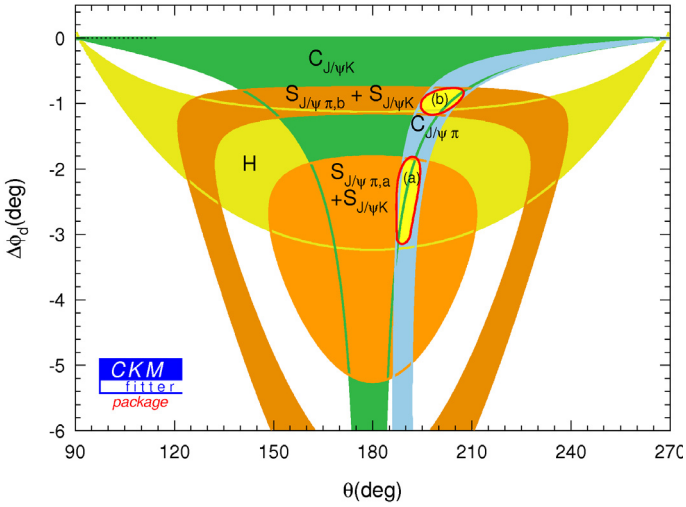


**Figure 4.9:** Future benchmark scenarios, as discussed in the text.

Since the experimental uncertainty of $(\phi_d)_{J/\psi K^0}$ could be reduced to $\sim 0.3^\circ$ at an upgrade of LHCb and an $e^+e^-$ Super-$B$ factory, these corrections will be essential. It is interesting to note that the quality of the data in flavour physics will soon reach a level, where subleading effects, i.e. doubly Cabibbo-suppressed penguin contributions, have to be taken into account. In particular, in the analyses of CP violation in the golden $B^0 \to J/\psi K_{\rm S,L}$ modes this is mandatory in order to fully exploit the physics potential for NP searches.

Obviously, this analysis does not rule out NP effects in the amplitude as the reason for the observed shift. It merely states that the relation between $B \to J/\psi K$ and $B \to J/\psi \pi$ seems to be SM-like, and that large hadronic SM effects therefore could be the explanation. Recently, in [138] the subleading effects in the SM have been re-estimated to be small, of order $\mathcal{O}(10^{-3})$, based of a non-perturbative estimation of rescattering effects. This estimate again relies on some assumptions, importantly in the expression for the matrix element of an operator

$T^c$ (proportional to $\lambda_{cs}$, leading to $\Delta C = 0$ and $|\Delta B| = |\Delta S| = 1$) the sum over all possible hadronic intermediate states $k$ appears,

$$\langle f|T^c|B^0\rangle = \sum_k \langle f|S_0|k\rangle\langle k|T^c|B^0\rangle\,, \tag{4.72}$$

where each term in the sum is assumed to be smaller than the left hand side. There is no obvious justification for that assumption. However, this estimate renders the analysis of the last section even more relevant, since the option of large SM effects would be ruled out. In that case, the analysis presented here confirms that a NP contribution in the amplitude is sufficient to explain the data, and that that contribution shows a SM-like transformation behaviour under $SU(3)$. In any case, this discussion shows that to finally identify NP in non-leptonic decays, the combination of several decay modes has to be taken into account, and that a better understanding of SM hadronic effects is necessary.

## 4.3 U-spin and its breaking

As seen in the previous section, $SU(3)$ and its breaking play an important role in distinguishing NP effects from SM ones. In this section, the formalism developed in section 3.3.4 will be applied to non-leptonic two-body $B$ decays. First, some general comments will be given regarding the decays of charged $B$ mesons in section 4.3.1, and two sample applications will be discussed in some detail, namely $B \to J/\psi(K \text{ or } \pi)$ and $B \to D(K \text{ or } \pi)$, in order to check how far one can get with present data without any restrictive ad-hoc assumptions. The decays of neutral $B$ mesons will then be discussed in section 4.3.2, fitting the present $B \to P^+P^-$ data in the $U$-spin limit to check for $U$-spin violations, and discussing decays to CP eigenstates in some detail. Finally, some concluding remarks are given.

Part of the work presented in this section has been published in [139], and most of it is included in [140].

### 4.3.1 Decays of charged B mesons

As mentioned in section 3.3.4, the charged $B$ mesons are $U$-spin singlets and hence — due to the simple $U$-spin structure of the effective Hamiltonian — the final state has to be a doublet or, when including $U$-spin breaking, a quadruplet.

Considering two-body decays, this corresponds to having one final-state meson in a $U$-spin doublet, while the second one has to be either $U$-spin singlet or -triplet.

Clearly the case of $\Delta C = \pm 1$ is the simplest one, since only a single CKM factor arises. This leads to a considerable reduction of parameters, but of course also of observables. An example will be discussed below.

In the case where one of the final state mesons is part of a triplet, there is another complication. Since $U$-spin breaking is not that small, the mass eigenstates are quite different from the $U$-spin eigenstates, i.e. there is not even an approximate mass eigenstate corresponding to an $s\bar{s} - d\bar{d}$ $U$-spin state. As already described in section 3.3.4 (see equations (3.59) ff.), there are three mass eigenstates contributing to $U_z = 0$, which all have to be taken into account. Due to that and the fact that in charged decays no time-dependent measurements are available, it is generally difficult to include breaking corrections without introducing too many parameters. Below two examples are discussed, where the neutral meson is chosen to be a $U$-spin singlet, thereby circumventing part of the complications described above.

### The decays $B \to J/\psi\,(K$ or $\pi)$

As a first application, the decays $B \to J/\psi\,(K \text{ or } \pi)$ are considered, which are under the simplest cases of $\Delta C = 0$ from the group-theoretical point of view, because of $B^-$ and $J/\psi$ being $U$-spin singlets. This results in the simple structure

$$\left\langle B^- | \mathcal{H}_{\text{eff}} | J/\psi\, K^-\,(\pi^-) \right\rangle = \sum_{q=u,c} \lambda_{q\,s/d} \left( A_{q,1/2} \pm A^{\epsilon}_{q,1/2} \right) . \tag{4.73}$$

The analysis is based on the data shown in tables 4.10 and 4.11.

| Decay | BR/$10^{-4}$ | $A_{\text{CP}}$ |
|---|---|---|
| $B^- \to J/\psi K^-$ | $10.07 \pm 0.035$ | $0.017 \pm 0.016(*)$ |
| $B^- \to J/\psi \pi^-$ | $0.49 \pm 0.06(*)$ | $0.09 \pm 0.08$ |

**Table 4.10:** Measurements for the decays $B^- \to J/\psi(K \text{ or } \pi)$, data taken from the PDG [35]. $(*)$: Error enhanced by PDG because of inconsistent measurements.

As a first step, it is checked for $U$-spin violation by testing relation (3.62).

Inserting the data from table 4.10 and neglecting tiny phase space differences results in

$$(A_{\mathrm{CP}} \times BR)_{B^- \to J/\psi K^-} + (A_{\mathrm{CP}} \times BR)_{B^- \to J/\psi \pi^-} = 0.22 \pm 0.17\,, \tag{4.74}$$

adding errors simply in quadrature. This result is not significant and a real test may only be performed, if at least one of the asymmetries is measured significantly different from zero.

In many applications naive factorization has been applied, which allows to include at least the factorizable part of $U$-spin breaking. In this picture one expects the ratio of branching ratios to be given only in terms of CKM factors and the ratio of form factors. One gets the theoretical prediction

$$\frac{BR(B^- \to J/\psi K^-)}{BR(B^- \to J/\psi \pi^-)} \sim \left( \frac{F^{B\to K}(M^2_{J/\psi})}{F^{B\to\pi}(M^2_{J/\psi})} \right)^2 \left| \frac{V^*_{cb} V_{cs}}{V^*_{cb} V_{cd}} \right|^2 = 33.9 \pm 6.1\,, \tag{4.75}$$

where the form factor ratio is evaluated as described in the last section (see equation (4.59) ff.). This has to be contrasted with the experimental number

$$\frac{BR(B^- \to J/\psi K^-)}{BR(B^- \to J/\psi \pi^-)} = \begin{cases} 19.2 \pm 1.5 & \text{(measurement of the ratio)} \\ 21.4 \pm 1.9 & \text{(combined single measurements).} \end{cases} \tag{4.76}$$

The sizable discrepancy indicates the well known fact that these decays have large non-factorizable contributions.

| Decay | BR/$10^{-4}$ | $A_{\mathrm{CP}}$ | $S_{\mathrm{CP}}$ |
|---|---|---|---|
| $\bar{B}^0 \to J/\psi \bar{K}^0$ | $8.71 \pm 0.32$ | $-0.002 \pm 0.020(*)$ | $0.657 \pm 0.025$ |
| $\bar{B}^0 \to J/\psi \pi^0$ | $0.205 \pm 0.024$ | $0.10 \pm 0.13$ | $-0.93 \pm 0.29(**)$ |

**Table 4.11:** Measurements for the decays $\bar{B} \to J/\psi(K \text{ or } \pi)$. Time-dependent measurements are taken from the HFAG [54], other data from the PDG [35]. $(*)$: Error enhanced by the PDG due to inconsistent measurements. $(**)$: Error enhanced according to the PDG prescription for the same reason.

On the other hand, the data in table 4.10 are not sufficient to allow a fit to the general group-theoretical expressions. Hence additional assumptions are necessary, which will be taken to be the following:

- The amplitude proportional to $\lambda_{ud/s} = V_{ub}V^*_{ud/s}$ is expected to be small compared to the one proportional to $\lambda_{cd/s} = V_{cb}V^*_{cd/s}$, because its tree contribution has only penguin matrix elements. Hence the breaking corrections to this amplitude will not be taken into account.

- In addition, isospin symmetry will be used. This means that also the decays of the neutral $B$ modes have to be taken into account, since they are the isospin partners of the charged $B$ mesons. When making use of isospin, the matrix elements identified in the $U$-spin analysis are splitted into their two isospin components as shown in table 3.4. Here the contribution with $\Delta I = 1, 3/2$ proportional to $\lambda_{cs/d}$ is neglected, which receives contributions from penguin matrix elements of electroweak penguin operators only; hence the corresponding penguin contributions are assumed to be a pure $\Delta I = 0(1/2)$ amplitude for both the $b \to s$ and $b \to d$ transition.

For the neutral $B$ mesons the data shown in table 4.11 are included. Using the above assumptions leads to the following parametrization:

$$\begin{aligned}
< B^-|\mathcal{H}_{\text{eff}}|J/\psi K^- > &= N_{J/\psi K}\left(1 + x_\epsilon + \epsilon\, e^{-i\gamma}\, r_0\, e^{i\phi_0}\right) , \\
< B^-|\mathcal{H}_{\text{eff}}|J/\psi \pi^- > &= \frac{\lambda}{1-\lambda^2/2} N_{J/\psi K}\left(-1 + x_\epsilon + e^{-i\gamma}\, r_0\, e^{i\phi_0}\right) , \\
< \bar{B}^0|\mathcal{H}_{\text{eff}}|J/\psi \bar{K}^0 > &= N_{J/\psi K}\left[1 + x_\epsilon + \epsilon\, e^{-i\gamma}\left(r_0\, e^{i\phi_0} - 2r_1^K\, e^{i\phi_1^K}\right)\right] , \\
< \bar{B}^0|\mathcal{H}_{\text{eff}}|J/\psi \pi^0 > &= \frac{\lambda}{1-\lambda^2/2} N_{J/\psi K}\left[-1 + x_\epsilon + e^{-i\gamma}\left(r_0\, e^{i\phi_0} - 2r_{3/2}^\pi\, e^{i\phi_{3/2}^\pi}\right)\right] ,
\end{aligned} \tag{4.77}$$

where the normalization factor $N_{J/\psi K}$ is chosen in such a way that its square fulfills $N^2_{J/\psi K} = \text{BR}(B^- \to J/\psi K^-)$ in absence of $U$-spin breaking and penguin effects. As a consequence, the corresponding ratios of lifetimes and phase space factors have to be taken into account when computing the branching ratios from the parametrization (4.77) for the other decays. Furthermore, the ratios $r_0$, $r_1^K$ and $r_{3/2}^\pi$ denote the penguin and $u$ quark tree contributions (normalized to $N_{J/\psi K}$), which are defined to contain a factor $R_u$. Finally, the complex parameter $x_\epsilon$ represents the $U$-spin breaking part in the leading contribution, again normalized to $N_{J/\psi K}$.

As inputs from the CKM fit, in addition to the ones described above, those from table 4.12 are used, taken from [29], where the data from $B \to J/\psi K$ is not part of the fit[4].

[4]In fact, the value obtained for the angle $\gamma$ is determined including the input of $B \to J/\psi K$.

| Parameter | Global fit value |
|---|---|
| $\lambda$ | $0.2252 \pm 0.0008$ |
| $\gamma$ | $\left(66.8^{+5.4}_{-3.8}\right)^\circ$ |
| $\beta_{w/oJ/\psi}$ | $0.48^{+0.02}_{-0.04}$ |

**Table 4.12:** CKM parameters taken from [29], results as of summer 08. The lower uncertainty of $\gamma$ and $\beta_{\mathrm{w/oJ/\psi}}$, which refers to the fit to $\beta$ excluding the measurement of $\sin(2\beta)$, has been slightly enhanced to reflect the non-gaussian behaviour of the distribution in a conservative way.

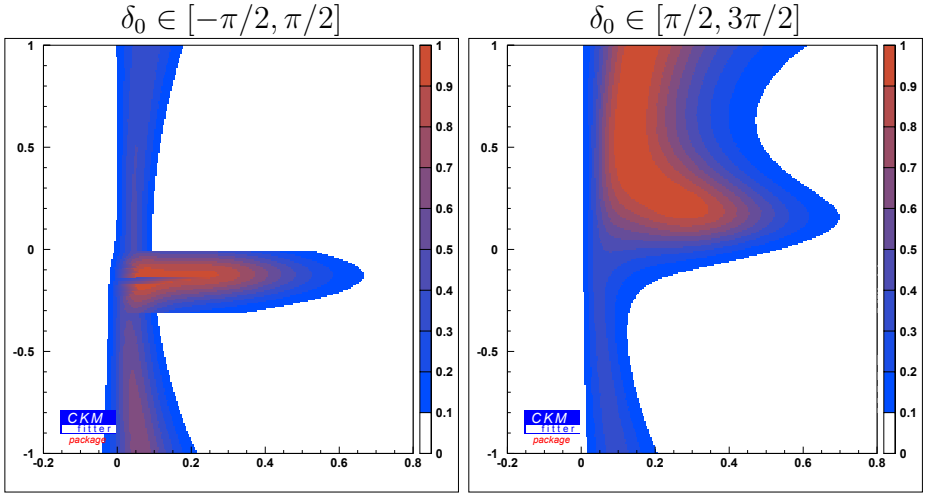


**Figure 4.10:** The fit results for the $U$-spin breaking parameter $x_\epsilon$ in $B \to J/\psi K$ and $B \to J/\psi\pi$ in the complex plane.

The results of the fit are given in table 4.13, and the results for the $U$-spin breaking parameters are additionally shown shown in figure 4.10. The fit shows three distinct solutions, two of which have $\phi_0 \sim 0$ while the third one has $\phi_0 \sim \pi$. As the solutions interfere in the fit and make it unstable, two separate fits are performed with the restrictons $\phi_0 \in [-\pi/2, \pi/2]$ and $\phi_0 \in [\pi/2, 3\pi/2]$, covering the whole parameter space.

The sizable difference between the branching ratios of the charged and the neutral $B \to J/\psi K$ modes is somewhat surprising. The isospin analysis discussed in section 4.1.1 shows that it is driven by the $\Delta I = 1$ contribution of the effective

However, for the preferred value of $\gamma$, this input has a negligible influence.

| $\phi_0 \in [-\pi/2, \pi/2]$ ($\chi^2 = 0.51$) | | | |
|---|---|---|---|
| Parameter | best fit value | $1\sigma$ range | $2\sigma$ range |
| $\mathrm{Re}(x_\epsilon)$ | 0.08 | $[\ 0.02,\ \ 0.41]$ | $[-0.03,\ \ 0.63]$ |
| $\mathrm{Im}(x_\epsilon)$ | -0.14 | $[-0.28, -0.04] \vee \leq -0.6$ | unconstrained |
| $N^2_{J/\psi K}$ | 8.39 | $[\ 4.60,\ \ 9.38]$ | $[\ 3.65, 10.17]$ |
| $r_0$ | 0.88 | $[\ 0.07,\ \ 0.26] \vee [\ 0.56, 1.47]$ | $[\ 0.00,\ \ 1.72]$ |
| $\phi_0$ | 0.09 | $[-0.22,\ \ 0.61]$ | unconstrained |
| $r_1^K$ | 1.60 | $[\ 1.18,\ \ 2.37]$ | $[\ 0.66,\ \ 2.85]$ |
| $\phi_1^K$ | -0.07 | $[-0.75, -0.50] \vee [-0.17, 0.04]$ | $[-0.90,\ \ 0.88]$ |
| $r^\pi_{3/2}$ | 0.49 | $[\ 0.00,\ \ 0.09] \vee [\ 0.24, 1.18]$ | $[\ 0.00,\ \ 1.46]$ |
| $\phi^\pi_{3/2}$ | (0.16) | unconstrained | unconstrained |
| $\phi_0 \in [\pi/2, 3\pi/2]$ ($\chi^2 = 0.01$) | | | |
| Parameter | best fit value | $1\sigma$ range | $2\sigma$ range |
| $\mathrm{Re}(x_\epsilon)$ | 0.13 | $[0.06, 0.45]$ | $[\ 0.01, 0.66]$ |
| $\mathrm{Im}(x_\epsilon)$ | (0.59) | $\geq 0.06$ | unconstrained |
| $N^2_{J/\psi K}$ | 6.27 | $[3.76, 8.60]$ | $[\ 2.96, 9.93]$ |
| $r_0$ | 0.29 | $[0.09, 1.03]$ | $[\ 0.00, 1.38]$ |
| $\phi_0$ | 2.78 | $[2.28, 3.25]$ | unconstrained |
| $r_1^K$ | 1.40 | $[0.78, 2.14]$ | $[\ 0.31, 2.58]$ |
| $\phi_1^K$ | 0.57 | $[0.05, 0.91]$ | $[-0.87, 1.11]$ |
| $r^\pi_{3/2}$ | 0.06 | $[0.00, 0.18]$ | $[\ 0.00, 0.31]$ |
| $\phi^\pi_{3/2}$ | (2.55) | unconstrained | unconstrained |

**Table 4.13:** Results for the fit to $J/\psi(K \text{ or } \pi)$ data, as explained in the text. The values in brackets indicate that due to a broad allowed range the central value is not significant.

hamiltonian, which is doubly CKM suppressed. Hence the ratio between these branching ratios should be given by the ratio of lifetimes which is close to unity, modified only by a doubly Cabbibo suppressed tree contribution and electroweak penguins. In the fit, the measured difference results in $r_1^K \sim 1 (\geq 0.78@1\sigma)$, which is quite large, but on the other hand not yet conclusive. Furthermore, the non-vanishing central values for the CP asymmetries imply a non-vanishing value for $r_0$, $r_0 \geq 0.06@1\sigma$, in combination with a non-trivial phase. However, as is obvious from the significance of the data, the allowed range at two standard devi-

ations includes zero. Concerning $U$-spin breaking, the fit prefers a non-vanishing imaginary part of the $U$-spin breaking parameter $x_\epsilon$, while it is not bounded from above. The first observation is due to relation (4.74) showing a deviation from zero and especially preferring equal signs for the CP asymmetries, while the branching ratios, as seen above, are compatible with no breaking at all. This is again a hint to non-factorizable $U$-spin breaking. The reason for the second observation lies in the fact, that no observable depends in leading order on $\mathrm{Im}(x_\epsilon)$, when assuming a power-counting $x_\epsilon, r_i \sim \lambda$. The other parameters lie within relatively large ranges, whithin or including the expected order of magnitude.

One possibility to further constrain this fit would be the approximate $SU(3)$ relation for $B \to J/\psi\pi^0$ and $B \to J/\psi K^0$ used in the last section, leading to the identification $r_1^K e^{i\phi_1^K} = r_{3/2}^\pi e^{i\phi_{3/2}^\pi}$. But as the purpose of this formalism is to avoid this kind of assumptions, it is not applied here. However, in table 4.13 it can be seen that, because of the large value for $r_1^K$, this identification would be problematic, thereby indicating a tension between charged and neutral modes in that scenario.

### $B^\pm \to D\,(K^\pm \text{ or } \pi^\pm)$ decays

As an example for $\Delta C = \pm 1$ transtions the decays $B^\pm \to D\,(K^\pm \text{ or } \pi^\pm)$ are considered. As can be seen in equation (3.56), these transitions are governed by a single CKM factor, since there are four different quark flavours in the final state. In particular, this leads to vanishing direct CP asymmetries in the corresponding decays, so the number of parameters as well as the one of observables is less by a factor of two.

However, it has been proposed a few years ago [141,142] to discuss observables from decays, where the (neutral) $D$ meson in the final state is reconstructed in a decay mode which is a CP eigenstate. This leads to interference between $B \to D$- and $B \to \bar{D}$-modes, where $B^- \to DK^-$ is the "golden mode" to extract $\gamma$ with negligible theoretical error. The analysis can be transferred to $B \to D\pi$ one to one, however, in this case the second amplitude, $B^- \to \bar{D}^0\pi^-$ is not only colour-, but in addition doubly Cabibbo-suppressed, which leads to very small interference effects.

Turning to $U$-spin, the analysis is as in the $B \to J/\psi(K \text{ or } \pi)$ modes, however,

with only a single CKM factor. The parametrization in this case reads

$$\begin{aligned}
\langle B^-|\mathcal{H}_{\text{eff}}|D^0K^-\rangle &= \lambda\tilde{A}_1\left(1+y_{1,\epsilon}e^{i\theta_1}\right)\,,\\
\langle B^-|\mathcal{H}_{\text{eff}}|D^0\pi^-\rangle &= (1-\lambda^2/2)\tilde{A}_1\left(1-y_{1,\epsilon}e^{i\theta_1}\right)\,,\\
\langle B^-|\mathcal{H}_{\text{eff}}|\bar{D}^0K^-\rangle &= \lambda e^{-i\gamma}\tilde{A}_2e^{i\theta_A}\left(1+y_{2,\epsilon}e^{i\theta_2}\right)\,,\\
\langle B^-|\mathcal{H}_{\text{eff}}|\bar{D}^0\pi^-\rangle &= -\lambda^2e^{-i\gamma}\tilde{A}_2e^{i\theta_A}\left(1-y_{2,\epsilon}e^{i\theta_2}\right)\,,
\end{aligned} \tag{4.78}$$

where a common factor $A\lambda^2$ is absorbed into the definition of $\tilde{A}_{1,2}$, and additionally a factor of $R_u$ in $\tilde{A}_2$. In the fit, the (to order 1%) common phase-space factor $\Phi$ and the lifetime of the $B$ meson are included by the definition

$$A_{1,2} = \sqrt{\Phi(m_B,m_\pi)\tau_{B^-}}\,\tilde{A}_{1,2}\,. \tag{4.79}$$

Note that $A_1$ is chosen to be real, while for $A_2$ one has to keep a phase, because of the interference effects described below. Furthermore, the $U$-spin breaking quantities $y_{1,\epsilon}$ and $y_{2,\epsilon}$ are real and positive, since their phases are taken into account explicitly.

Defining now the CP eigenstates[5]

$$|D^0_\pm\rangle = \frac{1}{\sqrt{2}}\left(|D_0\rangle \pm |\bar{D}_0\rangle\right)\,, \tag{4.80}$$

one has the additional eight observables

$$\bar{\Gamma}(B^-\to D^0_\pm K^-/\pi^-) = \frac{1}{2}\left[\Gamma(B^-\to D^0_\pm K^-/\pi^-)+\Gamma(B^+\to D^0_\pm(K^+/\pi^+)\right]\,, \tag{4.81}$$

$$\mathcal{A}_{\text{CP}}(B^-\to D^0_\pm K^-/\pi^-) = \frac{\Gamma(B^-\to D^0_\pm K^-/\pi^-)-\Gamma(B^+\to D^0_\pm K^+/\pi^+)}{\Gamma(B^-\to D^0_\pm K^-/\pi^-)+\Gamma(B^+\to D^0_\pm K^+/\pi^+)}\,, \tag{4.82}$$

with the four relations

$$\begin{aligned}
&\bar{\Gamma}(B^-\to D^0_+K^-/\pi^-)\mathcal{A}_{\text{CP}}(B^-\to D^0_+K^-/\pi^-) =\\
&\qquad -\bar{\Gamma}(B^-\to D^0_-K^-/\pi^-)\mathcal{A}_{\text{CP}}(B^-\to D^0_-K^-/\pi^-)\,,
\end{aligned} \tag{4.83}$$

$$\begin{aligned}
&\bar{\Gamma}(B^-\to D^0_+K^-/\pi^-)+\bar{\Gamma}(B^-\to D^0_-K^-/\pi^-) =\\
&\qquad \bar{\Gamma}(B^-\to D^0K^-/\pi^-)+\bar{\Gamma}(B^-\to \bar{D}^0K^-/\pi^-)\,,
\end{aligned} \tag{4.84}$$

[5]In the follwing any mixing in the $D$ system is neglected.

where the first relation requires in particular opposite signs for the corresponding CP asymmetries, leaving eight independent observables in total, which are chosen to be both from $\mathrm{BR}(B^- \to D^0 K^-/\pi^-)$, and six from $\mathrm{BR}(B^- \to D^0_\pm K^-/\pi^-)$ and $\mathcal{A}_{\mathrm{CP}}(B^- \to D^0_\pm K^-/\pi^-)$.

These face 7 parameters appearing in the parametrization (4.78), if the weak angle $\gamma$ is treated as an input, otherwise one has to deal with 8 parameters. However, one has to take into account parametric invariances: one observes one discrete invariance[6],

$$\gamma \to \pi - \gamma\,, \quad \theta_A \to \pi - \theta_A\,, \quad \theta_{1,2} \to -\theta_{1,2}\,, \tag{4.85}$$

which effectively replaces every phase by its negative value, leaving all observables invariant. In the future, as long as $\gamma$ does not lie near 90° (which is not the case, according to all present data), this ambiguity is trivially resolved by the observation of other $\gamma-$dependent processes.

In addition, there is one continuous invariance: One has the freedom to redefine the parametrization (4.78) in such a way, that

$$A_{1,2}(1 + y_{1,2}e^{i\theta_{1,2}}) \;\to\; A'_{1,2}(1 + y'_{1,2,\epsilon}e^{i\theta'_{1,2}}) = e^{i\theta^1_\xi}A_{1,2}(1 + y_{1,2}e^{i\theta_{1,2}})\,, \tag{4.86}$$

$$A_{1,2}(1 - y_{1,2}e^{i\theta_{1,2}}) \;\to\; A'_{1,2}(1 - y'_{1,2,\epsilon}e^{i\theta'_{1,2}}) = e^{i\theta^2_\xi}A_{1,2}(1 - y_{1,2}e^{i\theta_{1,2}})\,, \tag{4.87}$$

which is always possible in a restricted range for $\theta^i_\xi$. The restriction is given by the possible values of the corresponding parameter combinations, when considering $r_{1,2} \in [0, 0.6]$ in the fit.

The experimental results for these decays are given in table 4.14. The two colour suppressed decays have not been measured so far. The two CP asymmetries $B \to D^0 K^-/\pi^-$ do not enter the fit, because they are zero by construction, but are given mainly for completeness. Note that they are consistent with zero within one and two standard deviations respectively. Also the data is roughly consistent with relation (4.83). On the other hand, using relation (4.84), one observes that the data in both cases prefer vanishing colour-suppressed amplitudes by giving negative central values for both of them. While this is on one hand sensible, because they are expected to be small, it is at odds with the non-vanishing central values of the measured CP asymmetries. This is reflected in a bad $\chi^2_{\mathrm{min}}$-value in a global fit to the experimental data. Therefore the fit results are not shown explicitly here.

[6] $\gamma$ has been restricted to lie in $[0, \pi]$, which excludes additional solutions.

| Decay | BR/$10^{-4}$ | $\mathcal{A}_{\rm CP}$ |
|---|---|---|
| $B^- \to D^0 K^-$ | $4.02 \pm 0.21$ | $0.07 \pm 0.04$ |
| $B^- \to D_+^0 K^-$ | $1.81 \pm 0.27$ | $0.22 \pm 0.14(*)$ |
| $B^- \to D_-^0 K^-$ | $1.73 \pm 0.23$ | $-0.09 \pm 0.10$ |
| $B^- \to D^0 \pi^-$ | $48.4 \pm 1.5$ | $-0.008 \pm 0.008$ |
| $B^- \to D_+^0 \pi^-$ | $19.6 \pm 3.4$ | $0.035 \pm 0.024$ |
| $B^- \to D_-^0 \pi^-$ | $18 \quad \pm 4$ | $0.017 \pm 0.026$ |

**Table 4.14:** Experimental data for $B^- \to DK^-/\pi^-$ decays. Values are taken from the PDG [35]. $(*)$: Errors rescaled by the PDG due to inconsistent measurements.

It is interesting to note that for the colour allowed tree decays one may again check naive factorization. In this case the $U$-spin breaking is given by the ratio of the decay constants, i.e.

$$\frac{\langle B^-|\mathcal{H}_{\rm eff}|D^0K^-\rangle}{\langle B^-|\mathcal{H}_{\rm eff}|D^0\pi^-\rangle} = \frac{\lambda}{1-\frac{\lambda^2}{2}}\left(\frac{1+y_{1,\epsilon}e^{i\theta_1}}{1-y_{1,\epsilon}e^{i\theta_1}}\right) \simeq \frac{\lambda}{1-\frac{\lambda^2}{2}}\frac{f_K}{f_\pi} \sim 0.28\,. \tag{4.88}$$

In this approach one obtains $\theta_1 = 0$ and $y_{1,\epsilon} \sim 0.1$ from the ratio of the decay constants. The comparison with experiment

$$\sqrt{\frac{BR(B^- \to D^0K^-)}{BR(B^- \to D^0\pi^-)}} = \begin{cases} 0.28 \pm 0.02 & \text{(from table 4.14)}\,, \\ 0.281 \pm 0.005 & \text{(from direct measurement, see [54])}\,, \end{cases} \tag{4.89}$$

shows excellent agreement, indicating the well known fact that naive factorization works reasonably well in colour-allowed tree decays. This information could be used to fix one parameter in the fit (either the modulus to the ratio of decay constants or the corresponding phase to zero), which would break the continuous invariance, leaving part of the $U$-spin breaking in these decays and the one in the colour-suppressed decays to be extracted from the analysis.

It will be interesting to see what this analysis yields, once the data are consistent. Again, LHCb should clarify this situation, yielding a large sample for these decays.

### 4.3.2 Decays of neutral B mesons

The two neutral $B$ mesons form a doublet under $U$-spin. In the $U$-spin limit, the final states have to form either a singlet or a triplet, while there can also be

admixtures of $U = 2$ once $U$-spin breaking is included. When considering two-body decays, there are in total three possibilities: The decays into two charged final states necessarily have either $U = 0$ or $U = 1$, since the charged mesons form $U$-spin doublets. The neutral mesons form either $U$-spin singlets of triplets, in which case the two-body final states can have $U = 0, 1$ and 2. Clearly a final state with $U = 2$ can be reached only through $U$-spin breaking.

When considering decays of neutral $B$ mesons into two neutral mesons, one has again to deal with admixtures of $U$-spin multiplets. Using the decomposition

$$\begin{aligned}
\mathcal{H}_{\text{eff}}^{b\to d}\left|\bar{B}_d\right\rangle &= -\frac{1}{\sqrt{2}}\left|1,0\right\rangle_{d,0} - \frac{1}{\sqrt{3}}\left|1,0\right\rangle_{d,\epsilon(3/2)} + \frac{1}{\sqrt{6}}\left|1,0\right\rangle_{d,\epsilon(1/2)} \\
&\quad -\frac{1}{\sqrt{2}}\left|0,0\right\rangle_{d,0} + \frac{1}{\sqrt{6}}\left|0,0\right\rangle_{d,\epsilon} - \frac{1}{\sqrt{3}}\left|2,0\right\rangle_{d,\epsilon}\,, \qquad (4.90)\\
\mathcal{H}_{\text{eff}}^{b\to s}\left|\bar{B}_s\right\rangle &= +\frac{1}{\sqrt{2}}\left|1,0\right\rangle_{s,0} - \frac{1}{\sqrt{3}}\left|1,0\right\rangle_{s,\epsilon(3/2)} + \frac{1}{\sqrt{6}}\left|1,0\right\rangle_{s,\epsilon(1/2)} \\
&\quad -\frac{1}{\sqrt{2}}\left|0,0\right\rangle_{s,0} - \frac{1}{\sqrt{6}}\left|0,0\right\rangle_{s,\epsilon} + \frac{1}{\sqrt{3}}\left|2,0\right\rangle_{s,\epsilon}\,, \qquad (4.91)\\
\mathcal{H}_{\text{eff}}^{b\to d}\left|\bar{B}_s\right\rangle &= +\left|1,+1\right\rangle_{d,0} - \frac{1}{\sqrt{6}}\left|1,+1\right\rangle_{d,\epsilon(3/2)} - \frac{1}{\sqrt{3}}\left|1,+1\right\rangle_{d,\epsilon(1/2)} \\
&\quad +\frac{1}{\sqrt{2}}\left|2,+1\right\rangle_{d,\epsilon}\,, \qquad (4.92)\\
\mathcal{H}_{\text{eff}}^{b\to s}\left|\bar{B}_d\right\rangle &= -\left|1,-1\right\rangle_{s,0} - \frac{1}{\sqrt{6}}\left|1,-1\right\rangle_{s,\epsilon(3/2)} - \frac{1}{\sqrt{3}}\left|1,-1\right\rangle_{s,\epsilon(1/2)} \\
&\quad -\frac{1}{\sqrt{2}}\left|2,-1\right\rangle_{s,\epsilon}\,, \qquad (4.93)
\end{aligned}$$

one may express all the decay amplitudes in terms of $U$-spin amplitudes. Doing this in full generality leads to a large number of independent $U$-spin ampliutdes for $U_z = 0$ final states already in the symmetry limit, and does in general not allow for a determination of all breaking amplitudes. One very theoretical exception is given by the class of decays $B^0 \to P^0P^0$: when both final state particles belong to the same multiplet, Bose symmetry forbids antisymmetric final states[7], leading to a reduction of possible amplitudes[8]. However, this possibility remains a theoretical one, because in order to perform this fit, all decays of this class would have to be measured time-dependently, which seems not possible in the near future.

[7]This is true due to the $B$ and $P^0$ mesons being pseudoscalar.

[8]This fact has been overlooked in [95], the corrections to the corresponding decompositions are straight forward. For completeness, the corresponding final states are given in appendix 6.2.

Choosing the subset of decays formed by $b \to s$ transitions of $B_d$-mesons, combined with $b \to d$ transitions of $B_s$-mesons [95], results in 19 parameters facing up to 18 observables, therefore in this case one additional assumption is needed. From that paper, it also appears as if one could use the corresponding class of charmless $B \to P^0V^0$ decays, which should result in a determinable system. However, it has been overlooked there, that the states $|1_V 0_{8,P}\rangle$ and $|1_P 0_{8,V}\rangle$ are independent. As they receive also independent $U$-spin corrections, this class of decays has again not enough observables. The corrected decomposition of the decay amplitudes including the $U$-spin corrections is given in the appendix 6.2.

In any case, the current situation concerning the data is insufficient to perform such an analysis, since the $B_s$ system has not been fully explored yet. Clearly with the advent of LHC this situation will change once LHCb measures the decay rates and the CP asymmetries of the corresponding $B_s$ transitions.

Regarding decays into two charged mesons, the situation is similar: the breaking analysis without any assumptions is not possible, and for a full analysis one has to wait for LHCb data. However, some decays into charmless mesons have been measured at the Tevatron recently, with which one might perform an analysis in the $U$-spin limit, getting an impression of the present precision and possible hints of $U$-spin breaking in these decays.

In the $U$-spin limit, one has four amplitudes, leading to seven unknown parameters. Thanks to recent measurements at the CDF experiment at Tevatron [143], there are in principle enough data points to fix the problem unambiguously, see table 4.15. This remains true when taking into account relation (3.62), which leaves nine independent observables. Charmless $B_s$ decays involving vector mesons have not been measured yet, therefore no fit is possible at the moment for any other class of charmless decays.

The following parametrization is used:

$$\begin{aligned}
\left\langle \bar{B}_d|\mathcal{H}_{\text{eff}}|\pi^+K^-\right\rangle &= -A_1^c\left(1+\lambda^2 e^{-i\gamma}\, r_1^u\, e^{i\phi_1^u}\right), \\
\left\langle \bar{B}_s|\mathcal{H}_{\text{eff}}|\pi^-K^+\right\rangle &= -\lambda A_1^c\left(-1+e^{-i\gamma}\, r_1^u\, e^{i\phi_1^u}\right), \\
\left\langle \bar{B}_d|\mathcal{H}_{\text{eff}}|\pi^+\pi^-\right\rangle &= -\frac{1}{2}\lambda A_1^c\left[-1+r_0^c\, e^{i\phi_0^c}+e^{-i\gamma}\,\left(r_1^u\, e^{i\phi_1^u}-r_0^u\, e^{i\phi_0^u}\right)\right],
\end{aligned}$$

$$\begin{aligned}
\left\langle \bar{B}_s|\mathcal{H}_{\rm eff}|K^+K^-\right\rangle &= -\frac{1}{2}A_1^c\left[1-r_0^c\,e^{i\phi_0^c}+\lambda^2 e^{-i\gamma}\,\left(r_1^u\,e^{i\phi_1^u}-r_0^u\,e^{i\phi_0^u}\right)\right]\,,\\
\left\langle \bar{B}_d|\mathcal{H}_{\rm eff}|K^+K^-\right\rangle &= \frac{1}{2}\lambda A_1^c\left[-1-r_0^c\,e^{i\phi_0^c}+e^{-i\gamma}\,\left(r_1^u\,e^{i\phi_1^u}+r_0^u\,e^{i\phi_0^u}\right)\right]\,,\\
\left\langle \bar{B}_s|\mathcal{H}_{\rm eff}|\pi^+\pi^-\right\rangle &= \frac{1}{2}A_1^c\left[1+r_0^c\,e^{i\phi_0^c}+\lambda^2 e^{-i\gamma}\,\left(r_1^u\,e^{i\phi_1^u}+r_0^u\,e^{i\phi_0^u}\right)\right]\,, \quad (4.94)
\end{aligned}$$

choosing $A_0^c$ to be real and positive and including again a factor of $R_u$ in the definition of $r_{0,1}^u$. In addition, $A_0^c$ is rescaled in such a way that it again contains phase-space and lifetime, $\mathrm{BR}(\bar{B}_d\to\pi^+K^-)=|\left\langle \bar{B}_d|\mathcal{H}_{\rm eff}|\pi^+K^-\right\rangle|^2$, implying that the other branching ratios have to include correspondingly ratios of lifetimes and phase space factors.

| Decay | BR/$10^{-6}$ | $A_{\rm CP}$ | $S_{\rm CP}$ |
|---|---|---|---|
| $\bar{B}_d\to\pi^+\pi^-$ | $5.16\pm0.22$ | $0.38\pm0.14(*)$ | $-0.65\pm0.07$ |
| $\bar{B}_d\to\pi^+K^-$ | $19.4\pm0.6$ | $-0.098^{+0.012}_{-0.011}$ | – |
| $\bar{B}_d\to K^+K^-$ | $0.15^{+0.11}_{-0.10}$ | no data | no data |
| $\bar{B}_s\to\pi^+\pi^-$ | $0.53\pm0.51$ | no data | no data |
| $\bar{B}_s\to\pi^+K^-$ | $5.0\pm1.25$ | $0.39\pm0.17$ | – |
| $\bar{B}_s\to K^+K^-$ | $24.4\pm4.8$ | no data | no data |

**Table 4.15:** HFAG [54] averages for $B_{d,s}\to PP$ decays. $(*)$: Error inflated according to the PDG prescription, due to inconsistent measurements.

As additional input values in this fit $\lambda$ (error neglected) and $\beta=(21.11^{+1.9}_{-1.8})^\circ$ are used, where the latter value corresponds to the direct measurements in $B\to J/\psi K$ decays [54]. The fit results in

$$\gamma_{U-spin}=(75.8^{+4.8}_{-8.0})^\circ \quad (\chi^2_{\rm min}/\text{d.o.f.}=0.12/1)\,, \qquad (4.95)$$

in agreement with the determination $\gamma=(66.8^{+5.4}_{-3.8})^\circ$ by CKMfitter [29]. In addition, the fit results reflect the expectation, that the matrix elements proportional to $\lambda_{ud/s}$ are larger than the ones proportional to $\lambda_{cd/s}$, because there is no suppression for the tree contribution.

While the low $\chi^2$ for this fit is somewhat surprising, because it implies that the present data shows no sign of any $U$-spin breaking, this result shows that future analyses will be worthwile.

Decays into CP eigenstates (or, more generally, states which are not flavour-specific), play an exceptional role, because of the additional information coming from time-dependent measurements. Each of these decays forms a subset with its "$U$-spin partner" formed by exchanging all down and strange quarks in the process, because they have effectively only one amplitude. These subsets can be discussed separately from the rest of the corresponding class, which allows for fits with a small number of parameters, even when other decays of that class have not been measured yet. This feature has been extensively exploited in the $U$-spin limit, or including factorizable $U$-spin breaking only (see e.g. [96, 97]). In that case, the two decays in question have five independent observables (because of relation (3.62)), but only three parameters, so a fit for up to two weak phases is possible. However, these determinations suffer again from the systematic uncertainty related to $U$-spin breaking.

Including the breaking corrections to first order for these subsets, one observes that the breaking amplitudes form only one effective amplitude as well. However, again this does not suffice for an analysis of the breaking which is completely free from additional assumptions: the number of parameters increases by four, while only one additional independent observable becomes available. In these cases, for example the following two strategies may be used:

- If one amplitude is clearly dominating ($|A_1/A_2| \sim \delta$), one may consider the $U$-spin breaking for the leading ampliutde only, neglecting only terms of order $(\mathcal{O}(\epsilon^2), \mathcal{O}(\epsilon\delta))$. This is for example the case in $B_{d,s} \to D^+_{d,s} D^-_{d,s}$ decays, which are dominated by their colour allowed tree contribution.

- If one of the two parts in the leading amplitude is dominated by a colour allowed tree contribution, one may use the factorization assumption for that part only, as opposed to using it for the whole amplitude, and fit for the breaking amplitude in the other part.

In both cases, the number of free parameters increases only by two, so in principle a fit becomes possible; in addition, as one additional observable is available, one may determine that way one of the weak phases with correspondingly smaller systematic uncertainty. If for one class of decays the whole set is measured, these strategies may be used with the whole set, so the decays into flavour-specific modes can be included.

### 4.3.3 Conclusions

As discussed in section 3.2 for the example of QCDF, these kinds of computations of hadronic matrix elements suffer from large uncertainties due to non-factorizable corrections. The method of flavour symmetries therefore looks more promising. Clearly the latter will allow for performing precision calculations only if a reasonable control over symmetry breaking is gained.

Using the full $SU(3)$ flavour symmetry becomes quite complicated once the complete breaking is taken into account. However, the isospin subgroup of full $SU(3)$ may be assumed to be a reasonably good symmetry and hence only the breaking along the "orthogonal" directions in $SU(3)$ space has to be considered.

In this section the $U$-spin subgroup of $SU(3)$ has been studied, which has the advantage that the charge operator commutes with the symmetry generators and hence also the weak hamiltonian for $b$ decays has a simple structure under this symmetry. The breaking term is due to the mass difference between the down- and the strange quark mass and has a simple structure inferred from QCD.

Based on this the incorporation of $U$-spin breaking on a purely group theoretical basis has been discussed, together with some first applications, in which the $U$-spin breaking tuns out roughly of the order implied by the difference in the decay constants $f_\pi$ and $f_K$.

However, the full strength of this approach can be exploited only in the future. Since the $B_d$ and the $B_s$ form a $U$-spin doublet, the approach requires information on decay modes which will be gathered in the near future at the LHC. With a sufficient amount of data there will be a chance to obtain control over flavour $SU(3)$ breaking and hence a possible road to precise predictions for non-leptonic decay may be opened.

# Chapter 5

# Conclusions

Flavour Physics represents a powerful tool in the search for NP. From precision observables, its sensitivity reaches way beyond the scales that will be explored with the LHC or any foreseeable high-energy experiment. In addition, they are indispensable in order to determine the flavour structure of any model beyond the SM. However, in order to perform this task, it is essential to achieve control over the hadronic uncertainties in the SM, in order to be able to reliably differentiate between NP and SM effects.

In this work, mainly three projects related to these issues have been discussed. In order to receive quantitative results, the RFit approach has been used to treat the statistical and systematic uncertainties appropriately. The projects have been concluded separately in the corresponding sections. Main results are:

- The tensions observed in the $b \to s$ decays $B \to J/\psi K$, $B \to \phi K$, and $B \to \pi K$ can be fitted in a framework, which assumes dominance of one NP operator of the form $\mathcal{O} = (\bar{s}b)(\bar{q}q)$, leading to contributions with the expected order of magnitude for NP. In each of these cases a contribution with $\Delta I = 1$ is preferred. While an explanation in terms of enhanced SM contributions is always possible as well, the order of magnitude of these contributions is larger than expected in the SM.

- For $B \to J/\psi K$, the contrary assumption of large SM effects in combination with a NP phase has also been explored. In this case, an approximate $SU(3)$ relation can be used to determine the subleading contributions with aid of data for $B \to J/\psi\pi$ decays. The NP phase turns out to be compatible with zero, while a large penguin amplitude could explain the data in both decays,

leading to a shift in $\sin 2\beta$ of up to a few percent. While it has been argued in [138], that this is too large for a SM effect, the fact that $B \to J/\psi\pi$ data imply a shift in the observed direction is interesting, and should be taken into account in future analyses. In addition, if that estimate of SM effects is valid, it renders the previous analysis even more interesting.

- Finally, a framework for taking $U$-spin breaking corrections into accout model-independently has been developed. While in almost all cases this analysis is not possible without further assumptions, the related systematic uncertainties are still reduced, because it usually suffices to apply these assumptions to the breaking terms. For these kinds of analyses several proposals have been made. With respect to $B \to J/\psi(K \text{ or } \pi)$, the analysis shows that the breaking corrections deviate strongly from what is expected in naive factorization. In addition, the isospin breaking amplitudes seem to be different in the two decays, which, if confirmed with higher statistics, could imply a NP source.

While the present data do not allow for conclusive statements, there are hints for NP effects. However, as especially the present discussions regarding $B \to \pi K$ show, a more rigorous understanding of SM hadronic effects is necessary in order to meet the high precision expected from upcoming experiments, such as the LHC and hopefully a future Super-$B$ factory. In fact, lots of discoveries are to be made in NP, but in the SM as well.

# Chapter 6

# Appendix

## 6.1 Diagrammatic Parametrization in $B \to \pi K$

The diagramatic expansion for $B \to \pi K$, as used e.g. in [115], reads:

$$\begin{aligned}
\mathcal{A}(B^- \to \pi^- \bar{K}^0) &= -P^{'}_{tc} + P^{'}_{uc} e^{-i\gamma} - \frac{1}{3} P^{'C}_{EW} \,, \\
\sqrt{2}\,\mathcal{A}(B^- \to \pi^0 K^-) &= P^{'}_{tc} - P^{'}_{uc} e^{-i\gamma} - \frac{2}{3} P^{'C}_{EW} - P^{'}_{EW} - C^{'} e^{-i\gamma} - T^{'} e^{-i\gamma} \,, \\
\mathcal{A}(\bar{B}_d \to \pi^+ K^-) &= P^{'}_{tc} - P^{'}_{uc} e^{-i\gamma} - \frac{2}{3} P^{'C}_{EW} - T^{'} e^{-i\gamma} \,,
\end{aligned} \tag{6.1}$$

and again

$$\sqrt{2}\,\mathcal{A}(\bar{B}_d \to \pi^0 \bar{K}^0) = \mathcal{A}(B^- \to \pi^- \bar{K}^0) + \sqrt{2}\,\mathcal{A}(B^- \to \pi^0 K^-) - \mathcal{A}(\bar{B}_d \to \pi^+ K^-) \,. \tag{6.2}$$

The primes denote a $b \to s$ transition, $P^{'}_{ut,ct}$ are called gluonic penguin amplitudes, $P^{'(C)}_{EW}$ the (colour-suppressed) electroweak amplitudes, and $T^{'}(C^{'})$ denote the (colour-suppressed) tree amplitudes. Expressed in terms of the parametrization used in this work, the amplitudes read

$$\begin{aligned}
P^{'}_{tc} &= -P \left( 1 + \frac{1}{3} q_C e^{i\omega_C} \epsilon_T e^{i\phi_T} \right) \,, \\
P^{'}_{uc} &= P \epsilon_a e^{i\phi_a} \,, \\
T^{'} &= -P \epsilon_T e^{i\phi_T} \,, \\
C^{'} &= P \left( \epsilon_T e^{i\phi_T} - \epsilon_{3/2} e^{i\phi_{3/2}} \right) \,, \\
P^{'}_{EW} &= P \left( \epsilon_{3/2} e^{i\phi_{3/2}} q e^{i\omega} - q_C e^{i\omega_C} \epsilon_T e^{i\phi_T} \right) \,, \\
P^{'C}_{EW} &= P q_C e^{i\omega_C} \epsilon_T e^{i\phi_T} \,.
\end{aligned} \tag{6.3}$$

## 6.2 U-spin decompositions in charmless decays

For completeness, two $U$-spin decompositions are given explicitly, where the formulas in [95] included minor errors. The final states for two decays into two identical charmless pseudoscalar multiplets are listed in table 6.1. As discussed in section 4.3, this class of decays has in principle sufficient observables to determine the breaking parameters without further assumptions, but the necessary measurements are unlikely to be performed in the next years. In table 6.2 the amplitudes for $B \to P_0V_0$ decays are listed, where the breaking amplitudes are not determinable without further assumptions, due to $|1_V 0_{8,P}\rangle \neq |1_P 0_{8,V}\rangle$.

| $P_0P_0$ | $U_z$ | $\lvert 2\,U_z\rangle$ | $\lvert 1\,U_z\rangle_8$ | $\lvert 1\,U_z\rangle_1$ | $\lvert 0\,0\rangle$ | $\lvert 0\,0\rangle_{8\,8}$ | $\lvert 0\,0\rangle_{1\,8}$ | $\lvert 0\,0\rangle_{1\,1}$ |
|---|---|---|---|---|---|---|---|---|
| $\lvert\bar{K}^0\pi^0\rangle$ | $-1$ | $+\frac{1}{2}$ | $-\frac{\sqrt{3}}{2}$ | | | | | |
| $\lvert\bar{K}^0\eta\rangle$ | $-1$ | $-\frac{\sqrt{2}}{\sqrt{3}}$ | $-\frac{\sqrt{2}}{3}$ | $+\frac{1}{3}$ | | | | |
| $\lvert\bar{K}^0\eta'\rangle$ | $-1$ | $-\frac{1}{\sqrt{12}}$ | $-\frac{1}{6}$ | $-\frac{2\sqrt{2}}{3}$ | | | | |
| $\lvert K^0\pi^0\rangle$ | $+1$ | $-\frac{1}{2}$ | $+\frac{\sqrt{3}}{2}$ | | | | | |
| $\lvert K^0\eta\rangle$ | $+1$ | $+\frac{\sqrt{2}}{\sqrt{3}}$ | $+\frac{\sqrt{2}}{3}$ | $-\frac{1}{3}$ | | | | |
| $\lvert K^0\eta'\rangle$ | $+1$ | $+\frac{1}{\sqrt{12}}$ | $+\frac{1}{6}$ | $+\frac{2\sqrt{2}}{3}$ | | | | |
| $\lvert\bar{K}^0K^0\rangle$ | $0$ | $-\frac{1}{\sqrt{3}}$ | | | $-\frac{\sqrt{2}}{\sqrt{3}}$ | | | |
| $\lvert\pi^0\pi^0\rangle$ | $0$ | $+\frac{1}{2\sqrt{6}}$ | $-\frac{\sqrt{3}}{\sqrt{8}}$ | | $+\frac{1}{4\sqrt{3}}$ | $+\frac{3}{4}$ | | |
| $\lvert\pi^0\eta\rangle$ | $0$ | $-\frac{\sqrt{2}}{3}$ | $+\frac{\sqrt{2}}{3}$ | $+\frac{1}{6}$ | $+\frac{1}{3}$ | $+\frac{1}{\sqrt{3}}$ | $-\frac{1}{2\sqrt{3}}$ | |
| $\lvert\pi^0\eta'\rangle$ | $0$ | $-\frac{1}{6}$ | $+\frac{1}{6}$ | $-\frac{\sqrt{2}}{3}$ | $+\frac{1}{6\sqrt{2}}$ | $+\frac{1}{2\sqrt{6}}$ | $+\frac{\sqrt{2}}{\sqrt{3}}$ | |
| $\lvert\eta\eta\rangle$ | $0$ | $+\frac{2\sqrt{2}}{3\sqrt{3}}$ | $+\frac{2\sqrt{2}}{3\sqrt{3}}$ | $-\frac{2}{3\sqrt{3}}$ | $-\frac{2}{3\sqrt{3}}$ | $+\frac{2}{9}$ | $-\frac{2}{9}$ | $+\frac{1}{9}$ |
| $\lvert\eta\eta'\rangle$ | $0$ | $+\frac{\sqrt{2}}{3\sqrt{3}}$ | $+\frac{\sqrt{2}}{3\sqrt{3}}$ | $+\frac{7}{6\sqrt{3}}$ | $-\frac{1}{3\sqrt{3}}$ | $+\frac{1}{9}$ | $+\frac{7}{18}$ | $-\frac{4}{9}$ |
| $\lvert\eta'\eta'\rangle$ | $0$ | $+\frac{\sqrt{2}}{12\sqrt{3}}$ | $+\frac{1}{6\sqrt{6}}$ | $+\frac{2}{3\sqrt{3}}$ | $-\frac{1}{12\sqrt{3}}$ | $+\frac{1}{36}$ | $+\frac{2}{9}$ | $+\frac{8}{9}$ |

**Table 6.1:** $U$-spin decomposition for the final states in $B \to P_0P_0$. Note that for the coupling of parts belonging to the same multiplet the symmetric combination has to be taken, and $|00\rangle_{18} = |00\rangle_{81}$ holds. For identical particles, a factor $1/\sqrt{2}$ has to be applied.

| $V_0P_0$ | $U_z$ | $A_0^{(1)}$ | $A_{0,8V}^{(1)}$ | $A_{0,1V}^{(1)}$ | $A_{0,8P}^{(1)}$ | $A_{0,8V}^{(1)}$ | $A_\epsilon^{(1)}$ | $A_{\epsilon,8V}^{(1)}$ | $A_{\epsilon,1V}^{(1)}$ | $A_{\epsilon,8P}^{(1)}$ | $A_{\epsilon,1P}^{(1)}$ | $A_\epsilon^{(2)}$ |
|---|---|---|---|---|---|---|---|---|---|---|---|---|
| $\mathcal{H}^{b\to s}B_d$ | | | | | | | | | | | | |
| $\phi K^0$ | 1 | $-\frac{1}{2}$ | $+\frac{1}{\sqrt{6}}$ | $+\frac{1}{\sqrt{3}}$ | | | $+\frac{1}{2}$ | $-\frac{1}{\sqrt{6}}$ | $-\frac{1}{\sqrt{3}}$ | | | $+\frac{1}{2\sqrt{2}}$ |
| $\omega K^0$ | 1 | $+\frac{1}{2\sqrt{2}}$ | $-\frac{1}{2\sqrt{3}}$ | $+\frac{\sqrt{2}}{\sqrt{3}}$ | | | $-\frac{1}{2\sqrt{2}}$ | $+\frac{1}{2\sqrt{3}}$ | $-\frac{\sqrt{2}}{\sqrt{3}}$ | | | $-\frac{1}{4}$ |
| $\rho_0 K^0$ | 1 | $+\frac{1}{2\sqrt{2}}$ | $+\frac{\sqrt{3}}{2}$ | | | | $-\frac{1}{2\sqrt{2}}$ | $-\frac{\sqrt{3}}{2}$ | | | | $-\frac{1}{4}$ |
| $K^{0*}\pi^0$ | 1 | $-\frac{1}{2\sqrt{2}}$ | | | $+\frac{\sqrt{3}}{2}$ | | $+\frac{1}{2\sqrt{2}}$ | | | $-\frac{\sqrt{3}}{2}$ | | $-\frac{1}{4}$ |
| $K^{0*}\eta$ | 1 | $+\frac{1}{\sqrt{3}}$ | | | $+\frac{\sqrt{2}}{3}$ | $-\frac{1}{3}$ | $-\frac{1}{\sqrt{3}}$ | | | $-\frac{\sqrt{2}}{3}$ | $+\frac{1}{3}$ | $+\frac{1}{\sqrt{6}}$ |
| $K^{0*}\eta'$ | 1 | $+\frac{1}{2\sqrt{6}}$ | | | $+\frac{1}{6}$ | $+\frac{2\sqrt{2}}{3}$ | $-\frac{1}{2\sqrt{6}}$ | | | $-\frac{1}{6}$ | $-\frac{2\sqrt{2}}{3}$ | $+\frac{1}{4\sqrt{3}}$ |
| $\mathcal{H}^{b\to d}B_s$ | | | | | | | | | | | | |
| $\phi\bar{K}^0$ | -1 | $+\frac{1}{2}$ | $+\frac{1}{\sqrt{6}}$ | $+\frac{1}{\sqrt{3}}$ | | | $+\frac{1}{2}$ | $+\frac{1}{\sqrt{6}}$ | $+\frac{1}{\sqrt{3}}$ | | | $+\frac{1}{2\sqrt{2}}$ |
| $\omega\bar{K}^0$ | -1 | $-\frac{1}{2\sqrt{2}}$ | $-\frac{1}{2\sqrt{3}}$ | $+\frac{\sqrt{2}}{\sqrt{3}}$ | | | $-\frac{1}{2\sqrt{2}}$ | $-\frac{1}{2\sqrt{3}}$ | $+\frac{\sqrt{2}}{\sqrt{3}}$ | | | $-\frac{1}{4}$ |
| $\rho_0\bar{K}^0$ | -1 | $-\frac{1}{2\sqrt{2}}$ | $+\frac{\sqrt{3}}{2}$ | | | | $-\frac{1}{2\sqrt{2}}$ | $+\frac{\sqrt{3}}{2}$ | | | | $-\frac{1}{4}$ |
| $\bar{K}^{0*}\pi^0$ | -1 | $+\frac{1}{2\sqrt{2}}$ | | | $+\frac{\sqrt{3}}{2}$ | | $+\frac{1}{2\sqrt{2}}$ | | | $+\frac{\sqrt{3}}{2}$ | | $-\frac{1}{4}$ |
| $\bar{K}^{0*}\eta$ | -1 | $-\frac{1}{\sqrt{3}}$ | | | $+\frac{\sqrt{2}}{3}$ | $-\frac{1}{3}$ | $-\frac{1}{\sqrt{3}}$ | | | $+\frac{\sqrt{2}}{3}$ | $-\frac{1}{3}$ | $+\frac{1}{\sqrt{6}}$ |
| $\bar{K}^{0*}\eta'$ | -1 | $-\frac{1}{2\sqrt{6}}$ | | | $+\frac{1}{6}$ | $+\frac{2\sqrt{2}}{3}$ | $-\frac{1}{2\sqrt{6}}$ | | | $+\frac{1}{6}$ | $+\frac{2\sqrt{2}}{3}$ | $+\frac{1}{4\sqrt{3}}$ |

**Table 6.2:** Amplitudes for $B \to V_0P_0$ including $U$-spin breaking contributions to first order.

# Bibliography


[1] Glashow S.L. *Partial symmetries of weak interactions*. Nucl. Phys. **22**, (1961), 579.

[2] Weinberg S. *A model of leptons*. Phys. Rev. Lett. **19**, (1967), 1264.

[3] Salam A. *Weak and Electromagnetic Interactions*. In Svartholm W. (ed.), *Elementary Particle Theory*, Almquvist und Wiksell, 1968, 367.

[4] Quigg C. *Gauge Theories of the Strong, Weak, and Electromagnetic Interactions*. The Benjamin/Cummings Publishing Company Inc., 1983.

[5] Peskin M. and Schroeder D. *An Introduction to Quantum Field Theory*. Westview press, 1995.

[6] Donoghue J.F., Golowich E. and Holstein B.R. *Dynamics of the standard model*. Camb. Monogr. Part. Phys. Nucl. Phys. Cosmol. **2**, (1992), 1–540.

[7] Altarelli G. *Status of the Standard Model at the LHC Start*. Nuovo Cim. **123B**, (2008), 257–269. `[0804.4147 (hep-ph)]`.

[8] Langacker P. *Introduction to the Standard Model and Electroweak Physics*. arXiv: 0901.0241 (hep–ph).

[9] Dawson S. *Electroweak symmetry breaking circa 2005*. Int. J. Mod. Phys. **A21**, (2006), 1629–1641. `[hep-ph/0510385]`.

[10] Quigg C. *Unanswered Questions in the Electroweak Theory*. arXiv: 0905.3187 (hep–ph).

[11] Higgs P.W. *Broken symmetries, massless particles and gauge fields*. Phys. Lett. **12**, (1964), 132.

[12] Higgs P.W. *Broken Symmetries and the Masses of Gauge Bosons*. Phys. Rev. Lett. **13**, (1964), 508–509.

[13] Guralnik G.S., Hagen C.R. and Kibble T.W.B. *Global Conservation Laws and Massless Particles*. Phys. Rev. Lett. **13**, (1964), 585–587.

[14] Englert F. and Brout R. *Broken Symmetry and the Mass of Gauge Vector Bosons*. Phys. Rev. Lett. **13**, (1964), 321–322.

[15] Adriani O. et al. (PAMELA collaboration). *An anomalous positron abundance in cosmic rays with energies 1.5.100 GeV*. Nature **458**, (2009), 607–609. [0810.4995 (astro-ph)].

[16] Chang J. et al. (ATIC collaboration). *An excess of cosmic ray electrons at energies of 300.800 GeV*. Nature **456**, (2008), 362–365.

[17] Komatsu E. et al. (WMAP collaboration). *Five-Year Wilkinson Microwave Anisotropy Probe (WMAP) Observations: Cosmological Interpretation*. Astrophys. J. Suppl. **180**, (2009), 330–376. [0803.0547 (astro-ph)].

[18] Riess A.G. et al. (Supernova Search Team). *Observational Evidence from Supernovae for an Accelerating Universe and a Cosmological Constant*. Astron. J. **116**, (1998), 1009–1038. [astro-ph/9805201].

[19] Perlmutter S. et al. (Supernova Cosmology Project). *Measurements of Omega and Lambda from 42 High-Redshift Supernovae*. Astrophys. J. **517**, (1999), 565–586. [astro-ph/9812133].

[20] Weinberg S. *The cosmological constant problem*. Rev. Mod. Phys. **61**, (1989), 1–23.

[21] Frieman J., Turner M. and Huterer D. *Dark Energy and the Accelerating Universe*. Ann. Rev. Astron. Astrophys. **46**, (2008), 385–432. [0803.0982 (astro-ph)].

[22] Barate R. et al. (LEP Working Group for Higgs boson searches). *Search for the standard model Higgs boson at LEP*. Phys. Lett. **B565**, (2003), 61–75. Online updates available at http://lepewwg.web.cern.ch/LEPEWWG/, [hep-ex/0306033].

[23] Barbieri R. and Strumia A. *The 'LEP paradox'*. arXiv: hep–ph/0007265.

[24] Christenson J.H., Cronin J.W., Fitch V.L. and Turlay R. *Evidence for the 2 pi Decay of the k(2)0 Meson*. Phys. Rev. Lett. **13**, (1964), 138–140.

[25] Aubert B. et al. (BABAR collaboration). *Observation of CP violation in the $B^0$ meson system*. Phys. Rev. Lett. **87**, (2001), 091801. [hep-ex/0107013].

[26] Abe K. et al. (Belle collaboration). *Observation of large CP violation in the neutral B meson system*. Phys. Rev. Lett. **87**, (2001), 091802. [hep-ex/0107061].

[27] Cabbibo N. *Unitary Symmetry and Leptonic Decays*. Phys. Rev. Lett. **10**, (1963), 531.

[28] Kobayashi M. and Maskawa T. *CP violation in the renormalizable theory of weak interaction*. Prog. Theor. Phys. **49**, (1973), 652.

[29] Charles J. et al. (CKMfitter Group). *CP violation and the CKM matrix: Assessing the impact of the asymmetric B factories*. Eur. Phys. J. **C41**, (2005), 1–131. Updated results and plots available at: http://ckmfitter.in2p3.fr, [hep-ph/0406184].

[30] Baker C.A. et al. *An improved experimental limit on the electric dipole moment of the neutron*. Phys. Rev. Lett. **97**, (2006), 131801. [hep-ex/0602020].

[31] Peccei R.D. *The strong CP problem and axions*. Lect. Notes Phys. **741**, (2008), 3–17. [hep-ph/0607268].

[32] Peccei R.D. and Quinn H.R. *Constraints Imposed by CP Conservation in the Presence of Instantons*. Phys. Rev. **D16**, (1977), 1791–1797.

[33] Peccei R.D. and Quinn H.R. *CP Conservation in the Presence of Instantons*. Phys. Rev. Lett. **38**, (1977), 1440–1443.

[34] Hagmann C., Murayama H., Raffelt G.G., Rosenberg L.J. and Bibber K.v. *Axions* .

[35] Yao W.M. et al. (Particle Data Group). *Review of particle physics*. J. Phys. **G33**, (2006), 1–1232. Online updates: http://pdg.lbl.gov.

[36] Sakharov A.D. *Violation of CP Invariance, c Asymmetry, and Baryon Asymmetry of the Universe*. Pisma Zh. Eksp. Teor. Fiz. **5**, (1967), 32–35.

[37] Farrar G.R. and Shaposhnikov M.E. *Baryon asymmetry of the universe in the standard electroweak theory*. Phys. Rev. **D50**, (1994), 774. [hep-ph/9305275].

[38] Huet P. and Sather E. *Electroweak baryogenesis and standard model CP violation*. Phys. Rev. **D51**, (1995), 379–394. [hep-ph/9404302].

[39] Gavela M.B., Lozano M., Orloff J. and Pene O. *Standard model CP violation and baryon asymmetry. Part 1: Zero temperature*. Nucl. Phys. **B430**, (1994), 345–381. [hep-ph/9406288].

[40] Bigi I. and Sanda A. *CP Violation*. Cambridge University Press, 2000.

[41] Jarlskog C. (ed.). *CP Violation*. World Svientific Co. Pte. Ltd., 1989.

[42] Fleischer R. *CP violation in the B system and relations to $K \to \pi\nu\bar{\nu}$ decays*. Phys. Rept. **370**, (2002), 537–680. [hep-ph/0207108].

[43] Gronau M. *CP violation in beauty decays*. Int. J. Mod. Phys. **A22**, (2007), 1953–1982. [0704.0076 (hep-ph)].

[44] Nir Y. *CP violation in meson decays*. arXiv: hep–ph/0510413.

[45] Glashow S.L., Iliopoulos J. and Maiani L. *Weak Interactions with Lepton-Hadron Symmetry*. Phys. Rev. **D2**, (1970), 1285–1292.

[46] Jarlskog C. *A Basis independent formulation of the connection between quark mass matrices, CP violation and experiment*. Z. Phys. **C29**, (1985), 491.

[47] Jarlskog C. *Commutator of the Quark Mass Matrices in the Standard Electroweak Model and a measure of Maximal CP Violation*. Phys. Rev. Lett. **55**, (1985), 1039.

[48] Wolfenstein L. *Parametrization of the Kobayashi-Maskawa Matrix*. Phys. Rev. Lett. **51**, (1983), 1945.

[49] Buras A.J., Lautenbacher M.E. and Ostermaier G. *Waiting for the top quark mass, K+ → pi+ neutrino anti-neutrino, B(s)0 - anti-B(s)0 mixing and CP asymmetries in B decays*. Phys. Rev. **D50**, (1994), 3433–3446. [hep-ph/9403384].

[50] Ciuchini M. et al. *2000 CKM triangle analysis: A Critical review with updated experimental inputs and theoretical parameters*. JHEP **07**, (2001), 013. Updated results and plots available at: http://www.utfit.org, [hep-ph/0012308].

[51] Fleischer R. $B_{s,d} \to \pi\pi, \pi K, KK$*: Status and Prospects*. Eur. Phys. J. **C52**, (2007), 267–281. [0705.1121 (hep-ph)].

[52] Weisskopf V. and Wigner E.P. *Over the natural line width in the radiation of the harmonius oscillator*. Z. Phys. **65**, (1930), 18–29.

[53] Weisskopf V. and Wigner E.P. *Calculation of the natural brightness of spectral lines on the basis of Dirac's theory*. Z. Phys. **63**, (1930), 54–73.

[54] Barberio E. et al. (Heavy Flavor Averaging Group). *Averages of b−hadron and c−hadron Properties at the End of 2007*. arXiv: 0808.1297 (hep–ex). Online update available at http://www.slac.stanford.edu/xorg/hfag.

[55] D'Ambrosio G., Giudice G.F., Isidori G. and Strumia A. *Minimal flavour violation: An effective field theory approach*. Nucl. Phys. **B645**, (2002), 155–187. [hep-ph/0207036].

[56] Buras A.J., Gambino P., Gorbahn M., Jager S. and Silvestrini L. *Universal unitarity triangle and physics beyond the standard model*. Phys. Lett. **B500**, (2001), 161–167. [hep-ph/0007085].

[57] Botella F.J. and Silva J.P. *Reparametrization invariance of B decay amplitudes and implications for new physics searches in B decays*. Phys. Rev. **D71**, (2005), 094008. [hep-ph/0503136].

[58] Datta A. and London D. *Measuring new-physics parameters in B penguin decays*. Phys. Lett. **B595**, (2004), 453–460. [hep-ph/0404130].

[59] Dunietz I., Quinn H.R., Snyder A., Toki W. and Lipkin H.J. *How to extract CP violating asymmetries from angular correlations*. Phys. Rev. **D43**, (1991), 2193–2208.

[60] Grossman Y. and Quinn H.R. *Removing discrete ambiguities in CP asymmetry measurements*. Phys. Rev. **D56**, (1997), 7259–7266. [hep-ph/9705356].

[61] London D., Sinha N. and Sinha R. *Can one measure the weak phase of a penguin diagram?*. Phys. Rev. **D60**, (1999), 074020. [hep-ph/9905404].

[62] Baek S., Botella F.J., London D. and Silva J.P. *Can one detect new physics in I = 0 and / or I = 2 contributions to the decays B –> pi pi?*. Phys. Rev. **D72**, (2005), 036004. [hep-ph/0506075].

[63] Feldmann T., Jung M. and Mannel T. *Is there a non-Standard-Model contribution in non-leptonic b → s decays?*. JHEP **08**, (2008), 066. [0803.3729 (hep-ph)].

[64] Appelquist T. and Carazzone J. *Infrared Singularities and Massive Fields*. Phys. Rev. **D11**, (1975), 2856.

[65] Buchalla G., Buras A.J. and Lautenbacher M.E. *Weak decays beyond leading logarithms*. Rev. Mod. Phys. **68**, (1996), 1125–1144. [hep-ph/9512380].

[66] Neubert M. *Effective field theory and heavy quark physics*. arXiv: hep–ph/0512222.

[67] Mannel T. *Effective Field Theories in Flavor Physics*. Springer Tracts Mod. Phys. **203**, (2004), 1–175.

[68] Virto J. *Topics in Hadronic B Decays*. arXiv: 0712.3367 (hep–ph).

[69] Beneke M., Buchalla G., Neubert M. and Sachrajda C.T. *QCD factorization for exclusive, non-leptonic B meson decays: General arguments and the case of heavy-light final states*. Nucl. Phys. **B591**, (2000), 313–418. [hep-ph/0006124].

[70] Beneke M., Buchalla G., Neubert M. and Sachrajda C.T. *QCD factorization in B –> pi K, pi pi decays and extraction of Wolfenstein parameters*. Nucl. Phys. **B606**, (2001), 245–321. [hep-ph/0104110].

[71] Buchmuller W. and Wyler D. *Effective Lagrangian Analysis of New Interactions and Flavor Conservation*. Nucl. Phys. **B268**, (1986), 621.

[72] Froggatt C.D. and Nielsen H.B. *Hierarchy of Quark Masses, Cabibbo Angles and CP Violation*. Nucl. Phys. **B147**, (1979), 277.

[73] Leurer M., Nir Y. and Seiberg N. *Mass matrix models*. Nucl. Phys. **B398**, (1993), 319–342. [hep-ph/9212278].

[74] Leurer M., Nir Y. and Seiberg N. *Mass matrix models: The Sequel*. Nucl. Phys. **B420**, (1994), 468–504. [hep-ph/9310320].

[75] Bjorken J.D. *Topics in B Physics*. Nucl. Phys. Proc. Suppl. **11**, (1989), 325–341.

[76] Beneke M. and Neubert M. *QCD factorization for $B \to PP$ and $B \to PV$ decays*. Nucl. Phys. **B675**, (2003), 333–415. [hep-ph/0308039].

[77] Beneke M. and Jager S. *Spectator scattering at NLO in non-leptonic B decays: Tree amplitudes*. Nucl. Phys. **B751**, (2006), 160–185. [hep-ph/0512351].

[78] Beneke M. and Jager S. *Spectator scattering at NLO in non-leptonic B decays: Leading penguin amplitudes*. Nucl. Phys. **B768**, (2007), 51–84. [hep-ph/0610322].

[79] Pilipp V. *Hard spectator interactions in $B \to \pi\pi$ at order $\alpha_s^2$*. Nucl. Phys. **B794**, (2008), 154–188. [0709.3214 (hep-ph)].

[80] Kivel N. *Radiative corrections to hard spectator scattering in $B \to \pi\pi$ decays*. JHEP **05**, (2007), 019. [hep-ph/0608291].

[81] Jain A., Rothstein I.Z. and Stewart I.W. *Penguin Loops for Nonleptonic B-Decays in the Standard Model: Is there a Penguin Puzzle?*. arXiv: 0706.3399 (hep–ph).

[82] Bell G. *NNLO Vertex Corrections in charmless hadronic B decays: Imaginary part*. Nucl. Phys. **B795**, (2008), 1–26. [0705.3127 (hep-ph)].

[83] Bell G. *NNLO vertex corrections in charmless hadronic B decays: Real part*. arXiv: 0902.1915 (hep–ph).

[84] Bander M., Silverman D. and Soni A. *CP Noninvariance in the Decays of Heavy Charged Quark Systems*. Phys. Rev. Lett. **43**, (1979), 242.

[85] Bauer C.W., Fleming S., Pirjol D. and Stewart I.W. *An effective field theory for collinear and soft gluons: Heavy to light decays*. Phys. Rev. **D63**, (2001), 114020. [hep-ph/0011336].

[86] Bauer C.W., Fleming S., Pirjol D., Rothstein I.Z. and Stewart I.W. *Hard scattering factorization from effective field theory*. Phys. Rev. **D66**, (2002), 014017. [hep-ph/0202088].

[87] Beneke M., Chapovsky A.P., Diehl M. and Feldmann T. *Soft-collinear effective theory and heavy-to-light currents beyond leading power*. Nucl. Phys. **B643**, (2002), 431–476. [hep-ph/0206152].

[88] Beneke M. and Feldmann T. *Multipole-expanded soft-collinear effective theory with non-abelian gauge symmetry*. Phys. Lett. **B553**, (2003), 267–276. [hep-ph/0211358].

[89] Wigner E.P. *Einige Folgerungen aus der Schrödingerschen Theorie für die Termstrukturen*. Z. Physik **43**, (1927), 624–652.

[90] Eckart C. *The Application of Group Theory to the Quantum Dynamics of Monatomic Systems*. Rev. Mod. Phys. **2**, (1930), 305–380.

[91] Fleischer R. *Strategies for Fixing the CKM-angle $\gamma$ and Obtaining Experimental Insights into the World of Electroweak Penguins*. Phys. Lett. **B365**, (1996), 399–406. [hep-ph/9509204].

[92] Neubert M. and Rosner J.L. *New bound on gamma from B+- –> pi K decays*. Phys. Lett. **B441**, (1998), 403–409. [hep-ph/9808493].

[93] Zeppenfeld D. *SU(3) Relations for B Meson Decays*. Zeit. Phys. **C8**, (1981), 77.

[94] Savage M.J. and Wise M.B. *SU(3) Predictions for Nonleptonic B Meson Decays*. Phys. Rev. **D39**, (1989), 3346.

[95] Soni A. and Suprun D.A. *Determination of gamma from charmless B –> M(1) M(2) decays using U-spin*. Phys. Rev. **D75**, (2007), 054006. [hep-ph/0609089].

[96] Fleischer R. *New strategies to extract beta and gamma from B/d –> pi+ pi- and B/s –> K+ K-*. Phys. Lett. **B459**, (1999), 306–320. [hep-ph/9903456].

[97] Gronau M. *U-spin symmetry in charmless B decays*. Phys. Lett. **B492**, (2000), 297–302. [hep-ph/0008292].

[98] Hocker A., Lacker H., Laplace S. and Le Diberder F. *A New approach to a global fit of the CKM matrix*. Eur. Phys. J. **C21**, (2001), 225–259. [hep-ph/0104062].

[99] Charles J., Hocker A., Lacker H., Le Diberder F.R. and T'Jampens S. *Bayesian statistics at work: The troublesome extraction of the CKM phase alpha*. arXiv hep–ph/0607246.

[100] Bona M. et al. (UTfit collaboration). *Improved determination of the CKM angle alpha from B –> pi pi decays*. Phys. Rev. **D76**, (2007), 014015. [hep-ph/0701204].

[101] Charles J., Hocker A., Lacker H., Le Diberder F. and T'Jampens S. *Reply to: 'Improved determination of the CKM angle alpha from B –> pi pi decays'*. arXiv: hep–ph/0703073.

[102] Botella F.J. and Nebot M. *Reparametrization Invariance, the controversial extraction of $\alpha$ from $B \to \pi\pi$ and New Physics*. arXiv: 0704.0174 (hep–ph).

[103] Boos H., Mannel T. and Reuter J. *The gold-plated mode revisited: sin(2beta) and B0 –> J/psi K(S) in the standard model*. Phys. Rev. **D70**, (2004), 036006. [hep-ph/0403085].

[104] Li H.n. and Mishima S. *Penguin pollution in the B0 –> J/psi K(S) decay*. JHEP **03**, (2007), 009. [hep-ph/0610120].

[105] Ciuchini M., Pierini M. and Silvestrini L. *The effect of penguins in the B/d –> J/psi K0 CP asymmetry*. Phys. Rev. Lett. **95**, (2005), 221804. [hep-ph/0507290].

[106] Fleischer R. and Mannel T. *General analysis of new physics in $B \to J/\psi K$*. Phys. Lett. **B506**, (2001), 311–322. [hep-ph/0101276].

[107] Gronau M., Hernandez O.F., London D. and Rosner J.L. *Broken SU(3) symmetry in two-body B decays*. Phys. Rev. **D52**, (1995), 6356–6373. [hep-ph/9504326].

[108] Gronau M., Hernandez O.F., London D. and Rosner J.L. *Electroweak penguins and two-body B decays*. Phys. Rev. **D52**, (1995), 6374–6382. [hep-ph/9504327].

[109] Grossman Y., Ligeti Z., Nir Y. and Quinn H. *SU(3) relations and the CP asymmetries in B decays to eta' K(S), Phi K(S) and K+ K- K(S)*. Phys. Rev. **D68**, (2003), 015004. [hep-ph/0303171].

[110] Williamson A.R. and Zupan J. *Two body B decays with isosinglet final states in SCET*. Phys. Rev. **D74**, (2006), 014003. [hep-ph/0601214].

[111] Cheng H.Y., Chua C.K. and Soni A. *Effects of Final-state Interactions on Mixing-induced CP Violation in Penguin-dominated B Decays*. Phys. Rev. **D72**, (2005), 014006. [hep-ph/0502235].

[112] Beneke M. *Corrections to sin(2beta) from CP asymmetries in B0 –> (pi0, rho0, eta, eta', omega, Phi) K(S) decays*. Phys. Lett. **B620**, (2005), 143–150. [hep-ph/0505075].

[113] Fleischer R. and Mannel T. *Exploring New Physics in the $B \to \phi K$ System*. Phys. Lett. **B511**, (2001), 240–250. [hep-ph/0103121].

[114] Neubert M. *Model-independent analysis of B –> pi K decays and bounds on the weak phase gamma*. JHEP **02**, (1999), 014. [hep-ph/9812396].

[115] Baek S., Chiang C.W. and London D. *The B -> pi K Puzzle: 2009 Update* [0903.3086 (hep–ph)].

[116] Buras A.J. and Fleischer R. *A general analysis of gamma determinations from B –> pi K decays*. Eur. Phys. J. **C11**, (1999), 93–109. [hep-ph/9810260].

[117] Gronau M. and Rosner J.L. *Rate and CP-asymmetry sum rules in B –> K pi*. Phys. Rev. **D74**, (2006), 057503. [hep-ph/0608040].

[118] Fleischer R., Recksiegel S. and Schwab F. *On Puzzles and Non-Puzzles in $B \to \pi\pi$, $\pi K$ Decays*. Eur. Phys. J. **C51**, (2007), 55–61. [hep-ph/0702275].

[119] Buras A.J., Fleischer R., Recksiegel S. and Schwab F. *Anatomy of prominent B and K decays and signatures of CP- violating new physics in the electroweak penguin sector*. Nucl. Phys. **B697**, (2004), 133–206. [hep-ph/0402112].

[120] Ciuchini M., Franco E., Martinelli G., Pierini M. and Silvestrini L. *Searching For New Physics With B to K pi Decays*. Phys. Lett. **B674**, (2009), 197–203. [0811.0341 (hep-ph)].

[121] Fleischer R., Jager S., Pirjol D. and Zupan J. *Benchmarks for the New-Physics Search through CP Violation in $B^0 \to \pi^0 K_S$*. Phys. Rev. **D78**, (2008), 111501. [0806.2900 (hep-ph)].

[122] Gronau M. and Rosner J.L. *Implications for CP asymmetries of improved data on $B \to K^0\pi^0$*. Phys. Lett. **B666**, (2008), 467–471. [0807.3080 (hep-ph)].

[123] Gronau M. *A precise sum rule among four B –> K pi CP asymmetries*. Phys. Lett. **B627**, (2005), 82–88. [hep-ph/0508047].

[124] Feldmann T. and Hurth T. *Non-factorizable contributions to B –> pi pi decays*. JHEP **11**, (2004), 037. [hep-ph/0408188].

[125] Chiang C.W., Gronau M. and Rosner J.L. *Examination of Flavor SU(3) in B, $B_s \to K\pi$ Decays*. Phys. Lett. **B664**, (2008), 169–173. [0803.3229 (hep-ph)].

[126] Ciuchini M., Pierini M. and Silvestrini L. *The effect of penguins in the B/d –> J/psi K0 CP asymmetry*. Phys. Rev. Lett. **95**, (2005), 221804. [hep-ph/0507290].

[127] Faller S., Jung M., Fleischer R. and Mannel T. *The Golden Modes $B^0 - > J/psiK_{S,L}$ in the Era of Precision Flavour Physics*. Phys. Rev. **D79**, (2009), 014030. [0809.0842 (hep-ph)].

[128] Chen K.F. et al. (Belle collaboration). *Observation of time-dependent CP violation in B0 –> eta' K0 decays and improved measurements of CP asymmetries in B0 –> Phi K0, K0(S) K0(S) K0(S) and B0 –> J/psi K0 decays*. Phys. Rev. Lett. **98**, (2007), 031802. [hep-ex/0608039].

[129] Aubert B. et al. (BABAR collaboration). *Update of Time-Dependent CP Asymmetry Measurements in $b \to c\bar{c}s$ Decays*. arXiv: [0808.1903 (hep–ex)].

[130] Buras A.J. and Silvestrini L. *Non-leptonic two-body B decays beyond factorization*. Nucl. Phys. **B569**, (2000), 3–52. [hep-ph/9812392].

[131] Aubert B. et al. (BABAR collaboration). *Evidence for CP violation in $B^0 \to J/\psi\pi^0$ decays*. Phys. Rev. Lett. **101**, (2008), 021801. [0804.0896 (hep-ex)].

[132] Lee S.E. et al. (Belle collaboration). *Improved measurement of time-dependent CP violation in B0 -> J/Psi pi0 decays*. Phys. Rev. **D77**, (2008), 071101. [0708.0304 (hep-ex)].

[133] Fleischer R. *Extracting $\gamma$ from $B(s/d) \to J/\psi K_S$ and $B(d/s) \to D^+(d/s)D^-(d/s)$*. Eur. Phys. J. **C10**, (1999), 299–306. [hep-ph/9903455].

[134] Ball P. and Zwicky R. *New results on B –> pi, K, eta decay form-factors from light-cone sum rules*. Phys. Rev. **D71**, (2005), 014015. [hep-ph/0406232].

[135] Duplancic G., Khodjamirian A., Mannel T., Melic B. and Offen N. *Light-cone sum rules for $B \to \pi$ form factors revisited*. JHEP **04**, (2008), 014. [0801.1796 (hep-ph)].

[136] Duplancic G. and Melic B. *B, Bs -> K form factors: an update of light-cone sum rule results*. Phys. Rev. **D78**, (2008), 054015. [0805.4170 (hep-ph)].

[137] Becirevic D. and Kaidalov A.B. *Comment on the heavy –> light form factors*. Phys. Lett. **B478**, (2000), 417–423. [hep-ph/9904490].

[138] Gronau M. and Rosner J.L. *Doubly CKM-suppressed corrections to CP asymmetries in $B^0 \to J/\psi K^0$*. Phys. Lett. **B672**, (2009), 349–353. [0812.4796 (hep-ph)].

[139] Jung M. and Mannel T. *Model-independent analysis of U-spin breaking in non-leptonic B-decays*. In *International Workshop on Effective Field Theories: from the pion to the upsilon*. 2009, PoS(EFT09)003.

[140] Jung M. and Mannel T. *General Analysis of U-spin breaking in B Decays*. Preprint: SI–HEP–2009–01.

[141] Gronau M. and Wyler D. *On determining a weak phase from CP asymmetries in charged B decays*. Phys. Lett. **B265**, (1991), 172–176.

[142] Gronau M. and London. D. *How to determine all the angles of the unitarity triangle from B(d)0 → D K(s) and B(s)0 → D0*. Phys. Lett. **B253**, (1991), 483–488.

[143] Aaltonen T. et al. (CDF collaboration). *Observation of New Charmless Decays of Bottom Hadrons*. arXiv 0812.4271 (hep–ex).

# Acknowledgements


- I want to thank my advisor Thomas Mannel for countless discussions and insights, and for all the support you could ask for.
- Alexander Khodjamirian I thank for taking on the obligation as co-referee and for interesting discussions.
- I am grateful to Thorsten Feldmann for being a great tutor in innumerable discussions, seeing really to the root of problems.
- The working group in Siegen, including the honorary and former members, for a great atmosphere, discussions in the coffee room and an open ear for problems.
- Robert Feger impressed me by always being there in case of technical problems, dropping everything, and working until a solution had been found.
- I thank my new working group in Valencia for welcoming me warmly. Thanks especially to Toni Pich for giving me the opportunity to complete my thesis here.
- My friends Kai Grybel, Sven Faller, Nils Offen, Delia Brüser and Peter Kaufmann, I thank for really giving me something to look forward to at work every single day, Sven and Kai also for proof-reading the manuscript.
- My girlfriend Adeline Bieker for being with me through all the ups and downs of this work.
- I would like to thank my parents for their trust and support which has made me who I am today.
- All those of my family and friends not explicitly listed here: thanks for being part of my life!